

**The dynamics of bone augmentation with a TiO<sub>2</sub> graft material:  
Studies in challenging pre-clinical models**

Minh Khai Le Thieu



Department of Periodontology and Department of Biomaterials

Faculty of Dentistry

University of Oslo

2024

© Minh Khai Le Thieu, 2024

*Series of dissertations submitted to the  
Faculty of Dentistry, University of Oslo*

ISBN 978-82-8327-088-4

All rights reserved. No part of this publication may be  
reproduced or transmitted, in any form or by any means, without permission.

Cover: UiO.

Print production: Graphic center, University of Oslo.

*“All grown-ups were once children... but only few of them remember it.”*

The Little Prince

Antoine de Saint-Exupéry



## Table of contents

<b>Acknowledgment</b> .....	7
<b>List of papers</b> .....	9
<b>Abbreviations</b> .....	10
<b>Introduction</b> .....	11
<i>Replacement of missing teeth</i> .....	11
<i>Bone formation and bone augmentation</i> .....	11
<i>Timing of bone augmentation</i> .....	14
<i>Methods of bone augmentation</i> .....	15
<i>Bone graft materials</i> .....	17
<i>Ceramic bone grafts and TiO<sub>2</sub></i> .....	19
<i>Pre-clinical testing of graft materials</i> .....	20
<i>Choosing relevant test models</i> .....	20
<b>Aim of the research</b> .....	26
<i>General hypothesis of the thesis</i> .....	26
<i>General objective of the thesis</i> .....	26
<i>Specific aims of the thesis</i> .....	26
<b>Methodological considerations</b> .....	27
<i>Research models</i> .....	27
Considerations for <i>in vivo</i> models.....	27
Experimental designs .....	28
<i>In vivo</i> analytical methods .....	31
Microcomputed tomography .....	31
Histology and histomorphometry.....	33
Immunohistochemistry.....	35
Soft tissue measurements .....	37
<b>Summary of the results</b> .....	38
<i>Paper I</i> .....	38
<i>Paper II</i> .....	38
<i>Paper III</i> .....	38
<b>Discussion of the results</b> .....	39
<b>General conclusion</b> .....	44
<b>Conclusion related to specific aims</b> .....	44
<b>Concluding remarks</b> .....	44
<b>Future perspective</b> .....	46
<b>References</b> .....	49
<b>Errata</b> .....	57



## Acknowledgment

This work was conducted at the Department of Periodontology and the Department of Biomaterials, Faculty of Dentistry, University of Oslo. I am grateful to the Faculty of Dentistry for this opportunity and for the funding that made this project possible.

To Associate Professor Anders Verket, I would like to express my greatest gratitude. Thank you for opening your door to the fascinating world of periodontology and showing me the ropes. Despite working with a non-communicable disease, your passion for periodontology and research is truly contagious. I sincerely appreciated all our meetings discussion every sentences of every manuscript in the seventh-floor “bunker”. Your supervision has been invaluable.

To Professor Håvard J. Haugen, I want to thank you for supporting me and believing in me already when I was a dental student, after only a few lectures. I will never forget the opportunities you have given me. You only see the opportunities and always find a solution whenever a challenge presents itself, which has been truly inspirational. I have always left your office filled with coffee and motivation.

My sincerest thanks go to my co-authors, for extensive effort and comprehensive feedback, making this work such a fun project.

To Professor Mariano Sanz, Dr. Javier Sanz-Esporrin and your group at University Complutense of Madrid, I am grateful for your support and collaboration. It has been an honour working with such a dedicated and knowledgeable team.

To Professor Thaqif El Khassawna, Dr. Sabine Stötzl and Dr. Maryam Rahmati for invaluable collaboration in histology and immunohistochemistry.

To Professor Ståle Petter Lyngstadaas, your expertise in everything bone-related has been invaluable and your feedback was highly appreciated.

To Head of the Institute, Professor Jan Eirik Ellingsen, I am grateful for your support and for making this project possible.

I am thankful to all my friends and colleagues at the Department of Biomaterials for creating an environment where science and cakes are equally important. I am indebted to Liebert Parreiras Nogueira and Catherine Anne Heyward for sharing your technical expertise, but not least for your patience in showing a dentist how to do microCT and histology. A very special thanks goes to Hanna Tiainen. Your knowledge regarding anything biomaterials is unfathomable. I am truly grateful for your supervision and all our interesting discussions. You have shown me the beauty of science, but equally important the pitfalls of science.

A big thanks to all friends for distracting me with everything but periodontology and biomaterials. Thank you to John and Silje for keeping me physically active these years with tennis, cycling and running, and to Thea and Emma for showing me there is other food than canned mackerel and bread. Thank you Therese for your unlimited support, and for taking care of me. I am lucky to have you in my life.

Finally, I would like to thank my mom, my dad and my brother Kevin for always being there for me, and always believing in me.

Minh Thieu

Oslo, February 2024





## List of papers

### Paper I

**Impact of simultaneous placement of implant and block bone graft substitute: an in vivo peri-implant defect model**

Thieu, MKL; Homayouni, A; Hæren, LR; Tiainen, H; Verket, A; Ellingsen, JE; Rønold, HJ; Wohlfahrt, JC; Cantalapiedra, AG; Muñoz Guzon, FA; Permuy Mendaña, M; Lyngstadaas, SP & Haugen, HJ.

Biomaterials Research, 2021, 25(43).

ISSN 1226-4601. 25(43). doi: 10.1186/s40824-021-00245-3

### Paper II

**Guided bone regeneration of chronic non-contained bone defects using a volume stable porous block TiO<sub>2</sub> scaffold: An experimental in vivo study**

Thieu, MKL; Haugen, HJ; Sanz-Esporrin, J; Sanz, M; Lyngstadaas, SP & Verket, A. Clinical Oral Implants Research, 2021; 32: 369–381.

ISSN 0905-7161. doi: 10.1111/clr.13708.

### Paper III

**Immunohistochemical comparison of lateral bone augmentation using a synthetic TiO<sub>2</sub> block or a xenogeneic graft in chronic alveolar defects**

Thieu, MKL; Stoetzel, S; Rahmati, M; El Khassawna, T; Verket, A; Sanz-Esporrin, J; Sanz, M; Ellingsen, JE & Haugen, HJ.

Clinical Implant Dentistry and Related Research, 2023; 25(1): 57-67.

ISSN 1523-0899. doi: 10.1111/cid.13143.

All publications are reprinted with permission of the copyright holders.

## Abbreviations

<b><math>\alpha</math>-SMA</b>	alpha-smooth muscle actin
<b>ALP</b>	alkaline phosphatase
<b>BMP</b>	bone morphogenetic proteins
<b>DBBM</b>	deproteinized bovine bone mineral
<b>EDX</b>	energy-dispersive x-ray spectroscopy
<b>FTIR</b>	Fourier Transform infrared
<b>GBR</b>	guided bone regeneration
<b>IHC</b>	immunohistochemistry
<b>MCS-F</b>	macrophage colony-stimulating factor
<b>MicroCT</b>	microcomputed tomography
<b>MMA</b>	methyl methacrylate
<b>OC</b>	osteocalcin
<b>OP</b>	osteopontin
<b>OPG</b>	osteoprotegerin
<b>PTFE</b>	polytetrafluoroethylene
<b>RANKL</b>	nuclear factor $\kappa$ B ligand
<b>STL</b>	stereolithographic
<b>TFG-<math>\beta</math></b>	transforming growth factor- $\beta$
<b>TiO<sub>2</sub></b>	titanium dioxide
<b>TRAP</b>	tartrate-resistant acid phosphatase
<b>VAS</b>	visual analogue scale
<b>VOI</b>	volume of interest

## **Introduction**

### *Replacement of missing teeth*

Tooth loss is often the endpoint of several oral diseases, which 3.5 billion people are affected by worldwide [1]. Most common are dental caries and periodontal diseases, but also traumas, oral cancers, and congenital diseases may cause tooth loss [2]. Tooth loss is associated with reduced masticatory function, phonetical challenges, social stigma, and subsequently reduced quality of life [3, 4]. Nowadays, patients often expect a replacement for their missing teeth, and with increasing life expectancy, the replacement of missing teeth is ever more relevant.

Several options exist for replacing a missing tooth, including dental prostheses that are either removable or fixed. Removable dental prostheses have been widely used and may be used to replace everything from a single tooth to a complete dentition. Although the treatment is considered relatively low-cost, it is the solution for missing teeth in large parts of the world. Removable prostheses are a less invasive alternative as compared to fixed dental prostheses, but the treatment form may have disadvantages. As they are removable, achieving adequate retention may be challenging [5]. A prosthesis requires retention from the teeth and/or mucosa, and may be perceived as bulky and uncomfortable by the patients [6]. Studies demonstrate that patients prefer fixed over removable dental prostheses, reporting better stability, chewing function and pronunciation [7-9].

Fixed dental prostheses can be retained to either teeth, implants, or both. However, combinations of tooth- and implant-supported restorations have shown inferior survival rates [10, 11]. An implant is usually the preferred option when a patient presents pristine adjacent teeth and adequate bone volume [12]. However, it is not unusual that neighbouring teeth are pristine, but the dimension of the alveolar bone is limited. In such cases, bone augmentation procedures may facilitate prosthetically-driven implant placement in an acceptable recipient site.

### *Bone formation and bone augmentation*

When a dental implant is to be placed, adequate bone volume and quality are desired to ensure stability and aesthetic outcomes. However, in many cases, the clinical situation does not meet these requirements. Following oral diseases like periodontitis, apical periodontitis or tumors, bone destruction occurs around affected teeth. Likewise, traumas and tooth extraction can cause

bone defects. In the case of tooth extraction, following the healing of the extraction socket, resorption of the alveolar bone will follow [13]. Bone augmentation is, therefore, often required to gain sufficient bone for implant placement.

Bone is a living tissue that constitutes approximately 50-70% hydroxyapatite mineral  $[\text{Ca}_{10}(\text{PO}_4)_6(\text{OH})_2]$ , 5-10% water and only 20-40% organic matrix. Despite being predominantly an inorganic mineral, bone is a highly dynamic tissue under constant remodeling [14]. The total skeletal remodeling rates have been estimated to be approximately 10% per year [15]. Bone formation starts before birth, and remodeling is a continuous process until the end of life. The constant turnover allows the bone to maintain its mechanical strength and repairs damages [14].

Bone can be formed through two mechanisms: intramembranous ossification and endochondral ossification. During intramembranous ossification, bone develops directly from sheets of connective tissue. In endochondral ossification, bone develops by replacing hyaline cartilage [16]. Both processes take place during growth, but differ according to bone type. The lengthwise growth of long bones is primarily a result of endochondral ossification, whereas the appositional growth of flat bones, like the facial and most cranial bones, occurs by intramembranous ossification. Appositional growth and remodeling occur throughout life. In cases of traumas, repair may occur by either direct intramembranous healing when the fracture fragments are fixed together by direct contact, or through indirect healing involving both intramembranous and endochondral ossification [17].

Intramembranous bone formation is the pathway of intraoral bone augmentation and involves hematoma formation followed by an inflammatory reaction and the recruitment of mesenchymal stem cells [18, 19]. At the same time, blood is supplied by revascularization and neoangiogenesis of the area [20].

Mesenchymal stem cells recruited from the surrounding periosteum, cortical bone, bone marrow and peripheral blood can proliferate and differentiate into bone-forming osteoblasts [17, 21]. The osteoblasts synthesize and deposit bone matrix on the bone surface. During bone formation, some osteoblasts become trapped within the bone matrix in lacunae, which later differentiate into osteocytes (**Figure 1**). Their main function is to sense and respond to mechanical forces. These cells can express bone matrix proteins like osteocalcin (OC), galectin 3 and CD44 [14]. The osteocyte communicates with other osteocytes and cells on the bone

surface from the lacuna. Undifferentiated mesenchymal stem cells also reside within the bone marrow and endosteum and on the periosteum lining the surface.

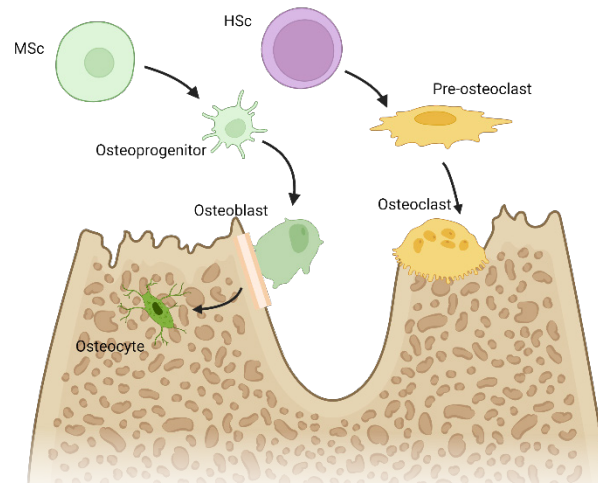


*Figure 1 - Pathways of osteoblast and osteoclast proliferation. MSc: mesenchymal stem cells, HSc: hematopoietic stem cells. Created With BioRender*

On the other hand, osteoclasts are bone-resorbing cells of the hematopoietic lineage. Osteoclasts are large multinucleated cells that resorb bone through chemical and enzymatic pathways. The activities of osteoblasts, osteocytes and osteoclasts altogether control the process of bone remodeling. Therefore, bone augmentation depends on the complex and finely coordinated processes required to stimulate new bone formation in a desired area.

Bone formation and resorption is mediated by nuclear factor  $\kappa$ B ligand (RANKL), its receptor RANK, and the decoy receptor osteoprotegerin (OPG). RANKL is primarily expressed in bone tissue by osteoblasts, osteocytes, stromal cells and T- and B-lymphocytes [22]. OPG is expressed by osteoblasts and stromal cells [23]. RANK receptors are located on osteoclast lineage cells, and binding to RANKL leads to the differentiation of the precursor cells into osteoclastic cells. In contrast, OPG acts as a decoy receptor by blocking RANKL. Macrophage colony-stimulating factor (M-CSF) binding to the pre-osteoclastic cells is also necessary for osteoclast development by promoting the proliferation of the osteoclast precursors [24].

During osteogenesis, a series of coordinated gene expressions must occur for the osteoblast to create mineralized bone tissue [25-27]. Four distinctive phases (**Figure 2**) have been described for this process [26, 27]. First, a proliferation phase where the osteoblasts expand and an increase in the expression of collagen type I takes place, and also fibronectin and transforming

growth factor- $\beta$  (TGF- $\beta$ ) are expressed. The matrix maturation phase comes after the downregulation of the genes in the proliferation phase. Alkaline phosphatase (ALP) enzymes, proteins associated with the bone cell phenotype increase. This leads to osteoblast differentiation, and the extracellular matrix composition and organization are prepared for mineralization. Entering the mineralization phase, gene expression of sialoprotein, osteopontin and osteocalcin reaches a peak expression. In the final phase, collagenase and collagen type I expression increase, and apoptotic activity occurs. This serves a remodeling function in mature cultures.

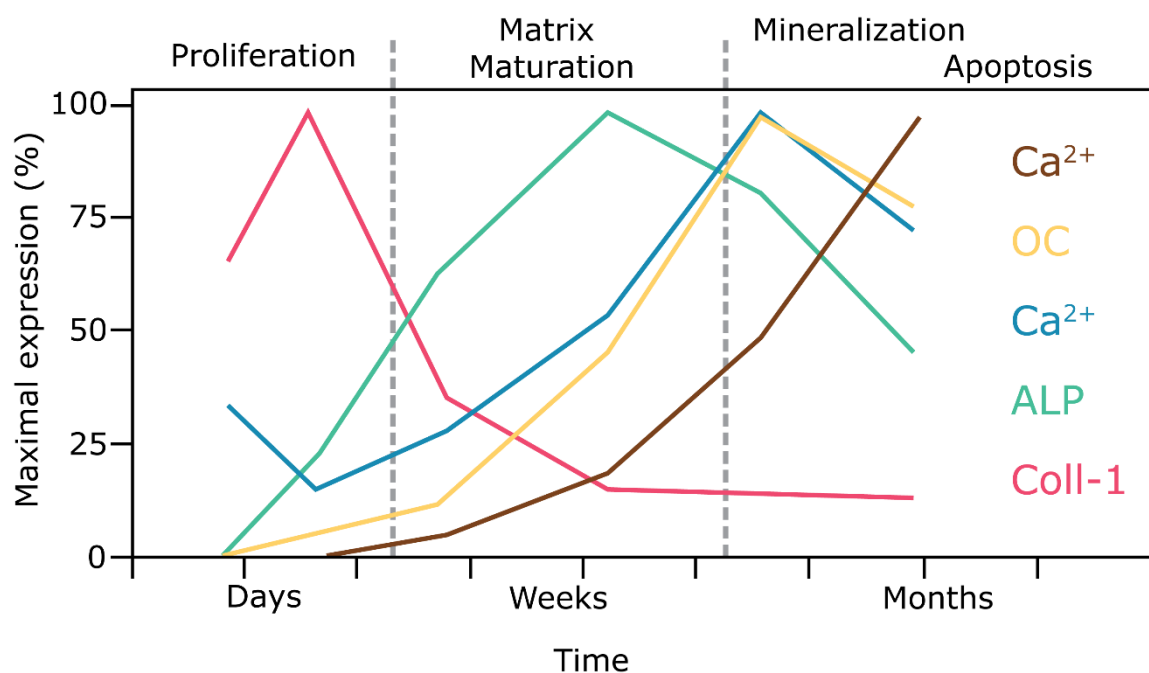
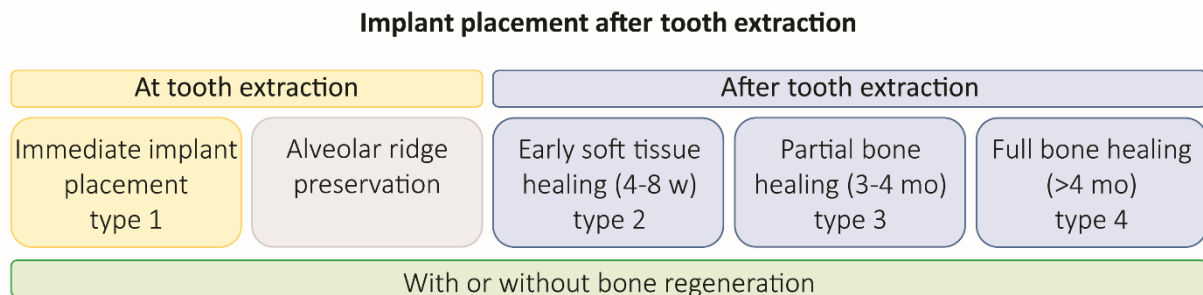


Figure 2 - The temporal osteoblast development sequence. OC: osteocalcin, ALP: alkaline phosphatase, Coll-1: collagen type I. Figure modified from the original article by Stein et al. (1996).

### Timing of bone augmentation

Bone augmentation can be performed prior to implant placement, at the time of implant placement, or after implant loading. The procedure is considered predictable and effective for the reconstruction of alveolar ridge defects [28-30]. When performed simultaneously, augmentation can be performed at either of the four time-points (type 1-4) of implant placement (**Figure 3**)[31]. Each type represents a different stage of bone healing and possibly a different bone condition, from the fresh extraction socket to an alveolar ridge under resorption and

remodeling and finally a fully healed ridge. Despite the differences, the consensus report and clinical recommendations of the European Workshop in Periodontology based on a systematic review recommend that clinicians to consider bone augmentation with a biomaterial combined with a barrier membrane [29, 31].



*Figure 3 - Four time points for implant placement (Type 1-4). Additionally alveolar ridge preservation can be performed at the time of tooth extraction, prior to type 3 or 4 placement. For each time point, bone regeneration may also be considered.*

In cases where augmentation is performed after loading, the situation is further complicated as the bone defect has been caused by a peri-implant disease. Accordingly, an inflammatory condition may be present [32]. However, comparing outcome measures is not straightforward as this field has only recently adopted core outcome sets and measurements, resulting in large heterogeneity in previously published papers [33, 34].

### *Methods of bone augmentation*

All intra-oral bone augmentation procedures are based on intramembranous bone formation and several surgical techniques have been described. A Cochrane review by Esposito *et al.* has divided the techniques according to the following main principles [35]:

Onlay grafting is where graft material is placed on a recipient bone bed. The onlay graft can be used to increase horizontal and/or vertical bone dimension. The graft needs to be immobilized during healing, which is often accomplished by fixation screws or dental implants.

Inlay grafting, where a section of the jawbone is surgically separated, and an inlay graft material is placed between the two bone sections to increase the vertical and horizontal dimensions [35-37].

Ridge expansion, where the alveolar ridge is surgically split and widened to create space for an implant, a graft material, or both in the space created. Laterally splitting the alveolar ridge can increase the horizontal bone dimension following healing.

Distraction osteogenesis is where a surgically prepared fracture segment is gradually moved to increase the alveolar bone volume. The gap creates space for immature non-calcified bone, gradually maturing into calcified bone.

These surgical techniques for augmentation can be used with different bone graft materials, osteoinductive proteins, or barrier membranes as in guided bone regeneration (GBR), and they can be used alone or in combination.

The concept of GBR using a barrier membrane was introduced in 1959 for spinal fusion [38]. GBR has since been adapted for alveolar ridge augmentation with proven efficacy [39-42]. The principle is to use a cell occlusive membrane to exclude non-osteogenic cell types migrating from the soft tissue, promoting slower-growing bone-forming cells from the patient's bone and creating space for new bone formation [40] (**Figure 4**). In addition to space maintenance and promoting osteogenic cell migration, a membrane may protect and stabilize the blood clot during healing [43]. Further investigations into the mechanism of GBR have demonstrated that membranes can also have an active role in promoting osteogenesis [44], as demonstrated by Hämmerle *et al.*, who found vascularization and bony islands near the membrane surface [45]. Membranes have been found to increase the expression of genes for bone formation proteins like osteocalcin, osteopontin and alkaline phosphatase [46, 47].

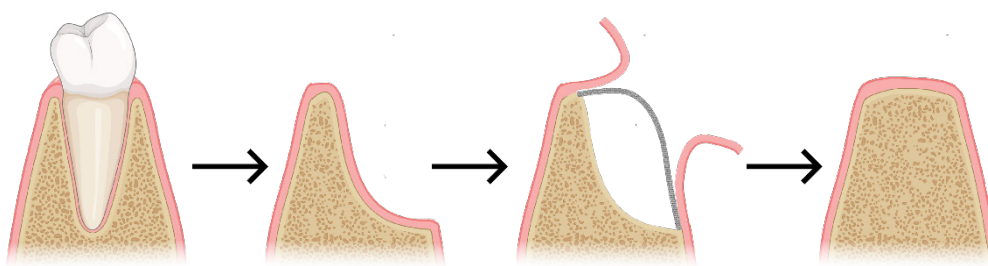


*Figure 4 - Principle of GBR for augmentation of a resorbed alveolar ridge following tooth loss. A cell-occlusive membrane is seen in the third figure. Created with BioRender.com*

Membranes can either be resorbable or non-resorbable. Non-resorbable barrier membranes are often made of expanded polytetrafluoroethylene (PTFE) reinforced with titanium, high-density PTFE or titanium mesh. While non-resorbable membranes have succeeded in bone augmentation, they require primary wound closure, as membrane exposure can lead to infection



and complications. A benefit of non-resorbable membranes is that they maintain their integrity throughout the healing period and may not collapse. As implied by their non-resorbable nature, a second intervention is required to remove the membrane, with the added risk of complications and bone loss following flap reflection [48]. However, most of the time, implant placement is planned following the healing of an augmentation procedure.

Resorbable membranes, on the other hand, overcome some of these limitations. Firstly, a second surgery is not required for removal. Secondly, if exposed to the oral cavity during healing, the resorption rate will accelerate, which may limit the consequences of exposure as compared to a non-resorbable membrane [49, 50]. These membranes can be of either synthetic polymer or natural origin. Generally, they lack mechanical strength for space maintenance to augment larger defect volumes and are often used in combination with a bone graft material.

### *Bone graft materials*

Bone grafts are often classified according to origin and are commonly grouped into autografts, allografts, xenografts and alloplasts [19, 51]. An ideal bone graft material should be osteogenic (e.g., possess osteoprogenitor cells), osteoinductive (stimulate bone formation by e.g. growth factors such as bone morphogenetic proteins (BMPs) or ion release) and osteoconductive (allow bone growth directly on the material, e.g., surface properties and three-dimensional structures that supports osteogenesis), and resorb at the time of new bone formation [52, 53]. Autogenous bone grafts possess all these properties and are generally considered the gold standard. However, since harvest requires an extended or another intervention, they involve increased morbidity. The amount of bone available for harvesting may also be limited. Clinically, autografts have proven efficacy for bone augmentation, but their resorption rates are unpredictable [54, 55]. As alternatives, allografts and xenogeneic bone grafts are commonly used. The bone must be processed before implantation to avoid the risk of disease transmission. Although the risk is minimal, it can not be eliminated entirely [56, 57] and requires stringent manufacturing process control [58]. During this process, organic components are removed, yielding a less osteoinductive material with no osteogenic cells and no osteoinductive proteins [59]. The final group of bone graft materials is the alloplastic. Like xenografts and allografts, alloplastic materials are abundant. Since they are synthetic, there is no risk of disease transmission.

Due to the drawbacks previously mentioned for autologous bone grafts, clinicians may favor other sources. Traditionally, this demand has been covered by allografts and xenografts, however, due to the risk mentioned above of disease transmission, ethical and religious considerations, and a politically-driven shift introduced in the latest directive for medical devices proposed by the European Union, a change towards more use of alloplastic materials is anticipated [53]. Alloplastic materials are generally divided into three main groups: Ceramics, polymers and metals. The most common may be ceramic calcium phosphate variants such as hydroxyapatites and tricalcium phosphates, but silicates like bioglasses are also commonly used [60, 61]. The major benefits of alloplasts are the eliminated risk of disease transmission, unlimited resources and the possibility to customize the size and shape of the materials. These materials can potentially be tailored to their specific use on a macroscopic scale, but also concerning the surface structures, porosity, mechanical strength and degradation properties. However, despite the ability to tweak synthetic materials, as of today, no one material exists that can be used for all bone graft applications. Inherent material properties like some metals' non-degradable nature and ceramics' brittleness limit their application areas. Compromises must often be made between increasing porosity, mechanical strength and degradability.

Clinically used bone grafts exist in various shapes arranged into two main groups: particulates and block materials. Particulate materials adapt readily to the recipient site and are inherently porous. However, they lack mechanical stability, have limited capacity for space maintenance, and depend on support and shielding from external forces. This makes granules technique-sensitive and operator-dependent, as the handling of the materials may affect how well they are stabilized and how much they are packed or compressed, which in turn affects the porosity. In cases where the defect is not self-contained, particulated graft materials often need to be supported by a membrane. It is shown that securing the membrane with tacks can improve the graft material's stability during healing and stabilize the augmented area from flap tension [62].

Block grafts, on the other hand, can be adapted to the desired shape. For example, their handling property may allow the clinician better control of the augmented area than granules. As with granules, blocks also require good stability at the recipient site for a successful outcome [63, 64]. The fixation can be achieved by specific bone fixation screws or simultaneous implant placement, such as onlay bone ring grafts [65, 66].

Today, autografts, allografts, xenografts and alloplasts are extensively used in the clinic, both in particulate and block form. However, due to the aforementioned increasing societal focus on animal welfare and ethical concerns of using human and animal products, as well as the political

drive to avoid biomaterials of animal origin, one may speculate that the use of synthetic materials will increase. A market report estimated the dental bone graft segment to be valued at 465 million USD in 2018, with a forecasted increase to 837 million USD by 2026, thereby increasing by 1.8 with the highest growth forecasted for synthetic bone graft materials [67].

### *Ceramic bone grafts and TiO<sub>2</sub>*

Ceramics are inorganic materials where strong ionic or covalent bonds bind the atoms together. They are typically known for high compressive strength but relatively weak in tensile. Certain ceramics have also demonstrated bioactive and osteoconductive properties when implanted in bone [68, 69]. This combination of mechanical strength and osteoconductivity makes ceramics suitable as bone graft material.

Ceramic titanium dioxide (TiO<sub>2</sub>) is another bioactive ceramic with promising properties as a bone graft material. The surface of a TiO<sub>2</sub> ceramic is bioactive and osteoconductive [70]. TiO<sub>2</sub> can be made into a porous scaffold by the relatively simple process of foam replication (**Figure 5**).



*Figure 5- Scaffold production. a) Original foam template, b) Coating of foam template with a TiO<sub>2</sub> slurry, c) Final scaffold. Note shrinkage of the ceramic following sintering.*

*In vitro* testing of such TiO<sub>2</sub> scaffolds has demonstrated porosity, pore size and interconnectivity suitable to support in-growth of bone [71, 72]. Mechanical testing has demonstrated similar strength to trabecular bone [73]. TiO<sub>2</sub> scaffolds have also been tested *in vivo*. The porous TiO<sub>2</sub> scaffold has been used in a rabbit peri-implant cortical defect model. After eight weeks of healing, the sites treated with a TiO<sub>2</sub> scaffold demonstrated significantly higher bone volume than a sham defect [74].

In studies by Tiainen and co-workers, TiO<sub>2</sub> scaffolds were placed in extraction sockets of minipigs and demonstrated biocompatibility, as seen by bone growth into the porous scaffold structures [75, 76]. However, alveolar sockets are expected to heal spontaneously without the use of biomaterials. Resorption of the alveolar ridge following extraction is also expected [13, 77], but the TiO<sub>2</sub> scaffold did not limit this compared to sham sites. Although the model was relevant evaluating alveolar ridge preservation, osteoconductivity, and biocompatibility, it could not provide relevant evidence for use of the TiO<sub>2</sub> graft material in bone augmentation. The scaffold has not been tested in chronic or circumferential peri-implant defects for this application. Apart from one *in vivo* study on acute peri-implant defects [78], there is limited evidence from *in vivo* studies where the material has been tested in clinically relevant models.

### *Pre-clinical testing of graft materials*

The purpose of every new bone graft material is to aid rehabilitation in patients. In dental applications, the final goal is usually to allow predictable implant placement to restore missing teeth. However, pre-clinical testing is always required to evaluate the interactions and mechanisms before a material is placed in humans. Although *in vitro* studies can evaluate cell responses and indicate cytotoxicity, they are simplified models that may not translate to living systems. *In vitro* testing may provide important answers before animal testing, but if the *in vitro* tests are promising *in vivo* testing is always required to simulate a clinical response. With animal testing follows an ethical responsibility. It is widely recognized that the "3Rs" and the ARRIVE guidelines should be followed during animal research [79]. The guidelines state that scientists should *replace* animals whenever possible, *reduce* the number of animals used and *refine* the care of the animals to maintain their welfare and keep pain and suffering to a minimum. The European Union monitor this matter and recently reported a decrease in animal use through stricter regulations [80]. Animal studies should therefore be carefully designed and the data collection optimized. This highlights the importance of choosing relevant experimental models and maximizing the collected data.

### *Choosing relevant test models*

A relevant experimental model should simulate the clinical situation and response to the material's intended use. A wide range of species is used in animal testing, from small fish to mice, rats and non-human primates. In 2017, fish, mice and rats accounted for 86% of the total

number of animals used in research in the European Union [80]. Smaller species are attractive to scientists due to easier handling, relatively simple husbandry and lower economical cost, but also because they have been extensively studied with large data and protocols described.

Mice are one of the most studied species and share 99% of its genome with a homolog in the human genome [81], and both display similar bone anatomy and physiology. Rodents are, therefore suited to evaluate a material's biocompatibility and osteoconductivity. However, rodent metabolism is significantly different from humans [82, 83], in addition to the apparent physical limitation for the simulation of surgical models.

Since it is impossible to evaluate material interactions on a macro scale in smaller animals, especially when it comes to dental implants and bone scaffolds, other models must be used. Large-animal models allow clinically relevant dimensions. Despite large interspecies variations, these are considered closer to humans. For bone graft materials, pigs, dogs, goats and sheep are often used [78, 84-86].

Non-human primates are the most similar animal species to humans in terms of anatomy, bone healing and genetics, but they are subject to ethical concerns and their use is highly limited by regulations and high cost [87, 88].

Dogs have traditionally been the most used larger animal model for orthopedic and dental implant research [89, 90]. They have bone composition that is similar to humans with respect to ash weight, hydroxyproline concentration, extractable proteins, bone density, and fracture stress [91]. Larger breeds can often support human-sized implants [90, 91]. However, canines have plexiform bone, which is a combination of lamellar and woven bone, as opposed to lamellar bone found in mature human bone [92, 93]. Dogs also have a significantly higher bone turnover than humans, averaging 140% yearly turnover of trabecular bone [94]

Pigs and miniature pigs are good animal models due to similar bone mineral density, anatomy, morphology and healing rate to humans [95-98]. Pigs, often used as commercial breeds, are considered undesirable for bone research due to their large growth rate and body weight. This, however, is overcome through the development of minipigs [90].

Sheep and goats are increasingly used for testing bone graft materials. Zeiter et al. reviewed sheep as the most frequently used large animal model, followed by dogs and goats when reviewing studies reporting on bone tissue engineering between 2008 and 2018 [99]. Compared to dogs and pigs, sheep have more similar dimensions of long bones to humans and easier

handling due to their calm nature and relatively lower economic cost [100]. They also have bone healing and remodeling rates similar to humans [101]. Goats are similar to sheep but are more challenging to house due to their curious and interactive nature [90]. Sheep have been suggested as a promising large animal model for periodontal tissue engineering, but currently, only limited studies are available [102].

*In vivo* research on bone augmentation in dentistry and for dental implants has until recently been concentrated around the dog and minipig models when larger animals are needed (**Figure 6**). Bone graft materials are usually intended for regenerating "critical-sized defects". Defining a critical-sized defect, which represents the smallest intraosseous wound in a particular bone and animal species that will not heal spontaneously during the animal's lifetime [103], is a challenging but essential part of bone regeneration studies. This challenge arises from the healing potentials varying across different locations and is influenced by factors such as tissue environment, age, and comorbidities [104, 105]. Local factors like the number of bone walls supporting the defect and the configuration of bone regeneration are critical for determining the healing potential [106-108]. The difference between acute and chronic defects also plays a major role in the kinetics of osteogenesis in a graft procedure.

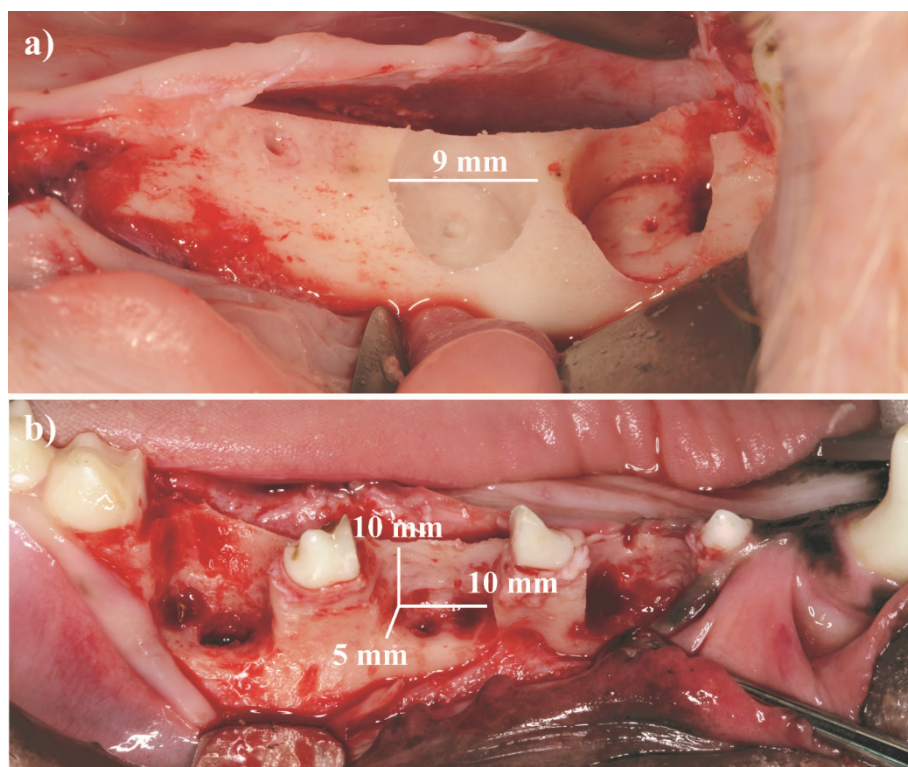


Figure 6 - Clinically relevant defect sizes with a) Minipig (paper II) and b) Beagle dog (paper II/III) models

In research, bone regeneration studies often employ different models of defects. Caton *et al.* have delineated four such models: naturally occurring defects, acute defects, chronic defects, and acute/chronic defects [87]. While naturally occurring defects offer a real-world scenario, their development is time-consuming and non-standardized. For example, naturally occurring periodontitis models take time to develop and are often seen late in the animal's life, especially if a defect of relevant size is desired. On the other hand, acute defects, created just prior to regeneration, offer cost-effectiveness and reduced experimental time. However, spontaneous healing sometimes undermines their utility, which can confound the results. The chronic and acute/chronic defect models aim to bridge this gap by simulating naturally occurring defects through induced inflammation or a surgically created defect, respectively. Advanced lesions can be created relatively quickly and resemble naturally occurring defects. Spontaneous regeneration is not observed, but the experimental time is still longer than for the acute defect model. The acute/chronic periodontal defect model is created by surgically creating a periodontal defect to the desired shape and location, and prior to flap closure, a foreign object is placed to induce a chronically inflamed state [109]. While these models are intended to evaluate regenerative treatments of periodontal and peri-implant defects, the principles can also be adapted to evaluate alveolar ridges when no teeth or implants are present. A chronic model evaluates the regeneration of the healed bone following extraction and defect creation, in contrast to an acute model where regeneration is performed on freshly prepared defects.

The nature of the defect, be it acute with exposed trabecular bone or marrow space or chronic with cortical bone, significantly impacts its interaction with graft materials. Furthermore, the preparation methods of a chronic defect site, such as perforation or decortication of the cortical bone, can influence the rate of bone formation and revascularization [63, 110]. Decortication is often performed as part of a GBR procedure, however there are limited clinical trials regarding the efficacy [111].

The animals' physiological response to surgery and pain should also be taken into consideration as the surgical stress response induces several changes in the animals, mainly activation of the sympathetic nervous system, endocrine response and immunologic and hematologic changes. In turn, this can result in impaired wound healing and immunosuppression. Furthermore, pain can affect the food and water intake of the animal, in addition to disrupting sleep and changing behaviour. For this reason, an optimized anesthetic protocol per- and postoperative is necessary to achieve a quick recovery and bone healing [112].

Therefore, choosing a relevant pre-clinical model is crucial to evaluate the clinical efficacy of a bone graft material. A bone graft material should be tested in the most similar and appropriate experimental model before clinical testing in humans. For bone augmentation in the clinic, acute defects are extremely rare. Accordingly, the use of a chronic defect model is required to test efficacy.

Following *in vivo* research, the samples also need appropriate methods of analysis. The chosen methods should be appropriate for the harvested samples. Each method often has its pros and cons, as well as the order of methods applied. Radiography is often used to non-destructively analyze hard tissue samples, like teeth, bone and implants. Microcomputed tomography (microCT) can also provide three dimensional images without sample destruction. However, considerations have to be taken as different materials have different attenuation, and large differences may not be captured within one scan, in addition metals can pose a challenge in tissue samples. On the other hand, histology is a destructive method that requires cutting the samples into thin sections. Traditionally, when a sample can be demineralized and embedded in paraffin, sections a few micrometer thick can be obtained by microtome sectioning (**Figure 7a**). However, in samples containing metals or ceramics resulting in a discrepancy of mechanical properties that may complicate the use of microtome, other techniques have to be exploited. One possible solution is embedding the samples in a harder material, like methyl methacrylate (MMA). MMA is sufficiently strong to support the cutting and grinding of metal implants or microtome sectioning of bone and even ceramics (**Figure 7b**)[113].

## Histology

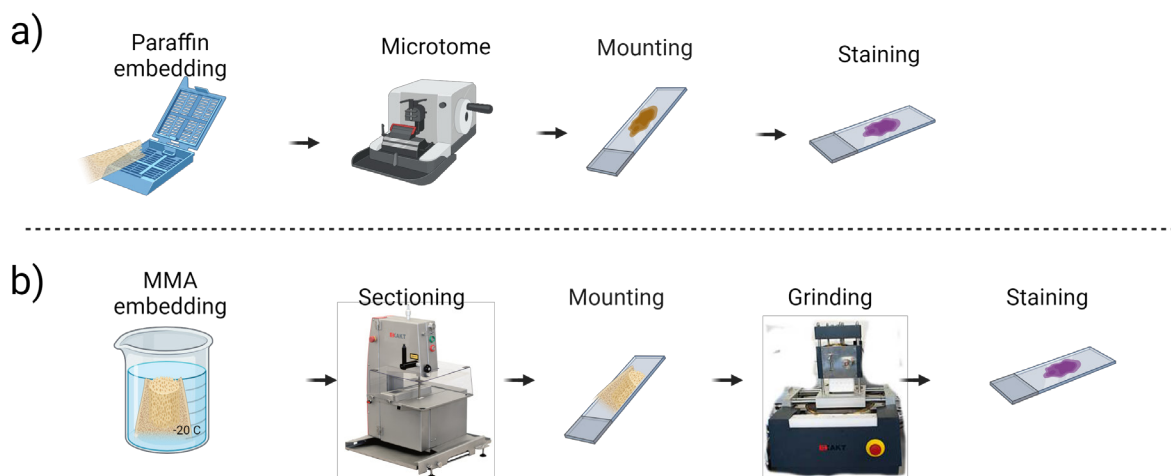
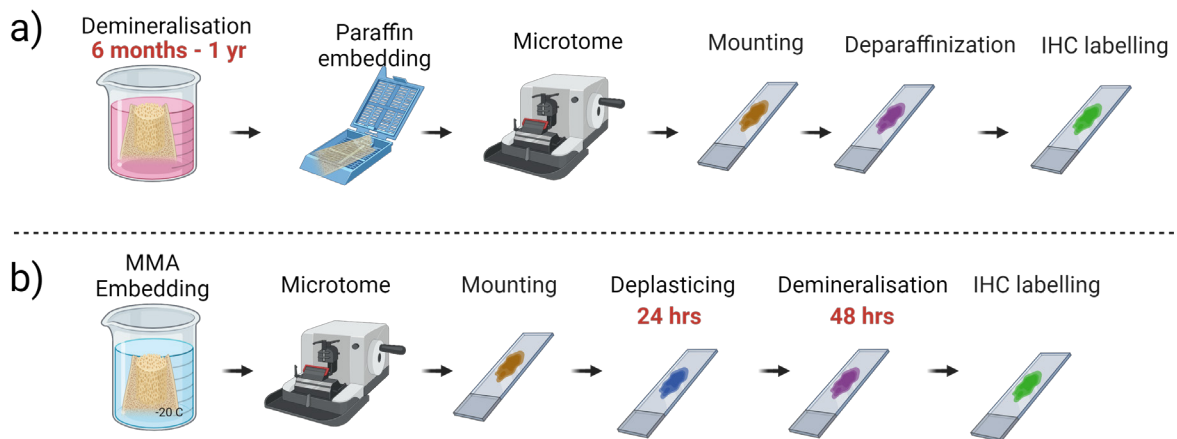


Figure 7 - Flowchart of histology processing for a) paraffin embedding and microtome sectioning and b) MMA embedding and cutting and grinding



Based on the aforementioned principles, it is also possible to identify specific proteins by using a primary antibody for the antigen of interest followed by a secondary antibody conjugated to a detectable marker, also known as immunohistochemistry (IHC). Traditionally, the tissue must be demineralized prior to paraffin embedding and staining, which can be time-consuming (**Figure 8a**). However, the MMA embedding method for histology also allows another approach for IHC. By deplastication of MMA embedded sections and demineralization of the section, demineralization is only needed for a section a few micrometres thick as opposed to a bulk tissue block [114]. The method thereby saves time, in addition to render a wider range of material properties possible as the microtome sectioning is performed on the MMA embedded material (**Figure 8b**).

## Immunohistochemistry



*Figure 8 - Flowchart of immunohistology processing for a) conventional demineralization and paraffin embedding and b) MMA embedding, deplastication and demineralization.*

### **Aim of the research**

This work focuses on *in vivo* evaluation of a porous ceramic TiO<sub>2</sub> scaffold for bone augmentation. The focus was to evaluate the scaffold in relevant experimental models. Previous research has demonstrated promising *in vitro* and *in vivo* results for the TiO<sub>2</sub> scaffold. The aim was to evaluate the TiO<sub>2</sub> scaffold in critical-size and chronic defects, which often represent the clinical challenges of bone augmentation procedures. Conventional immunohistochemical analysis methods usually require long demineralisation time of bulk samples and yields a limited number of labels, which then require manual scoring. The research also aimed to apply modern methods of IHC processing to label more markers from the samples and to use semi-automated quantification methods for analysis.

### **General hypothesis of the thesis**

The general null hypothesis (H<sub>0</sub>) of the thesis was:

Challenging bone defects will **not** show improved healing and restoration when treated with a TiO<sub>2</sub> scaffold.

The general alternate hypothesis (H<sub>A</sub>) was:

Challenging bone defects will show improved healing and restoration when treated with a TiO<sub>2</sub> scaffold.

### **General objective of the thesis**

The general objective of the thesis was to evaluate the effect of using a TiO<sub>2</sub> scaffold for bone augmentation *in vivo*.

### **Specific aims of the thesis**

- A) To evaluate bone augmentation by the use of a TiO<sub>2</sub> scaffold with simultaneous implant placement (Paper I)
- B) To evaluate bone augmentation by the use of a TiO<sub>2</sub> scaffold in chronic defects and investigate whether novel embedding methods enable more slides with IHC labeling and histology stains than conventional methods (Paper II and III).

## **Methodological considerations**

### *Research models*

The thesis comprises two *in vivo* experimental studies (papers I, II & II).

### **Considerations for *in vivo* models**

Previous studies have shown promising results when a TiO<sub>2</sub> scaffold was used in *in vitro* and *in vivo* models, being both biocompatible and allowing bone formation within its porous structures and in contact with titanium implants. The logical next step was to further evaluate the scaffold in clinically relevant models before clinical testing. As with every animal study, a main pillar is to design suitable experiments that confine to the guiding principles for animal research, the “three Rs”: replacement, reduction and refinement [115]. Since the goal of using the TiO<sub>2</sub> scaffold is to facilitate bone formation in critical-size bone defects and load-bearing areas, further *in vivo* testing on animal models was required.

A study by Verket *et al.* evaluated the TiO<sub>2</sub> scaffold in a peri-implant buccal dehiscence model in minipigs and found the percentage of bone-to-implant contact and distance from the implant shoulder to first bone contact similar to that of an autologous bone block control [78]. Paper I aimed to evaluate bone augmentation using the TiO<sub>2</sub> scaffold with simultaneous implant placement in a circumferential defect, which requires both horizontal and vertical bone formation for the implant to be fully embedded in bone. This is a clinically relevant challenge for implant placement in compromised ridges and also more challenging than horizontal regeneration alone. The minipig model was selected to test the scaffold in a critical size circumferential peri-implant defect with a buccal dehiscence. Defect configurations with a jumping distance from the bone to the implant of more than 2.25 mm with a buccal dehiscence have been shown to heal incompletely for acute defects [116]. Therefore, a gap size of 2.5 mm with removing the buccal wall was chosen to create a critical size defect (**Figure 9**). From previous experience, the minipig model also met the requirement of sufficiently wide alveolar ridges for implant placement and surgical defect creation. Another consideration was the ethical aspects of different animal models. The guiding principles of the three Rs are ubiquitous to all animal research, irrespective of species, but there are undoubtedly differences among public opinions. The European Union reports on non-humane primates and companion animals, cats and dogs, as species of particular public concern [80].

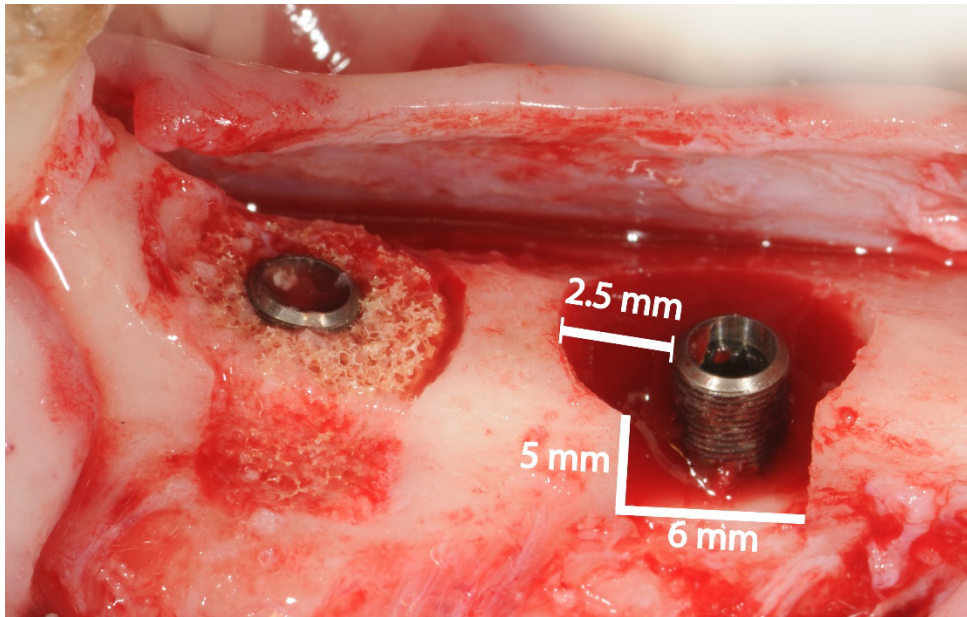


*Figure 9 - Critical size defect of paper I with buccal dehiscence*

Paper II and III evaluated the TiO<sub>2</sub> scaffold in chronic non-contained alveolar defects in dogs. The ceramic TiO<sub>2</sub> scaffolds have been tested in both small and large animal models, but never in dogs. Like minipigs, Beagle dogs also benefit from being of a clinically relevant size for the present model. In addition, dogs also have similar bone structure, composition, metabolism and mechanical properties [90, 91]. While both minipig and dog models could be considered for this defect model, Beagle dogs have been used in similar models [84, 117], and a proven model was considered a major benefit. Despite a study on Beagle dogs showing significant variations in bone formation and resorption within and between dogs, this model has been relevant for bone augmentation of defect dimensions seen clinically [94, 118]. Also, the mechanical properties of dog bone being closer to humans than pigs were considered a benefit when the augmentation of non-contained defects was analyzed. When placing a brittle block graft material on the cortical bone wall, forces exerted on the scaffold will consequently be transferred to the bone, and the interface between the recipient site and graft material should reflect the clinical situation.

### **Experimental designs**

Critical size defects were used for both experimental models (paper I and paper II/III). Otherwise, the models differed considerably. In paper II/III, defects were created and left to heal before the bone augmentation procedure, which was consequently performed in healed,

chronic defects and, therefore a more clinically relevant model. In paper I, augmentation was performed immediately following the preparation of the defect as an acute model. The chronic defect model has the benefit resembling the clinical situation closer, as acute defects are rarely present except for extraction sockets or following traumas. It is considered far more challenging to undertake regenerative procedures when the cortical bone border is denser and less vascularized than exposed trabecular bone and marrow spaces. To compensate for the challenging conditions, the cortical wall was perforated to enhance the regenerative potential [119, 120]. A major drawback of the chronic models was the defect shapes' heterogeneity. Even though all defects were initially made to the exact specification, healing occurred at different rates, both within and between individual animals. This made it challenging to define the baseline for the augmentation procedures. Another consideration was whether the defects were in a state of homeostasis or still undergoing healing or remodeling at the time of augmentation. This is in contrast to paper I, where the defects created just before regeneration were all prepared to identical dimensions. Although of critical size, the defect preparation in the alveolar bone created by a trephine bur resulted in a highly vascularized recipient bed for augmentation. As surgically created defects show great potential for regeneration [121, 122], this model has limited translation to clinical situations.

Another difference between the two models was the implant placement. Both models mimic regenerative bone formation procedures to allow implant placement. In paper I, augmentation was performed simultaneously with implant placement, whereas in papers II and III a staged approach was simulated, performing only bone augmentation. Since both approaches were considered relevant [35], the experimental model was based on previously published designs. In papers II and III a membrane was used to cover the TiO<sub>2</sub> scaffold. A resorbable collagen membrane was used, being the predominant choice of membrane for GBR procedures, and also since a graft material was used [67, 123]. In addition to creating a cell occlusive layer, a membrane provides mechanical support. Fixation of the membrane with metal tacks increased the stability of the TiO<sub>2</sub> scaffold and the particulated deproteinized bovine bone mineral (DBBM) [62, 124]. While GBR with a membrane is considered a predictable intervention [125, 126], there is a debate about whether membranes provide additional benefits [127-129]. For immediate implant placement and simultaneous grafting of peri-implant defects, studies have demonstrated similar or better bone formation results without using a membrane [130, 131]. Therefore, it was opted not to use a membrane in paper I. While it is questionable whether a membrane offers any clinical advantages, collagen membranes are commonly placed when

autogenous and allogeneic bone rings are used in clinical studies [132]. A membrane may provide additional stability and protection of the TiO<sub>2</sub> scaffold, possibly limit the observed scaffold fractures, and exclude soft tissue ingrowth into the grafted area.

In paper I, the mandibular premolars were extracted 4 weeks prior to implant placement. At the time of implantation, both sides of the mandible were treated during the same surgery and left to heal for 12 weeks before evaluation. Treatment allocation was assigned by a split-mouth design, where TiO<sub>2</sub> and empty control sites alternated between anterior and posterior locations for each side. By evaluating one time point only, limited information could be obtained about the dynamics of the regeneration process. For example, it was impossible to evaluate if the limit of bone formation was reached or whether regeneration was still ongoing. Paper II and III used a different split-mouth model, which enabled two healing times of 4 weeks and 12 weeks following regeneration (**Figure 10**). With this model, it was possible to evaluate bone formation at two-time points and gain insight into regeneration dynamics. However, it may be argued that an even longer observation time could be warranted for both studies as a healing period of six to ten months can be applied in humans [41], but it must be taken into consideration that the bone metabolism of animals is not directly translatable to humans. While the split-mouth model removes the intra-individual variability [133], it also halves the number of samples in each test group in paper II/III, thus reducing the statistical power of the test model.

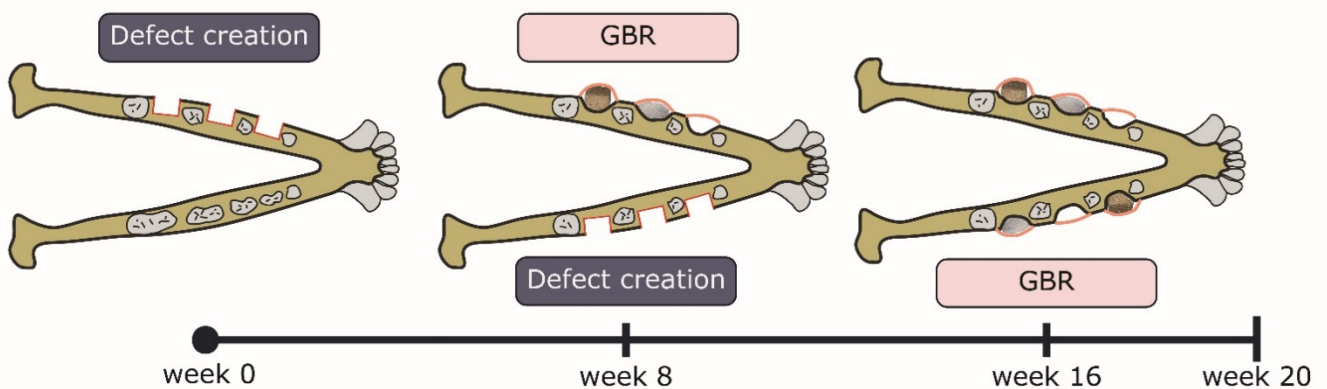


*Figure 10 - Flowchart of the split mouth experimental model of paper II/III*

## ***In vivo* analytical methods**

### Microcomputed tomography

Microcomputed tomography provides three-dimensional images, which is helpful for the evaluation of bone regeneration, both quantitatively and qualitatively (**Figure 11**). As a non-destructive method, microCT can be used in addition to other irreversible and destructive methods, like histology. In paper I, microCT was used to assess defect bone fill within a volume of interest (VOI), whereas in paper II, two-dimensional microCT sections of each defect were analyzed. In papers I and II, a scanning resolution of 7  $\mu\text{m}$  and 10  $\mu\text{m}$  was used, respectively. The chosen resolution resulted in high-resolution images where graft materials were readily distinguishable from bone and soft tissues. A higher resolution would have limited the scan volume, with the risk of not including the full VOI and yielding larger data files without providing additional helpful information. The chronic defect model used in paper II resulted in a different healing pattern for each defect. Since it was not possible to differentiate between old and new bone from the microCT images and no landmarks could be used to define the border of the original defect apart from the position of the graft materials, no accurate baseline concerning the extent of lateral bone formation could be determined for the microCT analyses. In contrast, the defects in paper I were standardized at the time of grafting and the implants served as a reference point. Therefore, in paper II the measurements were performed on several two-dimensional cross-sections within the grafted area for each defect. While not utilizing the microCT's capability of volumetric analysis in paper II, the three-dimensional images could still be used for precise alignment of the VOIs and measurements on images with a high resolution in a large number of sections per defect site.

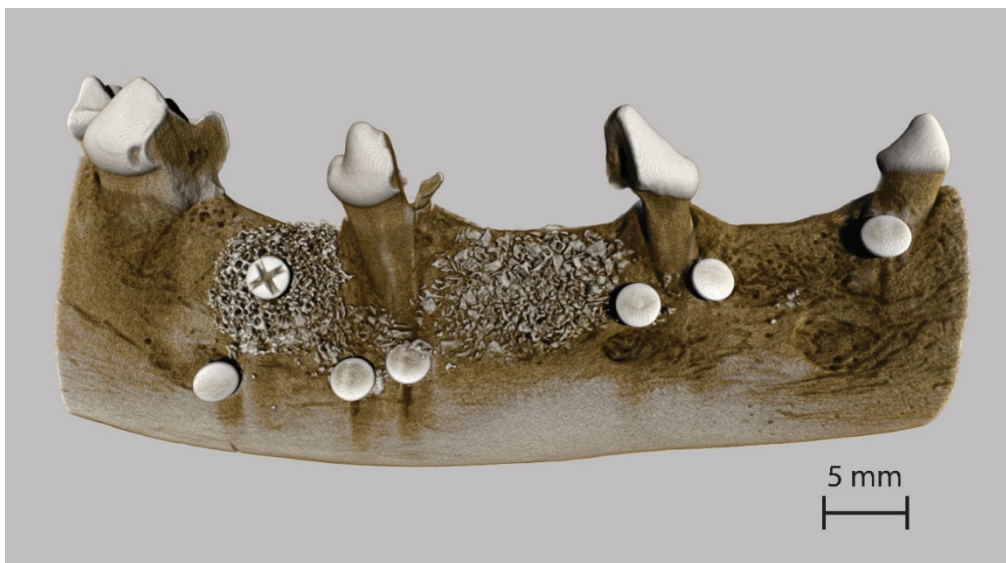


*Figure 11 - 3D reconstruction of microCT scan.*

A challenge with using microCT to evaluate bone formation adjacent to metal implants is the scattering. Since titanium absorbs X-rays much stronger than bone, the scattering during a microCT scan often causes a halation artifact called “partial volume effects” around the implant [134]. In paper I, a VOI slightly smaller than the TiO<sub>2</sub> scaffold and the circumferential defect was chosen to avoid possible artefacts at the interfaces (**Figure 12**). Copper and an aluminium filters were also used to reduce beam hardening. As the method aimed to evaluate the percentage of defect fill within the grafted area, the small interfacial area towards bone and implant was considered insignificant for the total values. This could instead be more accurately assessed by histology. In paper II, an aluminum filter was used during scanning in combination with beam hardening reduction in software reconstruction, which was set to 40%. Titanium fixation screws were used to secure the TiO<sub>2</sub> blocks to the bone and titanium tacks secured the membranes at the buccal corners. The titanium screws were placed at the center of the block and due to scattering from the screws, 0.5 mm on each side of the screws was excluded from the microCT analysis. An assumption was made that bone formation would arise by osteoconduction from the parent bone into the scaffold, so-called contact osteogenesis [135], and therefore bone formation would progress in bucco-lingual direction, thus the mesio-distal location of the measured sections would not be affected. To ensure only bone and scaffold material was included in the VOI, the threshold of the binarized images in paper I was individually adjusted for each sample. When the thresholding was performed manually and each scan was adjusted individually, a subjective source of error was also introduced.

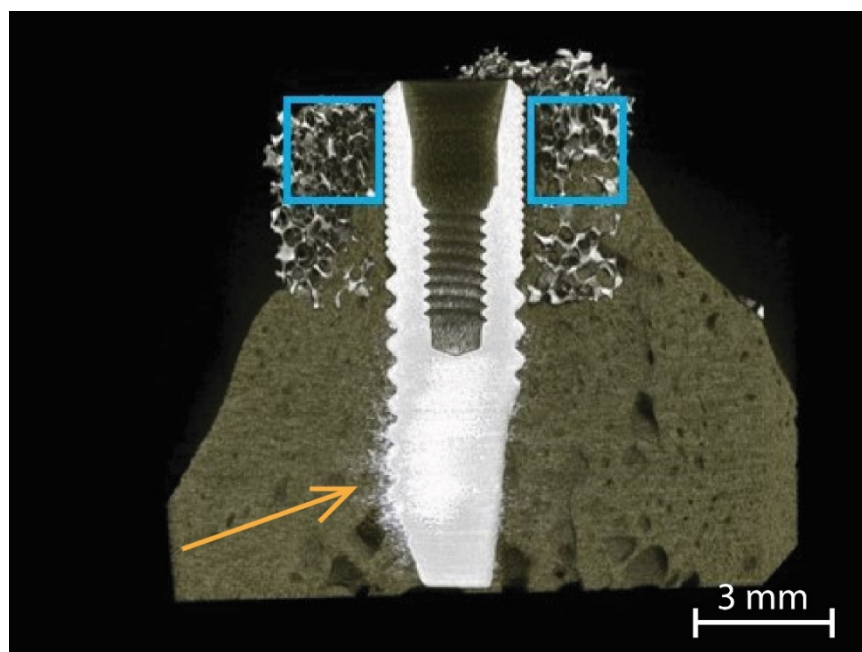


*Figure 12 - Scattering seen at the interface between bone and implant in paper II. Cross section of the VOI is marked in blue. Yellow arrow marking area with scattering.*



## Histology and histomorphometry

Through staining, microscopic study of cells and tissues provides images of structures not visible to the naked eye. Images obtained from histology reveal invaluable details for the qualitative evaluation of bone augmentation. Details of soft tissue structures and cells can be identified by histology, which may not readily be distinguished by microCT. In contrast to the non-destructive microCT, histology requires thin sectioning of the samples for microscope evaluation. In order to process and section tissue blocks, fixation and embedding are usually needed to preserve the biological tissue from degradation and provide mechanical stability. Paraffin is the most widely used embedding material. However, paraffin would not provide sufficient support for cutting the samples when handling materials with widely different mechanical properties like bone, soft tissues, metal implants and brittle ceramics. Therefore, the samples in paper I, II and III were embedded in MMA.

Paper I and II used the cutting and grinding technique [113, 136], thus allowing sectioning of titanium implants in paper I, and both TiO<sub>2</sub> scaffold and fixation screws in paper II. By cutting approximately 200 µm thick sections and gently polishing to a final thickness of 50-80 µm, it was possible to preserve even the ceramic scaffold in soft tissue. Cutting and grinding technique is great when handling materials of different properties, as gradually thinning the sections by grinding and polishing preserves the structures. However, the different hardness of the tissue and graft became evident when the sections were ground thinner than 50 µm. As the tissue abraded faster than the scaffold, grinding beyond 50 µm resulted in tissue chipped- or teared-off the sample. Accordingly, most sections were ground to a final thickness of 80 µm. When cutting a 200 µm section of the sample and subsequently grinding, a large portion of the sample was lost in addition to the width lost by the cutting blade for each histology slide prepared. Therefore, this method limited the number of slides obtained per site. Also, an 80 µm section is relatively thick regarding histological interpretation. More structures will overlap and denser material may limit light transmission by the microscope. This problem was pronounced in paper II, where dense structures between the DBBM and TiO<sub>2</sub> graft materials blocked the light and inhibited identifying structures in these areas (**Figure 13**). Methods such as Fourier Transform infrared (FTIR) spectroscopy and Raman spectroscopy were considered to characterize the bone's compositions and the unknown substance seen in **Figure 13**. Vibrational spectroscopy could have identified the chemistry and structure of the bone minerals. Energy-dispersive x-ray spectroscopy (EDX) may also identify the substances in questions, however other processing methods for histology was opted for further analysis.

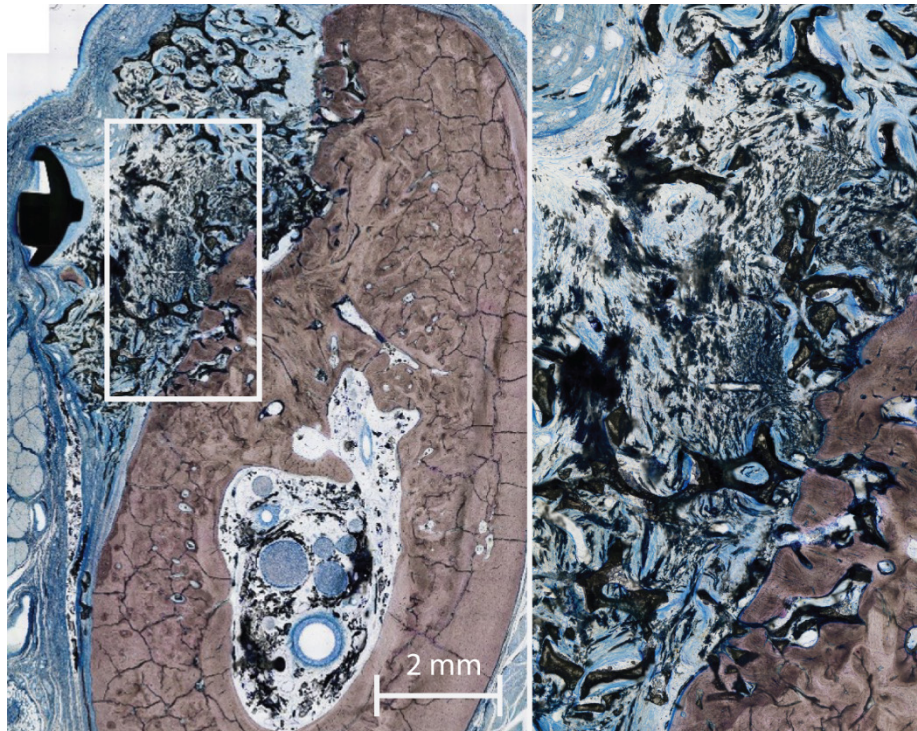


*Figure 13 - Levai-Laczko stained section following cutting and grinding slide to 80  $\mu\text{m}$ . Note the dark structures between the scaffold struts. Magnification of the white rectangle on the right.*

To circumvent the drawbacks of cutting and grinding techniques, the histological samples in paper III were prepared by microtome sectioning the MMA-embedded samples. The experimental model in paper II and III did not contain dental implants, so no metal-to-bone interface was required to be analyzed, and the fixation screws used to stabilize the  $\text{TiO}_2$  scaffolds could readily be excluded from the samples. Therefore, 5  $\mu\text{m}$  thin sections of the tissues were cut by the microtome, including the ceramic  $\text{TiO}_2$  scaffold (**Figure 14**). This method allowed for more sections of each defect, yielding more information from each animal. In paper III, this method enabled several histological stainings and immunohistochemical analyses of every defect.

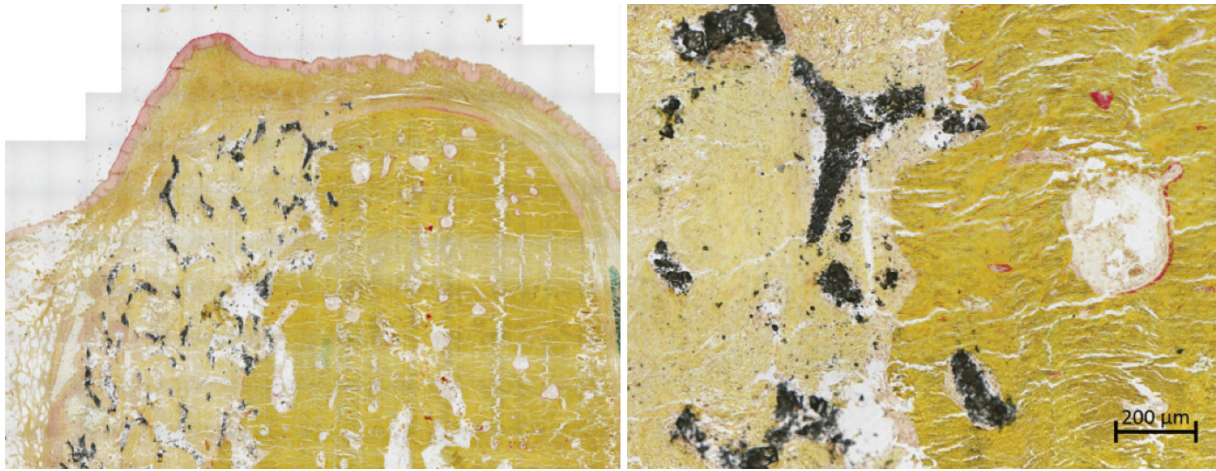


*Figure 14 - Movat Pentachrome stained section following microtome cutting slide of 5  $\mu\text{m}$*

All sections were scanned with a slide scanner (AxioScan Z1, Carl Zeiss, Germany), which provided the exact dimensions of the scanned images with the data files. This information could then be used to calibrate the images for linear and area measurements in ImageJ (National Institutes of Health, USA).

### Immunohistochemistry

In paper III, the 5  $\mu\text{m}$  sections obtained by microtome cutting also allowed for immunohistochemical staining of the samples (**Figure 15a**). By deplastifying the thin MMA section and then decalcifying, it was possible to stain specific antigens in addition to conventional histology staining. As compared to the traditional method of decalcifying bulk tissue blocks prior to paraffin embedding, decalcifying 5  $\mu\text{m}$  sections required a shorter time (**Figure 15b**). In addition, paraffin embedding would not provide sufficient mechanical strength when sectioning the ceramic  $\text{TiO}_2$  scaffold which would not be affected by the decalcifying process. Thus, paraffin embedding was not feasible for handling  $\text{TiO}_2$  scaffolds. In paper III the choice of markers for staining was based on the different proteins secreted during osteogenesis to gain insight into the dynamics of bone formation. The pure histological methods in paper II rendered no information on whether new bone formation was final at the 12 weeks end point, or if further bone formation could be expected. The aim of evaluating biomarkers at 4 and 12 weeks of healing was to explore if further bone growth could be expected.

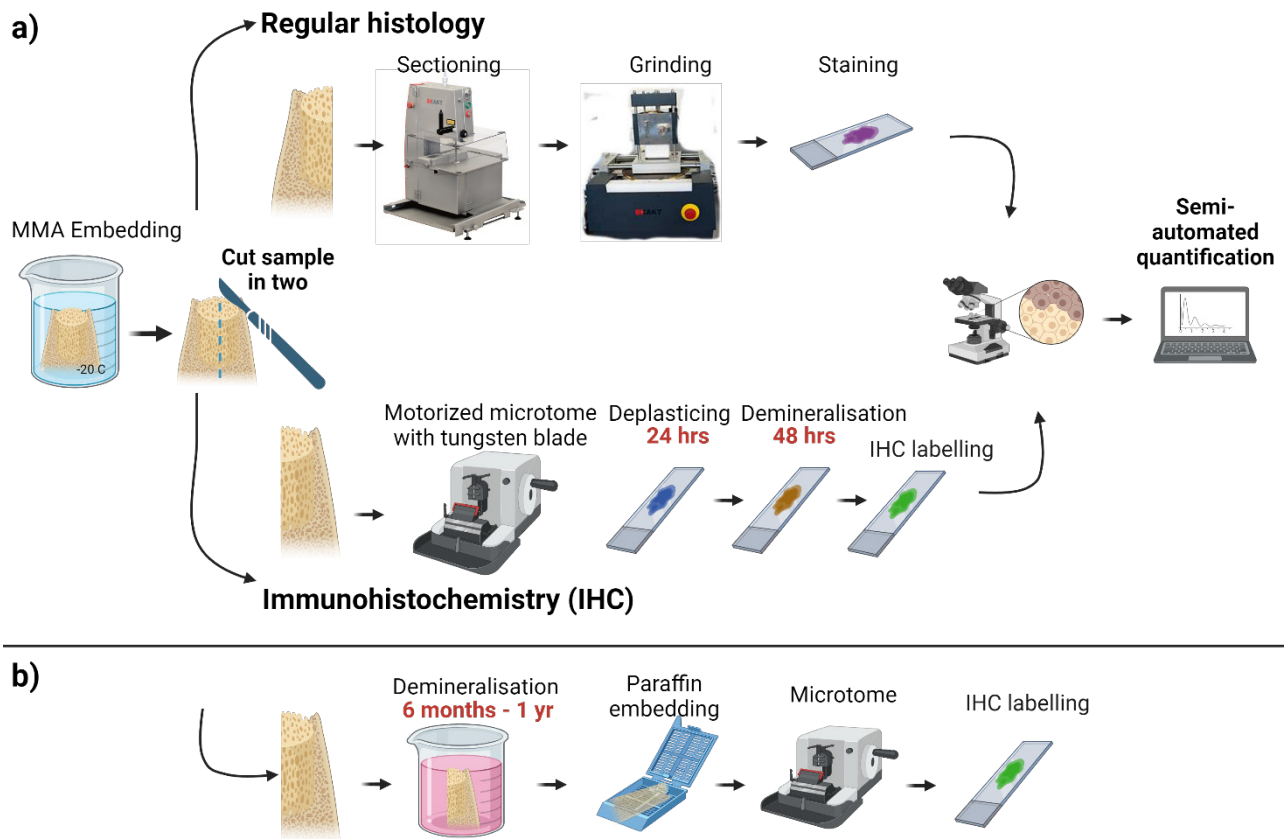


Figure 15 – a) Flowchart of slice preparation for histology in paper I and II and immunohistochemistry in paper III. b) Traditional processing for IHC labeling with paraffin embedding instead of MMA and demineralization of the bulk sample requires a significantly longer time. Created with BioRender.com

Bone remodeling has been studied with biomarkers of enzymes, proteins and by-products from bone metabolism. Several biomarkers are specific for bone formation, like alkaline phosphatase, osteocalcin, procollagen type 1 N-terminal propeptide and procollagen type 1 C-terminal propeptide. In contrast, others are markers of bone resorption, like hydroxyproline, hydroxylysine, bone sialoprotein, osteopontin (OP), tartrate-resistant acid phosphatase (TRAP), carboxy-terminal crosslinked telopeptide of type 1 collagen, amino-terminal crosslinked telopeptide of type 1 collagen and cathepsin K [137]. Biomarkers of angiogenesis are also relevant for bone formation and can be identified by markers like vascular endothelial growth factor, fibroblast growth factor, transglutaminase II and alpha-smooth muscle actin ( $\alpha$ -SMA) [138-140]. While all the markers mentioned earlier can be assessed, research on bone repair and bone graft materials has traditionally focused on a smaller selection such as RANKL OPG, TRAP, OC, OP and  $\alpha$ -SMA [141-144]. Based on relevance and previously reported techniques in the literature, the osteogenic markers osteocalcin, osteopontin, collagen type I,  $\alpha$ -SMA and TRAP were chosen as they represent different cues of bone formation and vascularization.

## Soft tissue measurements

We leveraged a range of methodologies to establish a baseline of the bone dimensions before augmentation, discussed in papers II and III. One such approach involved the determination of soft tissue dimensions via oral impressions taken before and after augmentation.

Custom-made impression trays were used for each test subject, with the resultant silicon impressions poured, scanned, and transformed into a stereolithographic (STL) model. This process was performed at three distinct stages: pre-extraction, pre-augmentation, and upon conclusion of the study. The teeth were employed as reference points when superimposing the images to facilitate comparison between images. This method for evaluating soft tissue changes and aesthetic outcomes has been substantiated in both pre-clinical and clinical studies [145-148].

Nevertheless, it is worth noting that the resultant dimensions represent an aggregate of soft tissues, hard tissues, and graft materials. Given the independent variability of these elements, the results may not provide an explicit indication of bone regeneration. Moreover, in one-stage/simultaneous implant placement and bone augmentation, the increase of the alveolar ridge width often remains the sole clinically measurable parameter.

During the linear measurements in the Beagle dog mandibles, we encountered a challenge: the vestibule needed to be positioned more consistently at the three-time points for impression. Paper II sought to measure the alveolar profile up to 6 mm apically from the alveolar crest. However, the positioning of the mucogingival border was a limiting factor, as it often appeared more coronal than anticipated. As such, these considerations should be recognized for future research.

## **Summary of the results**

### *Paper I*

Evaluation of bone augmentation using a TiO<sub>2</sub> scaffold with simultaneous implant placement was performed by microCT and histomorphometry. MicroCT demonstrated no differences in defect fill between TiO<sub>2</sub> and the negative control. However, at buccal sites, histomorphometric analysis demonstrated a higher bone fill, a higher fraction of bone-to-implant contact and a shorter distance to the bone in contact with the implant measured from the top of the implant in the negative control group as compared to the TiO<sub>2</sub> group. Three of the twelve scaffolds were partly fractured at the time of harvest. Five implants presented small mucosal perforation, four in the TiO<sub>2</sub> group and one in the sham group. The perforations were seen directly above the implant shoulders. Lingual bone resorption was seen at 7 of the sham sites and 8 of the TiO<sub>2</sub> sites.

### *Paper II*

A TiO<sub>2</sub> block was used for lateral bone augmentation of chronic, non-contained defects. Histomorphometry showed a higher fraction of new bone within the grafted area for the DBBM group than the TiO<sub>2</sub> group, although the total grafted area was also smaller. The osteoinductive properties were observed by histology. MicroCT demonstrated bone formation within the porous TiO<sub>2</sub> structures, which increased from 4 weeks to 12 weeks of healing. The greatest bone width was seen for the empty control group. The TiO<sub>2</sub> block group maintained the largest augmented volume compared to empty controls and DBBM group. Exposure of the TiO<sub>2</sub> scaffold was seen at three of the eight sites in the 4 week healing group. Fractures were also observed at the edges of the block and around the fixation screw. Migration of both TiO<sub>2</sub> particles and DBBM particles were frequently observed.

### *Paper III*

Immunohistochemical analysis was used to quantify markers for osteogenesis and angiogenesis, thus evaluating the potential for bone formation past the observed 12 weeks seen in paper II. In addition, histomorphometry was performed on Movat Pentachrome-stained and von Kossa/van Gieson-stained section and the alveolar ridge profile was evaluated by comparing stereolithographic models. The findings demonstrated an increase of  $\alpha$ -SMA and osteopontin from 4 weeks to 12 weeks of healing at the bone-scaffold interface, which may indicate a potential for bone formation at 12 weeks. Histological and histomorphometric

findings showed a collagen-rich extracellular matrix in the grafted area and soft tissue measurements showed an increased alveolar ridge profile in the areas with bone graft materials. Microtome sectioned slides were decalcified within a couple of days, substantially faster than decalcifying bulk tissue samples. Microtome sectioning also resulted in substantially more slides than cutting and grinding technique. Thus, the applied processing method of the MMA embedded samples allowed for IHC labeling with  $\alpha$ -SMA, collagen type I, osteocalcin, osteopontin and TRAP, in addition to the two histology staining.

### **Discussion of the results**

The peri-implant defect model applied in paper I aimed to replicate the clinical situation of insufficient bone volume at implant placement. It could be argued whether a two-step bone augmentation procedure would be preferred both clinically and in the experimental model. A benefit would be that bone growth could be evaluated independently of any implant interactions. Clinically, it would also allow implant placement at the bone level and not the graft material level, which for the TiO<sub>2</sub> scaffold was partly inferior following 12 weeks of healing in minipigs. However, one-step bone augmentation simultaneously with implant placement is commonly performed, both with the bone ring technique used in paper I and other augmentation techniques [35, 132, 149].

Bone growth into the porous scaffold structures was demonstrated by microCT and histology. However, a higher bone fraction, higher percentage of bone-to-implant contact and shorter distance from implant top to bone 0.5 mm lateral to the implant surface was found by histomorphometry for the empty controls as compared to the TiO<sub>2</sub> group. Both methods demonstrated bone formation within the TiO<sub>2</sub> structures but yielded different values. This was expected as different regions were evaluated. Histomorphometric analyses were performed on two-dimensional sections in bucco-lingual directions.

On the other hand, microCT analyses were performed for a three-dimensional region slightly smaller than the scaffold to avoid errors at the interfaces. Due to scattering from the titanium implants, the volume of interest had to be placed at a distance from the implant surface, and the interface between implant and graft/bone could not be evaluated. Therefore, histomorphometry and microCT complemented each other in the analyses.

Although similar defect and implant dimensions have been used in Beagle dogs, they evaluated autogenous bone ring grafts [150-153]. A new bone percentage of 31% at 3 months was reported by histomorphometry [151], similar to the defect fill of 29.8% found in paper I by

microCT. However, the group also reported no benefit of membrane application, but disruption of the soft tissue was a frequent complication independent of implant placement. Three out of twelve scaffolds fractured in paper I, so one might speculate whether a membrane would prevent scaffold fracture in addition to excluding soft tissue from the grafted area for GBR. Another plausible explanation for the fractures was during the placement of the scaffolds over the implant. A tight fit was necessary for a fixated scaffold, which again is required for bone formation. Especially given the brittle nature of the TiO<sub>2</sub> scaffold and the sharp edges of the individual struts, additional shielding could have been beneficial. Although membranes are also shown to provide healing stability [62], in the peri-implant model of paper I the graft was secured in a press-fit manner, shielded by three bone walls and an implant in the centre. Adding a membrane would also add a confounding factor to the bone regeneration processes, given the influences of a membrane on bone formation [44, 154].

The presence of new bone formation within parts the defect area for both the TiO<sub>2</sub> and the sham groups was anticipated even though the defects simulated were of critical size.

The designed defect simulated critical size defects. Following 12 weeks of healing, no sites were completely filled with new bone formation in either TiO<sub>2</sub> nor the sham group. The presence of bone in both groups was also expected as the defects were prepared at the same time as grafting and, therefore acute. Compared to the healing of extraction sockets, the radiographic bone fill can often be seen after three months in humans [13]. Compared to previously reported histomorphometric data by Catros *et al.* for circumferential defects around implants in minipigs who found a mean bone-to-implant contact of 60-71% and defect fill of 73-75%, the results in paper I demonstrated both a lower percentage of bone-to-implant contact of 14-22% and defect fill of 32% [155]. The authors used DBBM granules in similar defect dimensions and with the same healing time, but a major difference was the circumferential bone wall and the use of a collagen membrane compared to the exposed buccal wall and no membrane in paper I. It might be speculated whether the missing buccal bone wall could in part explain the lower defect fill at the buccal site of the TiO<sub>2</sub> group compared to the sham group as vascularization would have to come from the base of the defect and overcome the graft material's physical presence. On the other hand, the scaffold is supposed to stabilise the blood coagulum, and therefore facilitate healing in such circumstances. Although the focus of the design was to create a circumferential defect with a buccal dehiscence, no minimal lingual bone thickness was required at the time of grafting. The thickness of the lingual wall could contribute



to regenerative potential from the lingual side, but also resorption of the lingual side if it was too thin.

A positive control group with a bone graft material could have provided clinically relevant comparison, albeit outside the aim of the study, which was to evaluate bone healing using the TiO<sub>2</sub> block in the experimental model. An additional group would also require more animals, or smaller numbers of each group. Although membranes are usually intended to protect the graft material from the soft tissue, one might speculate if a membrane would also protect the soft tissue from the sharp struts of the scaffold. In turn, this may affect the occurrence of mucosal perforation.

On the other hand, a membrane would also lead to additional flap tension. Implant cover screws, which normally cover the implant lumen during healing, were not used. The lack of cover screws may have affected mucosal perforations. However, it may be hypothesized that the exposed implant lumen may affect the negative control group more negatively as a graft material does not support the area around the implant shoulder. Five of the 24 sites demonstrated mucosal perforation clinically; four were found in the scaffold group. Soft tissue thickness and the area above the implants were measured to investigate healing around the scaffold. No significant differences were found between the groups, which may indicate that the scaffolds were well tolerated even when suspended over the scaffold.

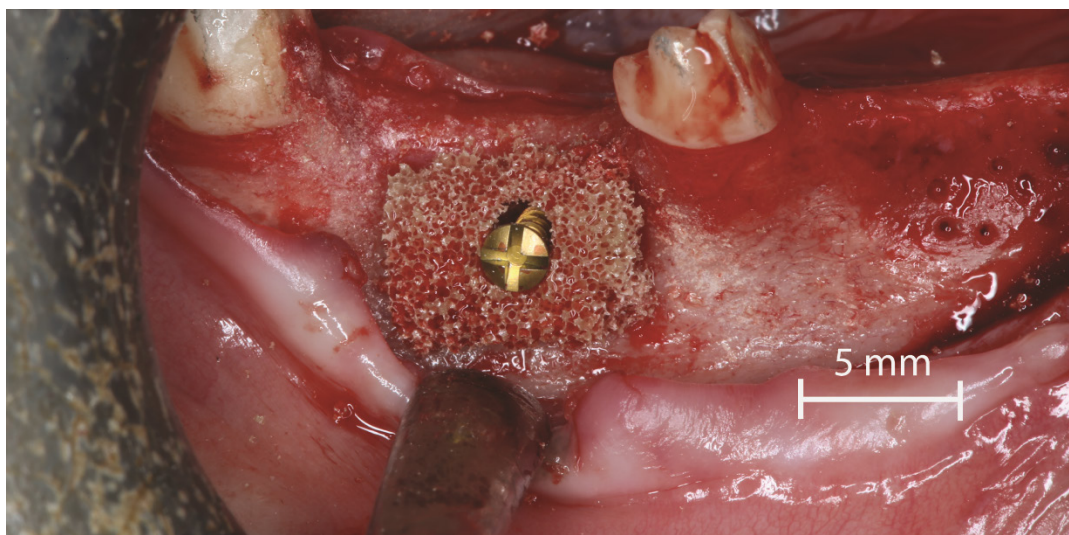


*Figure 16 - Fixation of scaffold in paper II/III. A small screw head concentrated the forces on a relatively small area of the scaffold, easily leading to fractures of the individual struts.*

For evaluation of the TiO<sub>2</sub> scaffold in a chronic defect model, paper II/III used the scaffold as an onlay graft in a GBR procedure with a resorbable collagen membrane. Also here, fractures of the scaffold were observed. Again this could have been due to the fixation method. The scaffold fracture observed in papers I and II/III might be due to the high force applied over a small area (**Figure 16**). Future studies could explore distributing this force over a larger area or using other fixation methods. A collagen membrane covered the grafted area, but despite this, fractures were seen, which raises questions about any additional stability or mechanical protection of a soft, resorbable membrane in the experimental model used.

While the weak individual ceramic struts presented a challenge for fixation of the scaffold, the same properties also made them ideal to handle and shape. A bur or scissor could easily shape the blocks to fit the defect and form a desired shape, and at the same time, be mechanically robust when even pressure is applied on the surface by, for example, a membrane or soft tissue. The handling properties may also be considered a convenience in case of future periodontitis or peri-implantitis where bone resection or implant removal is required, as the scaffold will also be removable by burs and debridement. A critical aspect not assessed by any studies is how suited the TiO<sub>2</sub> scaffold may be for a staged implant placement approach. Provided sufficient and successful lateral bone augmentation with the use of the TiO<sub>2</sub> scaffold, whether the non-resorbable ceramic material is suited for a subsequent osteotomy and implant placement remains to be researched. A previous study using oxidized porous titanium granules, rendering properties similar to the TiO<sub>2</sub>-scaffold demonstrated some potential challenges of such a procedure [156]. This needs to be assessed prior to clinical use.

It was considered an advantage of the experimental design used in paper II/III that pre-existing literature had used the same defect model [84], which allowed for historical comparison. Compared to a study by Sanz *et al.* the amount of graft material within the regions of interest was 16% after three months, similar to the 19.5% found in the DBBM group and 14.0% in the TiO<sub>2</sub> group of the present study [84]. The horizontal linear measurements for new mineralized tissue of  $0.79 \pm 0.39$  mm,  $0.35 \pm 0.24$  mm and  $0.46 \pm 0.6$  mm also coincided with results from paper II, ranging from 0.22 mm to 0.49 mm and 0.12 mm to 0.34 mm for the DBBM group and TiO<sub>2</sub> group, respectively. However, the authors reported a mineralized tissue amount of 36% after three months, considerably more than the 9.7% and 5.5% found in paper II for the DBBM group and TiO<sub>2</sub> group, respectively. The differences could be due to different processing and thresholding of the analyses, differences in total grafted area, antibiotic therapy following surgery, or differences in graft material, as Sanz *et al.* used DBBM blocks embedded in a

collagen matrix instead of DBBM granules. When compared to biphasic calcium phosphate and collagen membrane in a similar Beagle dog model, a study by Lee *et al.* found increased bone width ranging from 0.00 mm to 1.13 mm at eight weeks healing and 0.29 mm to 3.24 mm after 16 weeks [117]. The authors hypothesized that this chronic defect model resulted in slow bone formation.

In general, both experimental models in paper I and paper II yielded limited healing of the critical size defects. In paper I, the defect fill measured by microCT was only 30% for the TiO<sub>2</sub> group and 38% for sham group, whereas the histomorphometric defect fill was 25.2% and 44.1%, respectively when buccal and lingual sites were pooled. The histomorphometric defect fill after 12 week healing in paper II was 19.5% for the TiO<sub>2</sub> group and 29.2% for the DBBM group. As the grafted region was chosen as the ROI, no measurements were made for the sham group. Also, most of the material within the ROI did not constitute new bone, but the graft material was 14.0% and 19.5% respectively. The differences between the groups can also be attributed to the significantly larger grafted volume for the TiO<sub>2</sub> scaffold than DBBM granules.

Since no previous *in vivo* studies on TiO<sub>2</sub> scaffolds in relevant critical size defects have been conducted, data for sample size calculations was cumbersome. If one used the previous minipig extraction socket model [76] or implant dehiscence model [78], the sample size would be unethically high and not in accordance the principles of the three Rs. Furthermore, the outcomes assessed in these studies were not the same as evaluated in this thesis. For this reason, the statistical power for comparisons between the groups are limited. The sample sizes were therefore determined based on numbers in similar designs [117], and also takes into consideration the three R's regarding number of animals used, in addition to economical feasibility. Also, the use of two time points were chosen in order to explore the dynamics of bone formation over time.

Overall, this research demonstrates the potential of the TiO<sub>2</sub> as a scaffold. In the present form, the TiO<sub>2</sub> scaffold has not been shown to surpass DBBM xenografts or sham controls for new bone formation in the evaluated experimental models. A possible explanation could be that the non-resorbing scaffold needs a longer healing time for new bone formation. A meta-analysis by Al-Moraissi *et al.* suggested that slowly resorbing bone grafts had a slower new bone deposition than autologous bone grafts in sinus augmentation [157]. However, a longer observation time must be weighed against animal welfare and economic feasibility.

## **General conclusion**

The general null hypothesis ( $H_0$ ) was supported. Challenging bone defects did not show improved healing and restoration when treated with a  $TiO_2$  scaffold.

## **Conclusion related to specific aims**

A) The  $TiO_2$  scaffold demonstrated defect bone formation *in vivo* when placed simultaneously with implant placement in a peri-implant defect model after 12 weeks of healing time. However, the  $TiO_2$  scaffold demonstrated less bone formation as compared to empty control sites at the buccal aspect.

B) When placed in non-contained chronic defects, the  $TiO_2$  scaffold demonstrated less new bone formation as compared to particulate DBBM grafts and empty controls when evaluated by histology and microCT. The  $TiO_2$  scaffold maintained the largest augmented volume demonstrated by histology, microCT and measurements from impressions. Osteoconductive properties were demonstrated by bone formation outward from the parent bone. Immunohistochemical analysis indicated a potential for bone formation beyond 12 weeks as osteogenic markers increased from 4 to 12 weeks. The novel embedding and processing method for histology and IHC yielded more slides and more histology stains and IHC labels than conventional methods.

## **Concluding remarks**

The core of this research is the comprehensive exploration of the potential of the titanium dioxide scaffold as a bone graft substitute in challenging animal models. Despite the unique characteristics of  $TiO_2$  scaffolds, which provide specific advantages in terms of adaptability and ease of shaping, the outcomes did not indicate a significant enhancement in bone formation compared to other established bone grafts. In particular, when juxtaposed against demineralized bovine bone mineral xenografts or sham controls, the  $TiO_2$  scaffold did not exhibit superior new bone formation capabilities in the given experimental setups. While factors such as fixation methods and the intrinsic properties of the scaffold may have affected the results, it is noteworthy that the  $TiO_2$  scaffold's non-resorbing nature might necessitate a more prolonged healing duration. The porous  $TiO_2$  scaffold maintained the largest augmented volume, demonstrated by histology, microCT and soft tissue measurements. Still, it did not result in

increased new bone formation over DBBM particulate graft or empty controls in the tested models. Bone growth into the porous structure was also observed when the scaffold was placed simultaneously with an implant in an acute defect.

Whether supplementary techniques or materials to the TiO<sub>2</sub> scaffold could have affected bone formation should be investigated. In paper I, the TiO<sub>2</sub> scaffold was placed around an implant in an acute defect. On the other hand, in paper II/III, the scaffold was placed in a chronic defect, which was then covered by a collagen membrane secured with metal tacks. Both defect models in papers I and II/III did not fully heal with either regenerative materials or sham defects. The results suggest that the defect models were of critical sizes, as intended, though this needs to be confirmed by longer healing time. The IHC results indicate a further potential for bone growth at the final study time point, underlining the challenge of selecting an appropriate observation time. While a longer healing time could have resulted in more bone, it should be weighed against animal welfare and consider the three R's. This highlights the importance of relevant experimental models and methods to evaluate the dynamics of bone growth and healing bone growth and healing dynamics.

Comparative analyses, drawing parallels with prior studies, showcased variations that can be attributed to differing methodologies, graft materials, and other ancillary factors. It is critical to understand that while the TiO<sub>2</sub> scaffold exhibited osteoconductive properties and held potential for longer-term bone formation, the immediate outcomes were not congruent with the set expectations. This is further accentuated by the challenges faced in the chronic defect model, including scaffold fractures, which cast a shadow on the mechanical stability of the scaffold in certain situations. The research also showcased immunohistochemical technology advancements, facilitating more refined analyses enriching the overall data spectrum. However, the general hypothesis was upheld notwithstanding these advancements: the TiO<sub>2</sub> bone graft substitute did not meet the aspirational benchmarks for bone augmentation in compromised alveolar ridges.

In summation, while this research offers valuable insights into the potential and limitations of the TiO<sub>2</sub> scaffold, the overarching conclusion underscores the need for more nuanced explorations, alternative fixation methods, and longer observational periods.

## **Future perspective**

In recent years, the realm of bone regeneration research has witnessed significant strides, unearthing novel bone graft materials and methods to investigate their performance. This thesis has highlighted the intricate interplay between graft materials and the types of bone defects, showing a clearer path for further discovery in bone augmentation and regeneration. As we pivot towards the future of dental research, there is an evident shift towards synthetic alternatives to current xenografts. Notably, the revelations concerning the titanium dioxide scaffold form a foundational platform, pointing to new research horizons.

**Material advancements:** Although the TiO<sub>2</sub> scaffold has made its mark, there is room for refinement. The future may see composite materials or structural enhancements, bolstering mechanical integrity while ensuring adaptability. Different strategies have been proposed to introduce osteoinductive properties to the TiO<sub>2</sub> scaffolds. Effects of coatings like simvastatin, silica, calcium phosphate and peptide-containing hydrogels have been evaluated *in vitro* [70, 158, 159]. Doping of the TiO<sub>2</sub> with calcium, strontium, or magnesium has shown ion release, which could influence bone formation, and has also been evaluated [160-162]. Doping of TiO<sub>2</sub> may also increase mechanical strength, allowing the scaffold to be used in larger load-bearing, and possibly overcoming the drawback of being non-degradable.

**Refined defect models:** While our current models are invaluable, technological advancements, especially in imaging, might pave the way for other defect models, such as organoids. These would mirror human conditions more accurately, capturing the nuances of clinical situations, and replace the use of animals in research.

**Scaffold fixation methods:** Some scaffold fractures might stem from the existing fixation techniques. Exploring methods that evenly distribute pressure might mitigate these shortcomings.

**Long-term studies:** Given TiO<sub>2</sub>'s non-resorbable nature, prolonged healing phases might yield different outcomes. Hence, extensive longitudinal studies become vital in gauging the scaffold's potential to foster bone formation. The endgame remains clinical deployment. Considering diverse patient backgrounds and medical profiles, clinical studies will offer a holistic view of the TiO<sub>2</sub> scaffold in varied contexts.

**Comparative research with new technologies:** As dental research unfolds new solutions, contrasting them with the TiO<sub>2</sub> scaffold becomes crucial. Whether affirming the scaffold's

merits or spotlighting alternative graft substitutes, digital tools, like AI, could be pivotal in forecasting outcomes, refining graft properties, or simulating bone regeneration processes.

Exploring alternatives to xenografts may have begun, but the odyssey continues. The intricacies uncovered, and the inquiries indicated a promising phase teeming with innovation. Adopting a cross-disciplinary lens, tapping into parallel advancements, and consistently emphasizing patient welfare will guide the next phase in dental research. As we stand on the cusp of an exhilarating period, this thesis has underscored a truth: the future holds promise for more refined, efficient, and patient-focused bone grafting solutions. The roadmap for our journey is clear - innovate, inquire, and always prioritize the patient. The future of bone regeneration research appears replete with opportunities and challenges. Building on the foundation laid by rigorous studies like this thesis, we are poised to usher in a new era where bone grafting procedures become more predictable, efficient, and patient-centric. Embracing innovation, maintaining rigorous scientific inquiry, and keeping patient welfare at the forefront will be the guiding principles of this field of research.





## References

1. World Health Organization. Global oral health status report: towards universal health coverage for oral health by 2030: World Health Organization; 2022.
2. Bernabe E, Marcenes W, Hernandez CR, Bailey J, Abreu LG, Alipour V, et al. Global, Regional, and National Levels and Trends in Burden of Oral Conditions from 1990 to 2017: A Systematic Analysis for the Global Burden of Disease 2017 Study. *Journal of dental research*. 2020;99(4):362-73.
3. Gerritsen AE, Allen PF, Witter DJ, Bronkhorst EM, Creugers NHJ. Tooth loss and oral health-related quality of life: a systematic review and meta-analysis. *Health and Quality of Life Outcomes*. 2010;8(1):126.
4. Steele JG, Sanders AE, Slade GD, Allen PF, Lahti S, Nuttall N, et al. How do age and tooth loss affect oral health impacts and quality of life? A study comparing two national samples. *Community Dentistry and Oral Epidemiology*. 2004;32(2):107-14.
5. Bilhan H, Erdogan O, Ergin S, Celik M, Ates G, Geckili O. Complication rates and patient satisfaction with removable dentures. *jap*. 2012;4(2):109-15.
6. McCord JF, Grant AA. Identification of complete denture problems: a summary. *British Dental Journal*. 2000;189(3):128-34.
7. Quirynen M, Alsaadi G, Pauwels M, Haffajee A, Van Steenberghe D, Naert I. Microbiological and clinical outcomes and patient satisfaction for two treatment options in the edentulous lower jaw after 10 years of function. *Clinical oral implants research*. 2005;16(3):277-87.
8. Kapur KK. Veterans administration cooperative dental implant study—comparisons between fixed partial dentures supported by blade-vent implants and removable partial dentures. Part IV: Comparisons of patient satisfaction between two treatment modalities. *The Journal of Prosthetic Dentistry*. 1991;66(4):517-29.
9. Feine JS, de Grandmont P, Boudrias P, Brien N, LaMarche C, Taché R, et al. Within-subject comparisons of implant-supported mandibular prostheses: choice of prosthesis. *Journal of dental research*. 1994;73(5):1105-11.
10. Pjetursson BE, Brägger U, Lang NP, Zwahlen M. Comparison of survival and complication rates of tooth-supported fixed dental prostheses (FDPs) and implant-supported FDPs and single crowns (SCs). *Clinical oral implants research*. 2007;18 Suppl 3:97-113.
11. La Monaca G, Pranno N, Annibali S, Massimo C, Polimeni A, Patini R, et al. Survival and complication rates of tooth-implant versus freestanding implant supporting fixed partial prosthesis: a systematic review and meta-analysis. *J Prosthodont Res*. 2021;65(1):1-10.
12. Cosyn J, Raes S, De Meyer S, Raes F, Buyl R, Coomans D, et al. An analysis of the decision-making process for single implant treatment in general practice. *J Clin Periodontol*. 2012;39(2):166-72.
13. Schropp L, Wenzel A, Kostopoulos L, Karring T. Bone healing and soft tissue contour changes following single-tooth extraction: a clinical and radiographic 12-month prospective study. *The International journal of periodontics & restorative dentistry*. 2003;23(4):313-23.
14. Clarke B. Normal bone anatomy and physiology. *Clin J Am Soc Nephrol*. 2008;3 Suppl 3(Suppl 3):S131-9.
15. Heaney RP, Recker RR, Saville PD. Menopausal changes in bone remodeling. *J Lab Clin Med*. 1978;92(6):964-70.
16. Salhotra A, Shah HN, Levi B, Longaker MT. Mechanisms of bone development and repair. *Nature Reviews Molecular Cell Biology*. 2020;21(11):696-711.
17. Marsell R, Einhorn TA. The biology of fracture healing. *Injury*. 2011;42(6):551-5.
18. Ko FC, Sumner DR. How faithfully does intramembranous bone regeneration recapitulate embryonic skeletal development? *Developmental Dynamics*. 2021;250(3):377-92.
19. McAllister BS, Haghghat K. Bone augmentation techniques. *J Periodontol*. 2007;78(3):377-96.
20. Percival CJ, Richtsmeier JT. Angiogenesis and intramembranous osteogenesis. *Developmental Dynamics*. 2013;242(8):909-22.
21. Eghbali-Fatourechi GZ, Lamsam J, Fraser D, Nagel D, Riggs BL, Khosla S. Circulating Osteoblast-Lineage Cells in Humans. *New England Journal of Medicine*. 2005;352(19):1959-66.

22. Nakashima T, Hayashi M, Fukunaga T, Kurata K, Oh-hora M, Feng JQ, et al. Evidence for osteocyte regulation of bone homeostasis through RANKL expression. *Nature Medicine*. 2011;17(10):1231-4.
23. Silvestrini G, Ballanti P, Patacchioli F, Leopizzi M, Gualtieri N, Monnazzi P, et al. Detection of osteoprotegerin (OPG) and its ligand (RANKL) mRNA and protein in femur and tibia of the rat. *Journal of Molecular Histology*. 2005;36(1):59-67.
24. Hadjidakis DJ, Androulakis, II. Bone remodeling. *Ann N Y Acad Sci*. 2006;1092:385-96.
25. Weinreb M, Shinar D, Rodan GA. Different pattern of alkaline phosphatase, osteopontin, and osteocalcin expression in developing rat bone visualized by in situ hybridization. *Journal of Bone and Mineral Research*. 1990;5(8):831-42.
26. Stein GS, Lian JB. Molecular mechanisms mediating proliferation/differentiation interrelationships during progressive development of the osteoblast phenotype. *Endocr Rev*. 1993;14(4):424-42.
27. Stein GS, Lian JB, Stein JL, Van Wijnen AJ, Montecino M. Transcriptional control of osteoblast growth and differentiation. *Physiol Rev*. 1996;76(2):593-629.
28. Jepsen S, Schwarz F, Cordaro L, Derks J, Hämmerle CHF, Heitz-Mayfield LJ, et al. Regeneration of alveolar ridge defects. Consensus report of group 4 of the 15th European Workshop on Periodontology on Bone Regeneration. *Journal of Clinical Periodontology*. 2019;46(S21):277-86.
29. Thoma DS, Bienz SP, Figuero E, Jung RE, Sanz-Martín I. Efficacy of lateral bone augmentation performed simultaneously with dental implant placement: A systematic review and meta-analysis. *Journal of Clinical Periodontology*. 2019;46(S21):257-76.
30. Naenni N, Lim H-C, Papageorgiou SN, Hämmerle CHF. Efficacy of lateral bone augmentation prior to implant placement: A systematic review and meta-analysis. *Journal of Clinical Periodontology*. 2019;46(S21):287-306.
31. Tonetti MS, Jung RE, Avila-Ortiz G, Blanco J, Cosyn J, Fickl S, et al. Management of the extraction socket and timing of implant placement: Consensus report and clinical recommendations of group 3 of the XV European Workshop in Periodontology. *Journal of Clinical Periodontology*. 2019;46(S21):183-94.
32. Schwarz F, Derks J, Monje A, Wang H-L. Peri-implantitis. *Journal of Clinical Periodontology*. 2018;45(S20):S246-S66.
33. Shi J-Y, Montero E, Wu X-Y, Palombo D, Wei S-M, Sanz-Sánchez I. Bone preservation or augmentation simultaneous with or prior to dental implant placement: A systematic review of outcomes and outcome measures used in clinical trials in the last 10 years. *Clinical oral implants research*. 2023;34(S25):68-83.
34. Tonetti MS, Sanz M, Avila-Ortiz G, Berglundh T, Cairo F, Derks J, et al. Relevant domains, core outcome sets and measurements for implant dentistry clinical trials: The Implant Dentistry Core Outcome Set and Measurement (ID-COSM) international consensus report. *Clinical oral implants research*. 2023;34(S25):4-21.
35. Esposito M, Grusovin MG, Felice P, Karatzopoulos G, Worthington HV, Coulthard P. Interventions for replacing missing teeth: horizontal and vertical bone augmentation techniques for dental implant treatment. *Cochrane Database of Systematic Reviews*. 2009(4).
36. Schettler D. Sandwich technic with cartilage transplant for raising the alveolar process in the lower jaw. *Fortschr Kiefer Gesichtschir*. 1976;20:61-3.
37. Bianchi A, Felice P, Lizio G, Marchetti C. Alveolar distraction osteogenesis versus inlay bone grafting in posterior mandibular atrophy: a prospective study. *Oral Surgery, Oral Medicine, Oral Pathology, Oral Radiology, and Endodontology*. 2008;105(3):282-92.
38. Hurley LA, Stinchfield FE, Bassett AL, Lyon WH. The role of soft tissues in osteogenesis. An experimental study of canine spine fusions. *J Bone Joint Surg Am*. 1959;41-a:1243-54.
39. Buser D, Dula K, Belser U, Hirt HP, Berthold H. Localized ridge augmentation using guided bone regeneration. 1. Surgical procedure in the maxilla. *The International journal of periodontics & restorative dentistry*. 1993;13(1):29-45.
40. Nyman S, Gottlow J, Karring T, Lindhe J. The regenerative potential of the periodontal ligament. An experimental study in the monkey. *J Clin Periodontol*. 1982;9(3):257-65.
41. Buser D, Brägger U, Lang NP, Nyman S. Regeneration and enlargement of jaw bone using guided tissue regeneration. *Clinical oral implants research*. 1990;1(1):22-32.

42. Calciolari E, Corbella S, Gkranias N, Viganó M, Sculean A, Donos N. Efficacy of biomaterials for lateral bone augmentation performed with guided bone regeneration. A network meta-analysis. *Periodontology* 2000.n/a(n/a).
43. Jovanovic SA, Schenk RK, Orsini M, Kenney EB. Supracrestal bone formation around dental implants: an experimental dog study. *Int J Oral Maxillofac Implants*. 1995;10(1):23-31.
44. Omar O, Elgali I, Dahlin C, Thomsen P. Barrier membranes: More than the barrier effect? *Journal of Clinical Periodontology*. 2019;46(S21):103-23.
45. Hämmerle CHF, Schmid J, Lang NP, Olah AJ. Temporal dynamics of healing in rabbit cranial defects using guided bone regeneration. *Journal of Oral and Maxillofacial Surgery*. 1995;53(2):167-74.
46. Tanaka S, Matsuzaka K, Sato D, Inoue T. Characteristics of Newly Formed Bone During Guided Bone Regeneration: Analysis of cbfa-1, Osteocalcin, and VEGF Expression. *Journal of Oral Implantology*. 2007;33(6):321-6.
47. Lima LL, Gonçalves PF, Sallum EA, Casati MZ, Nociti Jr FH. Guided tissue regeneration may modulate gene expression in periodontal intrabony defects: a human study. *Journal of Periodontal Research*. 2008;43(4):459-64.
48. Brägger U, Pasquali L, Kornman KS. Remodelling of interdental alveolar bone after periodontal flap procedures assessed by means of computer-assisted densitometric image analysis (CADIA). *Journal of Clinical Periodontology*. 1988;15(9):558-64.
49. Tal H, Kozlovsky A, Artzi Z, Nemcovsky CE, Moses O. Cross-linked and non-cross-linked collagen barrier membranes disintegrate following surgical exposure to the oral environment: a histological study in the cat. *Clinical oral implants research*. 2008;19(8):760-6.
50. Simion M, Maglione M, Iamoni F, Scarano A, Piattelli A, Salvato A. Bacterial penetration through Resolut resorbable membrane in vitro. An histological and scanning electron microscopic study. *Clinical oral implants research*. 1997;8(1):23-31.
51. Bartold PM, Gronthos S, Ivanovski S, Fisher A, Hutmacher DW. Tissue engineered periodontal products. *Journal of Periodontal Research*. 2016;51(1):1-15.
52. Amini AR, Laurencin CT, Nukavarapu SP. Bone tissue engineering: recent advances and challenges. *Crit Rev Biomed Eng*. 2012;40(5):363-408.
53. Haugen HJ, Lyngstadaas SP, Rossi F, Perale G. Bone grafts: which is the ideal biomaterial? *Journal of Clinical Periodontology*. 2019;46(S21):92-102.
54. Widmark G, Andersson B, Ivanoff CJ. Mandibular bone graft in the anterior maxilla for single-tooth implants: Presentation of a surgical method. *International Journal of Oral and Maxillofacial Surgery*. 1997;26(2):106-9.
55. Sbordone L, Toti P, Menchini-Fabris GB, Sbordone C, Piombino P, Guidetti F. Volume changes of autogenous bone grafts after alveolar ridge augmentation of atrophic maxillae and mandibles. *International Journal of Oral and Maxillofacial Surgery*. 2009;38(10):1059-65.
56. Mellonig JT, Prewett AB, Moyer MP. HIV Inactivation in a Bone Allograft. *Journal of Periodontology*. 1992;63(12):979-83.
57. Sogal A, Tofe AJ. Risk Assessment of Bovine Spongiform Encephalopathy Transmission Through Bone Graft Material Derived From Bovine Bone Used for Dental Applications. *Journal of Periodontology*. 1999;70(9):1053-63.
58. Wenz B, Oesch B, Horst M. Analysis of the risk of transmitting bovine spongiform encephalopathy through bone grafts derived from bovine bone. *Biomaterials*. 2001;22(12):1599-606.
59. Bae HW, Zhao L, Kanim LEA, Wong P, Delamarter RB, Dawson EG. Intersubject and Intra-subject Variability of Bone Morphogenetic Proteins in Commercially Available Demineralized Bone Matrix Products. *Spine*. 2006;31(12).
60. Guillaume B. Filling bone defects with  $\beta$ -TCP in maxillofacial surgery: A review. *Morphologie*. 2017;101(334):113-9.
61. Zimmermann G, Moghaddam A. Allograft bone matrix versus synthetic bone graft substitutes. *Injury*. 2011;42:S16-S21.
62. Mir-Mari J, Wui H, Jung RE, Hämmerle CHF, Benic GI. Influence of blinded wound closure on the volume stability of different GBR materials: an in vitro cone-beam computed tomographic examination. *Clinical oral implants research*. 2016;27(2):258-65.

63. de Carvalho PS, Vasconcellos LW, Pi J. Influence of bed preparation on the incorporation of autogenous bone grafts: a study in dogs. *Int J Oral Maxillofac Implants*. 2000;15(4):565-70.
64. Lin KY, Bartlett SP, Yaremchuk MJ, Fallon M, Grossman RF, Whitaker LA. The effect of rigid fixation on the survival of onlay bone grafts: an experimental study. *Plast Reconstr Surg*. 1990;86(3):449-56.
65. Giesenhausen B, Martin N, Jung O, Barbeck M. Bone augmentation and simultaneous implant placement with allogenic bone rings and analysis of its purification success. *Materials (Basel)*. 2019;12(8):1291.
66. Miller RJ, Korn RJ, Miller RJ. Indications for simultaneous implantation and bone augmentation using the allograft bone ring technique. *Int J Perio Res Dent*. 2020;40:345-52.
67. Coherent Market Insights. Bone graft, substitutes and membrane market, Global Industry Insights, Trends, Outlook, and Opportunity Analysis, 2018–2026. Coherent Market Insights; 2018.
68. Hao L, Lawrence J, Chian KS. Osteoblast cell adhesion on a laser modified zirconia based bioceramic. *Journal of Materials Science: Materials in Medicine*. 2005;16(8):719-26.
69. Hench LL. Bioceramics. *Journal of the American Ceramic Society*. 1998;81(7):1705-28.
70. Verket A, Tiainen H, Haugen HJ, Lyngstadaas SP, Nilsen O, Reseland JE. Enhanced osteoblast differentiation on scaffolds coated with TiO<sub>2</sub> compared to SiO<sub>2</sub> and CaP coatings. *Biointerphases*. 2012;7(1-4):36.
71. Sabetrasekh R, Tiainen H, Lyngstadaas SP, Reseland J, Haugen H. A Novel Ultra-porous Titanium Dioxide Ceramic with Excellent Biocompatibility. *Journal of Biomaterials Applications*. 2010;25(6):559-80.
72. Tiainen H, Lyngstadaas SP, Ellingsen JE, Haugen HJ. Ultra-porous titanium oxide scaffold with high compressive strength. *J Mater Sci Mater Med*. 2010;21(10):2783-92.
73. Tiainen H, Wiedmer D, Haugen HJ. Processing of highly porous TiO<sub>2</sub> bone scaffolds with improved compressive strength. *Journal of the European Ceramic Society*. 2013;33(1):15-24.
74. Haugen HJ, Monjo M, Rubert M, Verket A, Lyngstadaas SP, Ellingsen JE, et al. Porous ceramic titanium dioxide scaffolds promote bone formation in rabbit peri-implant cortical defect model. *Acta Biomaterialia*. 2013;9(2):5390-9.
75. Tiainen H, Verket A, Haugen HJ, Lyngstadaas SP, Wohlfahrt JC. Dimensional Ridge Preservation with a Novel Highly Porous TiO<sub>2</sub> Scaffold: An Experimental Study in Minipigs. *International Journal of Biomaterials*. 2012;2012:851264.
76. Tiainen H, Wohlfahrt JC, Verket A, Lyngstadaas SP, Haugen HJ. Bone formation in TiO<sub>2</sub> bone scaffolds in extraction sockets of minipigs. *Acta Biomaterialia*. 2012;8(6):2384-91.
77. Amler MH, Johnson PL, Salman I. Histological and histochemical investigation of human alveolar socket healing in undisturbed extraction wounds. *The Journal of the American Dental Association*. 1960;61(1):32-44.
78. Verket A, Muller B, Wohlfahrt JC, Lyngstadaas SP, Ellingsen JE, Jostein Haugen H, et al. TiO<sub>2</sub> scaffolds in peri-implant dehiscence defects: an experimental pilot study. *Clinical oral implants research*. 2016;27(10):1200-6.
79. Percie du Sert N, Hurst V, Ahluwalia A, Alam S, Avey MT, Baker M, et al. The ARRIVE guidelines 2.0: Updated guidelines for reporting animal research. *PLoS Biol*. 2020;18(7):e3000410.
80. European Commission. 2019 Report on the Statistics on the Use of Animals for Scientific Purposes in the Member States of the European Union in 2015–2017. European Commission Brussels, Belgium; 2020.
81. Chinwalla AT, Cook LL, Delehaunty KD, Fewell GA, Fulton LA, Fulton RS, et al. Initial sequencing and comparative analysis of the mouse genome. *Nature*. 2002;420(6915):520-62.
82. Mosekilde L, Danielsen CC, Knudsen UB. The effect of aging and ovariectomy on the vertebral bone mass and biomechanical properties of mature rats. *Bone*. 1993;14(1):1-6.
83. Castañeda S, Largo R, Calvo E, Rodríguez-Salvanés F, Marcos ME, Díaz-Curiel M, et al. Bone mineral measurements of subchondral and trabecular bone in healthy and osteoporotic rabbits. *Skeletal Radiol*. 2006;35(1):34-41.
84. Sanz M, Ferrantino L, Vignoletti F, de Sanctis M, Berglundh T. Guided bone regeneration of non-contained mandibular buccal bone defects using deproteinized bovine bone mineral and a

- collagen membrane: an experimental in vivo investigation. *Clinical oral implants research*. 2017;28(11):1466-76.
85. Jinno Y, Jimbo R, Lindström M, Sawase T, Lilin T, Becktor JP. Vertical Bone Augmentation Using Ring Technique with Three Different Materials in the Sheep Mandible Bone. *Int J Oral Maxillofac Implants*. 2018;33(5):1057-63.
  86. Zou D, Guo L, Lu J, Zhang X, Wei J, Liu C, et al. Engineering of bone using porous calcium phosphate cement and bone marrow stromal cells for maxillary sinus augmentation with simultaneous implant placement in goats. *Tissue Eng Part A*. 2012;18(13-14):1464-78.
  87. Caton J, Mota L, Gandini L, Laskaris B. Non-Human Primate Models for Testing the Efficacy and Safety of Periodontal Regeneration Procedures. *Journal of Periodontology*. 1994;65(12):1143-50.
  88. Pellegrini G, Seol YJ, Gruber R, Giannobile WV. Pre-clinical Models for Oral and Periodontal Reconstructive Therapies. *Journal of dental research*. 2009;88(12):1065-76.
  89. Martini L, Fini M, Giavaresi G, Giardino R. Sheep Model in Orthopedic Research: A Literature Review. *Comparative Medicine*. 2001;51(4):292-9.
  90. Pearce AI, Richards RG, Milz S, Schneider E, Pearce SG. Animal models for implant biomaterial research in bone: a review. *European cells & materials*. 2007;13:1-10.
  91. Aerssens J, Boonen S, Lowet G, Dequeker J. Interspecies Differences in Bone Composition, Density, and Quality: Potential Implications for in Vivo Bone Research\*. *Endocrinology*. 1998;139(2):663-70.
  92. Smith JW. Collagen fibre patterns in mammalian bone. *J Anat*. 1960;94(Pt 3):329-44.
  93. Liebschner MA. Biomechanical considerations of animal models used in tissue engineering of bone. *Biomaterials*. 2004;25(9):1697-714.
  94. Kimmel DB, Jee WS. A quantitative histologic study of bone turnover in young adult beagles. *Anat Rec*. 1982;203(1):31-45.
  95. Kragstrup J, Richards A, Fejerskov O. Effects of fluoride on cortical bone remodeling in the growing domestic pig. *Bone*. 1989;10(6):421-4.
  96. Mosekilde L, Kragstrup J, Richards A. Compressive strength, ash weight, and volume of vertebral trabecular bone in experimental fluorosis in pigs. *Calcified Tissue International*. 1987;40(6):318-22.
  97. Mosekilde L, Weisbrode SE, Safron JA, Stills HF, Jankowsky ML, Ebert DC, et al. Calcium-restricted ovariectomized sinclair S-1 minipigs: An animal model of osteopenia and trabecular plate perforation. *Bone*. 1993;14(3):379-82.
  98. Raab DM, Crenshaw TD, Kimmel DB, Smith EL. A histomorphometric study of cortical bone activity during increased weight-bearing exercise. *Journal of Bone and Mineral Research*. 2020;6(7):741-9.
  99. Zeiter S, Koschitzki K, Alini M, Jakob F, Rudert M, Herrmann M. Evaluation of Preclinical Models for the Testing of Bone Tissue-Engineered Constructs. *Tissue Eng Part C Methods*. 2020;26(2):107-17.
  100. Berner A, Reichert JC, Woodruff MA, Saifzadeh S, Morris AJ, Epari DR, et al. Autologous vs. allogenic mesenchymal progenitor cells for the reconstruction of critical sized segmental tibial bone defects in aged sheep. *Acta Biomaterialia*. 2013;9(8):7874-84.
  101. Petite H, Viateau V, Bensaïd W, Meunier A, de Pollak C, Bourguignon M, et al. Tissue-engineered bone regeneration. *Nature Biotechnology*. 2000;18(9):959-63.
  102. Fawzy El-Sayed KM, Dörfer CE. (\*) Animal Models for Periodontal Tissue Engineering: A Knowledge-Generating Process. *Tissue Eng Part C Methods*. 2017;23(12):900-25.
  103. Schmitz JP, Hollinger JO. The critical size defect as an experimental model for craniomandibulofacial nonunions. *Clinical orthopaedics and related research*. 1986(205):299-308.
  104. Sanders DW, Bhandari M, Guyatt G, Heels-Ansdell D, Schemitsch EH, Swiontkowski M, et al. Critical-sized defect in the tibia: is it critical? Results from the SPRINT trial. *J Orthop Trauma*. 2014;28(11):632-5.
  105. Keating JF, Simpson AH, Robinson CM. The management of fractures with bone loss. *J Bone Joint Surg Br*. 2005;87(2):142-50.
  106. Schwarz F, Sahm N, Schwarz K, Becker J. Impact of defect configuration on the clinical outcome following surgical regenerative therapy of peri-implantitis. *J Clin Periodontol*. 2010;37(5):449-55.

107. Tsitoura E, Tucker R, Suvan J, Laurell L, Cortellini P, Tonetti M. Baseline radiographic defect angle of the intrabony defect as a prognostic indicator in regenerative periodontal surgery with enamel matrix derivative. *J Clin Periodontol*. 2004;31(8):643-7.
108. Aghazadeh A, Persson RG, Renvert S. Impact of bone defect morphology on the outcome of reconstructive treatment of peri-implantitis. *Int J Implant Dent*. 2020;6(1):33.
109. Ellegaard B, Karring T, Davies R, Loe H. New Attachment After Treatment of Intrabony Defects in Monkeys. *Journal of Periodontology*. 1974;45(5P2):368-77.
110. Majzoub Z, Berengo M, Giardino R, Aldini NN, Cordioli G. Role of intramarrow penetration in osseous repair: a pilot study in the rabbit calvaria. *J Periodontol*. 1999;70(12):1501-10.
111. Tresguerres FGF, Tresguerres IF, Iglesias O, Leco I, Tamimi F, Torres J. The role of cortical perforations in allogeneic block grafting for lateral augmentation in maxilla: A randomized clinical trial. *Clinical Implant Dentistry and Related Research*. 2021;23(4):530-42.
112. Alonso-Fernández I, Haugen HJ, López-Peña M, González-Cantalapiedra A, Muñoz F. Use of 3D-printed polylactic acid/bioceramic composite scaffolds for bone tissue engineering in preclinical in vivo studies: A systematic review. *Acta Biomaterialia*. 2023;168:1-21.
113. Rohrer MD, Schubert CC. The cutting-grinding technique for histologic preparation of undecalcified bone and bone-anchored implants: Improvements in instrumentation and procedures. *Oral Surgery, Oral Medicine, Oral Pathology*. 1992;74(1):73-8.
114. Knabe C, Kraska B, Koch C, Gross U, Zreiqat H, Stiller M. A method for immunohistochemical detection of osteogenic markers in undecalcified bone sections. *Biotechnic & Histochemistry*. 2006;81(1):31-9.
115. Russell WMS, Burch RL. *The principles of humane experimental technique*: Methuen; 1959.
116. Botticelli D, Berglundh T, Lindhe J. Resolution of bone defects of varying dimension and configuration in the marginal portion of the peri-implant bone. *Journal of Clinical Periodontology*. 2004;31(4):309-17.
117. Lee J-T, Cha J-K, Kim S, Jung U-W, Thoma DS, Jung RE. Lateral onlay grafting using different combinations of soft-type synthetic block grafts and resorbable collagen membranes: An experimental in vivo study. *Clinical oral implants research*. 2020;n/a(n/a):303-14.
118. Coelho PG, Granjeiro JM, Romanos GE, Suzuki M, Silva NRF, Cardaropoli G, et al. Basic research methods and current trends of dental implant surfaces. *Journal of Biomedical Materials Research Part B: Applied Biomaterials*. 2009;88B(2):579-96.
119. Greenstein G, Greenstein B, Cavallaro J, Tarnow D. The Role of Bone Decortication in Enhancing the Results of Guided Bone Regeneration: A Literature Review. *Journal of Periodontology*. 2009;80(2):175-89.
120. Danesh-Sani SA, Tarnow D, Yip JK, Mojaver R. The influence of cortical bone perforation on guided bone regeneration in humans. *International Journal of Oral and Maxillofacial Surgery*. 2017;46(2):261-6.
121. Sun Z, Kennedy KS, Tee BC, Damron JB, Allen MJ. Establishing a Critical-Size Mandibular Defect Model in Growing Pigs: Characterization of Spontaneous Healing. *Journal of Oral and Maxillofacial Surgery*. 2014;72(9):1852-68.
122. Hanisch O, Sorensen RG, Kinoshita A, Spiekermann H, Wozney JM, Wikesjö UME. Effect of Recombinant Human Bone Morphogenetic Protein-2 in Dehiscence Defects with Non-Submerged Immediate Implants: An Experimental Study in Cynomolgus Monkeys. *Journal of Periodontology*. 2003;74(5):648-57.
123. Sanz M, Dahlin C, Apatzidou D, Artzi Z, Bozic D, Calciolari E, et al. Biomaterials and regenerative technologies used in bone regeneration in the craniomaxillofacial region: Consensus report of group 2 of the 15th European Workshop on Periodontology on Bone Regeneration. *J Clin Periodontol*. 2019;46 Suppl 21:82-91.
124. Mertens C, Braun S, Krisam J, Hoffmann J. The influence of wound closure on graft stability: An in vitro comparison of different bone grafting techniques for the treatment of one-wall horizontal bone defects. *Clin Implant Dent Relat Res*. 2019;21(2):284-91.
125. Hämmerle CH, Karring T. Guided bone regeneration at oral implant sites. *Periodontology* 2000. 1998;17(1):151-75.

126. Buser D, Dula K, Belser UC, Hirt H-P, Berthold H. Localized ridge augmentation using guided bone regeneration. II. Surgical procedure in the mandible. *International Journal of Periodontics & Restorative Dentistry*. 1995;15(1).
127. Gielkens P, Schortinghuis J, De Jong J, Paans A, Ruben J, Raghoobar G, et al. The influence of barrier membranes on autologous bone grafts. *Journal of dental research*. 2008;87(11):1048-52.
128. Gielkens P, Stegenga B. Is there evidence that barrier membranes prevent bone resorption in autologous bone grafts during the healing period? An update. *International Journal of Oral and Maxillofacial Surgery*. 2011;40(10):1050-1.
129. Regidor E, Ortiz-Vigón A, Romandini M, Dionigi C, Derks J, Sanz M. The adjunctive effect of a resorbable membrane to a xenogeneic bone replacement graft in the reconstructive surgical therapy of peri-implantitis: A randomized clinical trial. *Journal of Clinical Periodontology*. 2023;50(6):765-83.
130. Al-Hazmi BA, Al-Hamdan KS, Al-Rasheed A, Babay N, Wang H-L, Al-Hezaimi K. Efficacy of Using PDGF and Xenograft With or Without Collagen Membrane for Bone Regeneration Around Immediate Implants With Induced Dehiscence-Type Defects: A Microcomputed Tomographic Study in Dogs. *Journal of Periodontology*. 2013;84(3):371-8.
131. Chen ST, Darby IB, Reynolds EC. A prospective clinical study of non-submerged immediate implants: clinical outcomes and esthetic results. *Clinical oral implants research*. 2007;18(5):552-62.
132. Sáez-Alcaide LM, Brinkmann JC-B, Sánchez-Labrador L, Pérez-González F, Molinero-Mourelle P, López-Quiles J. Effectiveness of the bone ring technique and simultaneous implant placement for vertical ridge augmentation: a systematic review. *Int J Implant Dent*. 2020;6(1):82.
133. Lesaffre E, Philstrom B, Needleman I, Worthington H. The design and analysis of split-mouth studies: what statisticians and clinicians should know. *Stat Med*. 2009;28(28):3470-82.
134. Swain MV, Xue J. State of the Art of Micro-CT Applications in Dental Research. *International Journal of Oral Science*. 2009;1(4):177-88.
135. Rossi F, Botticelli D, Pantani F, Pereira FP, Salata LA, Lang NP. Bone healing pattern in surgically created circumferential defects around submerged implants: an experimental study in dog. *Clinical oral implants research*. 2012;23(1):41-8.
136. Donath K, Breuner G. A method for the study of undecalcified bones and teeth with attached soft tissues. The Sage-Schliff (sawing and grinding) technique. *J Oral Pathol*. 1982;11(4):318-26.
137. Kuo T-R, Chen C-H. Bone biomarker for the clinical assessment of osteoporosis: recent developments and future perspectives. *Biomarker Research*. 2017;5(1):18.
138. Skalli O, Ropraz P, Trzeciak A, Benzonana G, Gillesen D, Gabbiani G. A monoclonal antibody against alpha-smooth muscle actin: a new probe for smooth muscle differentiation. *J Cell Biol*. 1986;103(6 Pt 2):2787-96.
139. Hanahan D, Folkman J. Patterns and Emerging Mechanisms of the Angiogenic Switch during Tumorigenesis. *Cell*. 1996;86(3):353-64.
140. Haroon ZA, Hettasch JM, Lai T-S, Dewhirst MW, Greenberg CS. Tissue transglutaminase is expressed, active, and directly involved in rat dermal wound healing and angiogenesis. *The FASEB Journal*. 1999;13(13):1787-95.
141. Becker K, Drescher D, Hönscheid R, Golubovic V, Mihatovic I, Schwarz F. Biomechanical, micro-computed tomographic and immunohistochemical analysis of early osseous integration at titanium implants placed following lateral ridge augmentation using extracted tooth roots. *Clinical oral implants research*. 2017;28(3):334-40.
142. Torquato LC, Suárez EAC, Bernardo DV, Pinto ILR, Mantovani LO, Silva TIL, et al. Bone repair assessment of critical size defects in rats treated with mineralized bovine bone (Bio-Oss®) and photobiomodulation therapy: a histomorphometric and immunohistochemical study. *Lasers in Medical Science*. 2021;36(7):1515-25.
143. Ramires GAD, Helena JT, Oliveira JCSD, Faverani LP, Bassi APF. Evaluation of Guided Bone Regeneration in Critical Defects Using Bovine and Porcine Collagen Membranes: Histomorphometric and Immunohistochemical Analyses. *International Journal of Biomaterials*. 2021;2021:8828194.
144. Bai Y, Dai X, Yin Y, Wang J, Sun X, Liang W, et al. Biomimetic piezoelectric nanocomposite membranes synergistically enhance osteogenesis of deproteinized bovine bone grafts. *International Journal of Nanomedicine*. 2019;14:3015-26.

145. Di Raimondo R, Sanz-Esporrin J, Sanz-Martin I, Pla R, Luengo F, Vignoletti F, et al. Hard and soft tissue changes after guided bone regeneration using two different barrier membranes: an experimental in vivo investigation. *Clin Oral Investig*. 2021;25(4):2213-27.
146. Di Raimondo R, Sanz-Esporrin J, Plá R, Sanz-Martín I, Luengo F, Vignoletti F, et al. Alveolar crest contour changes after guided bone regeneration using different biomaterials: an experimental in vivo investigation. *Clinical Oral Investigations*. 2020;24(7):2351-61.
147. Basler T, Naenni N, Schneider D, Hämmerle CHF, Jung RE, Thoma DS. Randomized controlled clinical study assessing two membranes for guided bone regeneration of peri-implant bone defects: 3-year results. *Clinical oral implants research*. 2018;29(5):499-507.
148. Bienz SP, Jung RE, Sapata VM, Hämmerle CHF, Hüsler J, Thoma DS. Volumetric changes and peri-implant health at implant sites with or without soft tissue grafting in the esthetic zone, a retrospective case–control study with a 5-year follow-up. *Clinical oral implants research*. 2017;28(11):1459-65.
149. Gaikwad AM, Joshi AA, Padhye AM, Nadgere JB. Autogenous bone ring for vertical bone augmentation procedure with simultaneous implant placement: A systematic review of histologic and histomorphometric outcomes in animal studies. *The Journal of Prosthetic Dentistry*. 2020.
150. Nakahara K, Haga-Tsujimura M, Sawada K, Kobayashi E, Schaller B, Saulacic N. Single-staged vs. two-staged implant placement in vertically deficient alveolar ridges using bone ring technique - Part 2: implant osseointegration. *Clinical oral implants research*. 2017;28(7):e31-e8.
151. Nakahara K, Haga-Tsujimura M, Sawada K, Kobayashi E, Mottini M, Schaller B, et al. Single-staged vs. two-staged implant placement using bone ring technique in vertically deficient alveolar ridges – Part 1: histomorphometric and micro-CT analysis. *Clinical oral implants research*. 2016;27(11):1384-91.
152. Nakahara K, Haga-Tsujimura M, Igarashi K, Kobayashi E, Schaller B, Lang NP, et al. Single-staged implant placement using the bone ring technique with and without membrane placement: Micro-CT analysis in a preclinical in vivo study. *Clinical oral implants research*. 2020;31(1):29-36.
153. Haga-Tsujimura M, Nakahara K, Kobayashi E, Igarashi K, Schaller B, Saulacic N. Single-staged implant placement using bone ring technique with and without membrane placement: An experimental study in the Beagle dog. *Clinical oral implants research*. 2018;29(3):263-76.
154. Hammerle CH, Olah AJ, Schmid J, Fluckiger L, Gogolewski S, Winkler JR, et al. The biological effect of natural bone mineral on bone neoformation on the rabbit skull. *Clinical oral implants research*. 1997;8(3):198-207.
155. Catros S, Sandgren R, Pippenger BE, Fricain JC, Herber V, El Chaar E. A Novel Xenograft Bone Substitute Supports Stable Bone Formation in Circumferential Defects Around Dental Implants in Minipigs. *Int J Oral Maxillofac Implants*. 2020;35(6):1122-31.
156. Verket A, Lyngstadaas SP, Rønold HJ, Wohlfahrt JC. Osseointegration of dental implants in extraction sockets preserved with porous titanium granules – an experimental study. *Clinical oral implants research*. 2014;25(2):e100-e8.
157. Al-Moraissi EA, Alkhutari AS, Abotaleb B, Altairi NH, Del Fabbro M. Do osteoconductive bone substitutes result in similar bone regeneration for maxillary sinus augmentation when compared to osteogenic and osteoinductive bone grafts? A systematic review and frequentist network meta-analysis. *International Journal of Oral and Maxillofacial Surgery*. 2020;49(1):107-20.
158. Rubert M, Pullisaar H, Gómez-Florit M, Ramis JM, Tiainen H, Haugen HJ, et al. Effect of TiO<sub>2</sub> scaffolds coated with alginate hydrogel containing a proline-rich peptide on osteoblast growth and differentiation in vitro. *Journal of Biomedical Materials Research Part A*. 2013;101A(6):1768-77.
159. Pullisaar H, Reseland JE, Haugen HJ, Brinchmann JE, Ostrup E. Simvastatin coating of TiO<sub>2</sub> scaffold induces osteogenic differentiation of human adipose tissue-derived mesenchymal stem cells. *Biochem Biophys Res Commun*. 2014;447(1):139-44.
160. Klemm A, Gomez-Florit M, Carvalho PA, Wachendörfer M, Gomes ME, Haugen HJ, et al. Grain boundary corrosion in TiO<sub>2</sub> bone scaffolds doped with group II cations. *Journal of the European Ceramic Society*. 2019;39(4):1577-85.
161. Pors Nielsen S. The biological role of strontium. *Bone*. 2004;35(3):583-8.
162. Yoshizawa S, Brown A, Barchowsky A, Sfeir C. Magnesium ion stimulation of bone marrow stromal cells enhances osteogenic activity, simulating the effect of magnesium alloy degradation. *Acta Biomater*. 2014;10(6):2834-42.



## Errata

Page	Line	Original text	Type of correction	Corrected text
9	13	Removable prostheses is a less invasive alternative...	Cor	Removable prostheses are a less invasive alternative...
29	7	...a volume of interest (VOI) , whereas...	Cor	...a volume of interest (VOI), whereas...
26	figure legend 9	Critical size defect of paper II with buccal dehiscence	Cor	Critical size defect of paper I with buccal dehiscence
31	15	...thickness of 50-80 $\mu\text{m}$ , it...	Cor	...thickness of 50-80 $\mu\text{m}$ , it...
41	18	...not in accordance the principles of the three Rs.	Cor	...not in accordance the principles of the three Rs.
43	27		Paragraph removed	

Cor - correction







RESEARCH ARTICLE

Open Access

# Impact of simultaneous placement of implant and block bone graft substitute: an in vivo peri-implant defect model



Minh Khai Le Thieu<sup>1</sup>, Amin Homayouni<sup>1</sup>, Lena Ringsby Hæren<sup>1</sup>, Hanna Tiainen<sup>1</sup>, Anders Verket<sup>2</sup>, Jan Eirik Ellingsen<sup>3</sup>, Hans Jacob Rønold<sup>3</sup>, Johan Caspar Wohlfahrt<sup>2</sup>, Antonio Gonzalez Cantalapedra<sup>4,5</sup>, Fernando Maria Guzon Muñoz<sup>4,5</sup>, Maria Permuy Mendaña<sup>4,5</sup>, Ståle Petter Lyngstadaas<sup>1</sup> and Håvard Jostein Haugen<sup>1\*</sup>

## Abstract

**Background:** Insufficient bone volume around an implant is a common obstacle when dental implant treatment is considered. Limited vertical or horizontal bone dimensions may lead to exposed implant threads following placement or a gap between the bone and implant. This is often addressed by bone augmentation procedures prior to or at the time of implant placement. This study evaluated bone healing when a synthetic TiO<sub>2</sub> block scaffold was placed in circumferential peri-implant defects with buccal fenestrations.

**Methods:** The mandibular premolars were extracted and the alveolar bone left to heal for 4 weeks prior to implant placement in six minipigs. Two cylindrical defects were created in each hemi-mandible and were subsequent to implant placement allocated to treatment with either TiO<sub>2</sub> scaffold or sham in a split mouth design. After 12 weeks of healing time, the samples were harvested. Microcomputed tomography (MicroCT) was used to investigate defect fill and integrity of the block scaffold. Distances from implant to bone in vertical and horizontal directions, percentage of bone to implant contact and defect fill were analysed by histology.

**Results:** MicroCT analysis demonstrated no differences between the groups for defect fill. Three of twelve scaffolds were partly fractured. At the buccal sites, histomorphometric analysis demonstrated higher bone fraction, higher percentage bone to implant contact and shorter distance from implant top to bone 0.5 mm lateral to implant surface in sham group as compared to the TiO<sub>2</sub> group.

**Conclusions:** This study demonstrated less bone formation with the use of TiO<sub>2</sub> scaffold block in combination with implant placement in cylindrical defects with buccal bone fenestrations, as compared to sham sites.

**Keywords:** Bone substitute, Animal experimentation, Bone ring technique

\* Correspondence: [hj.haugen@odont.uio.no](mailto:hj.haugen@odont.uio.no)

<sup>1</sup>Department of Biomaterials, Institute of Clinical Dentistry, University of Oslo, 0317 Oslo, Norway

Full list of author information is available at the end of the article



© The Author(s). 2021 **Open Access** This article is licensed under a Creative Commons Attribution 4.0 International License, which permits use, sharing, adaptation, distribution and reproduction in any medium or format, as long as you give appropriate credit to the original author(s) and the source, provide a link to the Creative Commons licence, and indicate if changes were made. The images or other third party material in this article are included in the article's Creative Commons licence, unless indicated otherwise in a credit line to the material. If material is not included in the article's Creative Commons licence and your intended use is not permitted by statutory regulation or exceeds the permitted use, you will need to obtain permission directly from the copyright holder. To view a copy of this licence, visit <http://creativecommons.org/licenses/by/4.0/>. The Creative Commons Public Domain Dedication waiver (<http://creativecommons.org/publicdomain/zero/1.0/>) applies to the data made available in this article, unless otherwise stated in a credit line to the data.

## Background

Dental implants are commonly used to replace missing teeth. Implants were originally placed in healed alveolar ridges following physiologic bone resorption after tooth extraction [1]. With the change towards prosthetically-driven implant placement, the ideal implant position may present challenging bone architecture which may render exposure of implant threads or a gap between the alveolar bone and the implant. A peri implant gap of less than 2–2.25 mm often leads to spontaneous healing as demonstrated in several studies [2, 3]. For gaps exceeding 2 mm or exposed implant threads, the use of a graft material has been recommended, but there is a controversy as to which material is superior [4].

Autologous bone grafts are considered the gold standard for bone augmentation, but are associated with donor site morbidity and unpredictable graft resorption [5–7]. Allografts and xenografts are widely used and well documented [8], but run the risk of disease transmission from graft to host [9]. Synthetic bone graft substitutes circumvent many disadvantages with auto-, allo- and xenografts, which may lead to its increased use also reflected by recent regulatory changes by the European Union [10].

Clinical procedures combining vertical bone augmentation and implant placement are often performed in two stages. Currently, only few studies have reported on the use of block grafts in circumferential peri-implant defects in conjunction with implant placement, such as the bone ring technique [11, 12]. However the technique is scarcely reported in the literature, lacking control groups and only reporting short follow-up times [13]. Gaikwad et al. suggested that results from animal studies on autogenous bone rings were not sufficiently robust to support this technique in humans [14]. Previous studies on the bone ring technique are also widely heterogeneous with regard to graft materials, surgical protocols and peri-implant defect size and shape. As described by Botticelli et al., circumferential defects with a gap distance to the implant of up to 2.25 mm heal spontaneously, but if a concomitant buccal dehiscence was present, healing was incomplete [2].

This study evaluates a porous ceramic TiO<sub>2</sub> bone graft substitute in a peri-implant defect model with a buccal dehiscence. TiO<sub>2</sub> scaffolds have documented biocompatible properties with compressive strength similar to trabecular bone [15, 16]. The average pore size close to 400 μm, high porosity and interconnectivity gives a favourable pore architecture for osteogenesis [17–19]. Studies in minipigs have demonstrated bone ingrowth and angiogenesis within the structures of the TiO<sub>2</sub> scaffolds in extraction sockets and in peri-implant dehiscence defects [18, 19].

In a buccal dehiscence model by Botticelli et al. particulate graft materials were assessed [20]. Using a synthetic block material may be more advantageous in such a model as targeted porosity and interconnectivity can be designed, which is impossible with the use of particulate grafts. Therefore, in the present study a TiO<sub>2</sub> block scaffold was used simultaneous to implant placement for bone augmentation of 2.5 mm circumferential defects with buccal dehiscences in an experimental minipig model.

The aim of this experimental study was to evaluate the use of a TiO<sub>2</sub> block scaffold in the bone ring technique for peri-implant bone defects with buccal fenestrations, without the use of barrier membranes, to evaluate bone healing.

## Methods

Ceramic TiO<sub>2</sub> scaffolds were fabricated by polymer foam replication as described by Tiainen et al. [16]. TiO<sub>2</sub> slurry was prepared by gradually dispersing 65 g of TiO<sub>2</sub> powder (Kronos 1171, Kronos Titan GmbH, Leverkusen, Germany) cleaned with 1 M NaOH into 25 ml of sterilised H<sub>2</sub>O and stirred at 5000 rpm for 2.5 h. The slurry was adjusted to pH 1.5 during the stirring with 1 M HCl. Cylindrical polyurethane foam templates (60 ppi, Bulbren S, Eurofoam GmbH, Wiesbaden, Germany) were soaked in the slurry and squeezed to remove excess slurry. The polymer sponge was burned out before sintering at 1500 °C for 20 h. After sintering, the scaffolds were immersed with a slurry containing 40 g of powder dispersed in 25 ml of sterilised water. Excess slurry was removed by centrifugation and the second coating was sintered at 1500 °C for 20 h. The finished scaffolds were 7.0–7.5 mm in diameter and 5 mm in height. Prior to use, the scaffolds were steam sterilised at 121 °C for 20 min.

## Animals

Six female minipigs (Göttingen minipig, *Sus scrofa*, Ellegaard AS, Dalmose, Denmark) aged 27–32 months and weighing 42–51 kg were used. The animals were kept in a centre for large experimental animals at the Veterinary Teaching Hospital Rof Codina in Lugo, Spain. The animals were kept on a soft diet and subjected to oral hygiene by mechanical cleaning once every 3 weeks during the experimental study. The Regional Ethics Committee for Animal Research of the University of Santiago de Compostela approved the protocol (Ref. AE-LU-001/002/14).

All surgical procedures were performed under general anaesthesia and sterile conditions in an operating room using propofol (2 mg/kg/i.v., Propovet, Abbott Laboratories, Kent, UK) and 2.5–4% of isoflurane (Isoba-vet, Schering-Plough, Madrid Spain) for the entire period of

the surgery. Lidocaine 2% with epinephrine 1:100.000 (2% Xylocaine Dental, Dentsply, York, PA, USA) was infiltrated locally to reduce intra-operative bleeding and provide local analgesia. The animals were premedicated with acepromazine (0.05 mg/kg/i.m., Calmo Neosan, Pfizer, Madrid, Spain) and pain controlled with the administration of morphine (0.3 mg/kg/i.m., Morfina Braun 2%, B. Braun Medical, Barcelona, Spain). During anaesthesia, a veterinarian continuously monitored the animals.

### Experimental design

Mandibular premolars were extracted 4 weeks before implant placement. Mucoperiosteal flaps were bilaterally reflected and teeth carefully removed after tooth separation. Primary healing was accomplished by mattress sutures. Prophylactic administration of cefovecin sodium (8 mg/kg body weight S.C. S.I.D., Convenia®, Zoetis, Spain) was given postoperatively.

Four weeks after extraction, full thickness flaps were raised on the buccal and lingual side and the alveolar crest was levelled to create a flat surface for osteotomies. In each mandibular quadrant, two implant osteotomies were prepared. Thereafter, peri-implant defects were made with a trephine bur, 8 mm in diameter and 5 mm in height (Meisinger Bone Management® Systems, Hager & Meisinger GmbH, Neuss, Germany). The defects were placed with a minimum of 10 mm between the osteotomy centres, and at least 6 mm from neighbouring teeth. The defects were made so that the buccal portion of the defect wall was missing. Dental implants (OsseoSpeed

TX 3.0 S 11 mm, Dentsply) were placed in the centre of the defect with the coronal 5 mm of the implants exposed.

The treatment allocation was assigned by a split mouth design where sham and TiO<sub>2</sub> alternated between anterior and posterior location for every other animal. For the sites allocated to treatment with the TiO<sub>2</sub> scaffold, a cylindrical block scaffold was perforated in the centre, creating a donut-shaped scaffold to fit around the implant and shaped to fit the defect with burs or scissors. The scaffold was secured in the defect by press-fit installation before the flap was passively adapted and primary wound closure was obtained (Fig. 1). After 12 weeks of healing, the animals were euthanized using a lethal dose of sodium Pentothal (40–60 mg/kg/i.v., Dolethal, Vetoquinol, France) and the mandibles were dissected and fixed in formalin.

### Micro-computed tomography scanning

Microcomputed tomographic imaging (microCT) of the samples was performed (SkyScan 1172, Bruker microCT, Kontich, Belgium) with a resolution of 7 µm, using 100 kV and 100 µA, with 3 average images every 0.4 degrees for a 360-degree rotation with an aluminium and copper filter. The data were reconstructed using NRecon software (Bruker microCT, Kontich, Belgium) with ring artefact correction of 10%.

The defect fill volume was analysed for a volume of interest (VOI) slightly smaller than the scaffold, to avoid possible errors at the interfaces of the scaffold's outer and inner border (Fig. 2). The VOI was a cylindrical

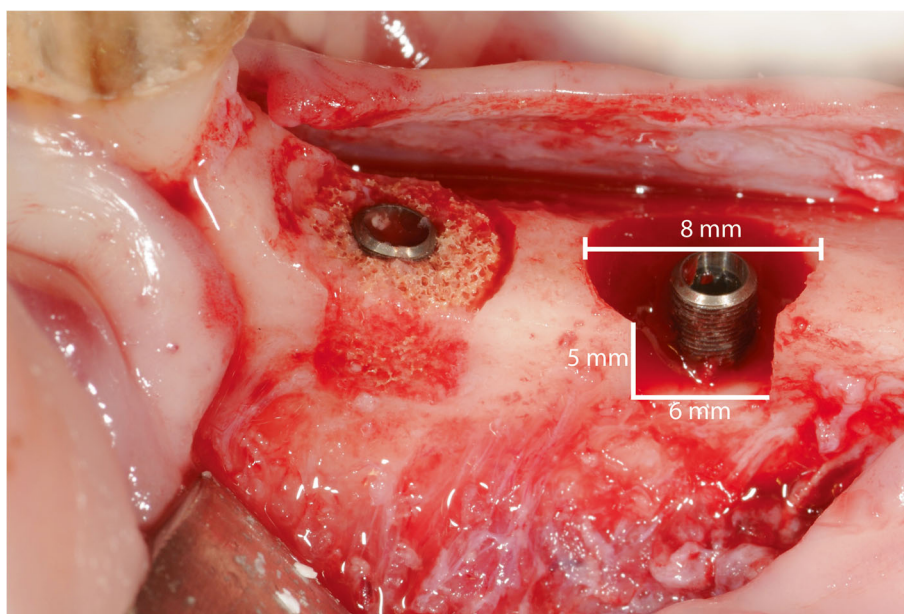


**Fig. 1** Clinical photos depicting the experimental model. Circumferential defects were created before implant placement with a block scaffold (TiO<sub>2</sub> group) and implant only (sham)

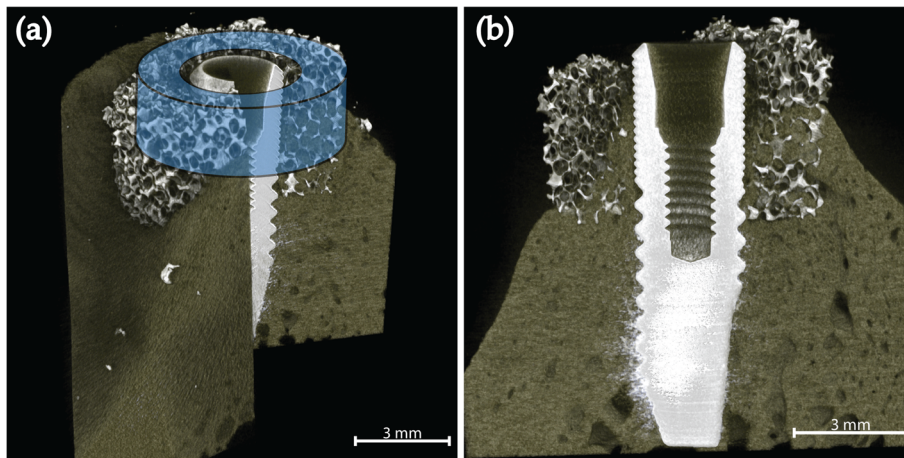


**Fig. 2** 3D reconstructions of the microCT scan (a) Illustration of circumferential area evaluated for defect fill in blue. (b) Cross section of the same sample in bucco-lingual direction (buccal left)

donut-shaped area with a height of approximately 2.3 mm (including the first ten upper threads of the implant) and a diameter of 6.0 mm concentric with the implant. Individual thresholds were set to measure the defect fill of bone and scaffold. Percentage of defect fill was analysed in CTan (Bruker microCT, Kontich, Belgium).

**Histological preparation**

The tissue blocks were dehydrated in different graded ethanol series (70-100%), and infiltrated with four different graded mixtures of ethanol and infiltrating resin, glycometacrylate (Technovit 7200<sup>®</sup> VLC, Heraeus Kulzer GMBH, Werheim, Germany). The samples were then polymerised, first under low intensity UV light for 4 h, followed by high intensity UV light for 12 h. Finally, the

samples were placed in an oven at 37 °C for 24 h to assure a complete polymerisation. Longitudinal sections in bucco-lingual direction were obtained by cutting with a band saw and mechanically micropolished (Exakt Apparatebau, Norderstedt, Germany) with silicon carbide papers until a thickness for approximately 50 µm was obtained. The slides were stained with Levaï Laczko for both histological examination and histomorphometric analysis.

All sections were observed using light microscopy and a PC-based image capture system (BX51, DP71, Olympus Corporation, Japan) and histometrically analysed. Quantitative histology was performed by a masked examiner using PC-based image analysis programs: Cell-sens 1.13 (Olympus Corporation, Japan) and Image Pro-Premier 9.0 (Media cybernetics, Bethesda, MD, USA).

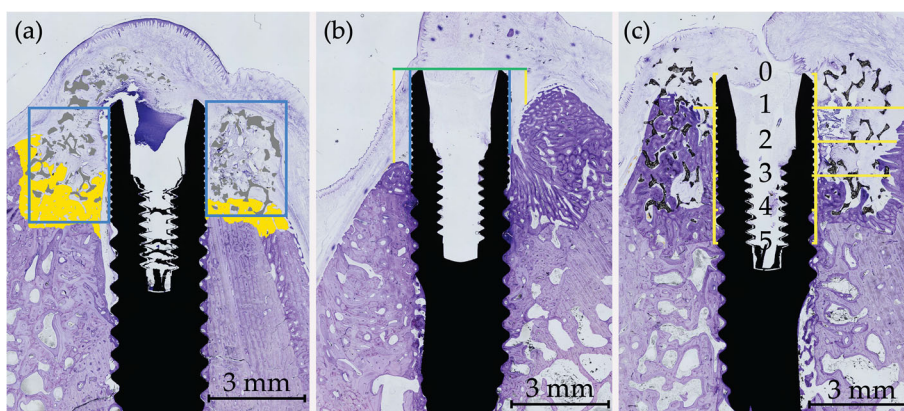


**Fig. 3** Histological samples (a) Illustration of defect analysis. Blue box depicting regions of interest in the buccal and lingual sides, yellow = bone, grey = TiO<sub>2</sub> scaffold. (b) Vertical linear measurements from the implant top (green line) to the first bone contact at the implant surface (blue line) and 0.5 mm lateral to the implant (yellow line). (c) Horizontal linear measurements from implant surface to the first bone contact. Measured from implant top and five consecutive millimetres apically. Lingual side left and buccal side right for all figures



### Histological analyses

The images were painted with a digital tablet (Cintiq, Wacom, Japan) and Photoshop CS (Adobe, USA). The region of interest was the buccal and lingual rectangles defined from the top of the implant to the bottom of the defect created and from the surface of the implant to the lateral portion of the defect. The fraction of possible bone fill within each rectangle was calculated, excluding scaffold material in the TiO<sub>2</sub> group (Fig. 3a).

Vertical linear measurements were made for two distances: 1) Implant shoulder to the first bone contact (first bone-to-implant contact, FBIC) and 2) Implant shoulder to the first bone contact 500 μm lateral to the implant (FBIC500) (Fig. 3b). Percentage of bone-to-implant contact (%BIC) was calculated for the first 5 mm from the implant top.

Horizontal bone growth within the defect was measured from the implant surface to the first bone contact in the buccal and lingual direction. Measurements were done in millimetre increments from the top of the implant to defect bottom 5 mm apically. The defect dimensions were set as reference points, hence when no bone was seen the value was set at a maximum 3 mm (Fig. 3c).

All measurements were done for both the buccal and lingual side of the implants using ImageJ.

(ImageJ 1.52a, National Institutes of Health, USA).

Linear measurements of soft tissue dimensions were performed for the shortest distance from implant shoulder to the oral cavity using ImageJ (Fig. 4a). The area of soft tissue above the implants was measured in

Photoshop CS6 (Fig. 4b). One sample was excluded from the analysis due to missing soft tissue following the histological preparation.

### Statistics

Comparison across the two groups was performed using a paired t-test between contralaterals when normality was assumed and Wilcoxon Signed Rank Test when normality test failed. All statistical analyses were performed using SigmaPlot 14 (Systat Software, San Jose, CA, USA). Statistical significance was set at the 0.05 level.

### Results

Post-operative healing following surgery was uneventful. Five implants presented small mucosal perforations to the oral cavity at the time of harvest (Fig. 3c), four in the TiO<sub>2</sub> scaffold sites and one in the sham sites.

### MicroCT

The apical portion of the implants placed in sound bone showed osseointegration at all sites, but the defect areas showed large variation of bone fill. The largest variations were seen in the TiO<sub>2</sub> scaffold sites. One site was missing most of the scaffold and was subsequently excluded from further microCT analysis. Two sites demonstrated a fracture of approximately one fourth of the scaffold, one of which was missing while the other remained in the defect. The remaining nine scaffolds maintained their structural integrity. All but the excluded scaffold demonstrated bone growth within the porous scaffold structures in various degrees. As for the sham sites,

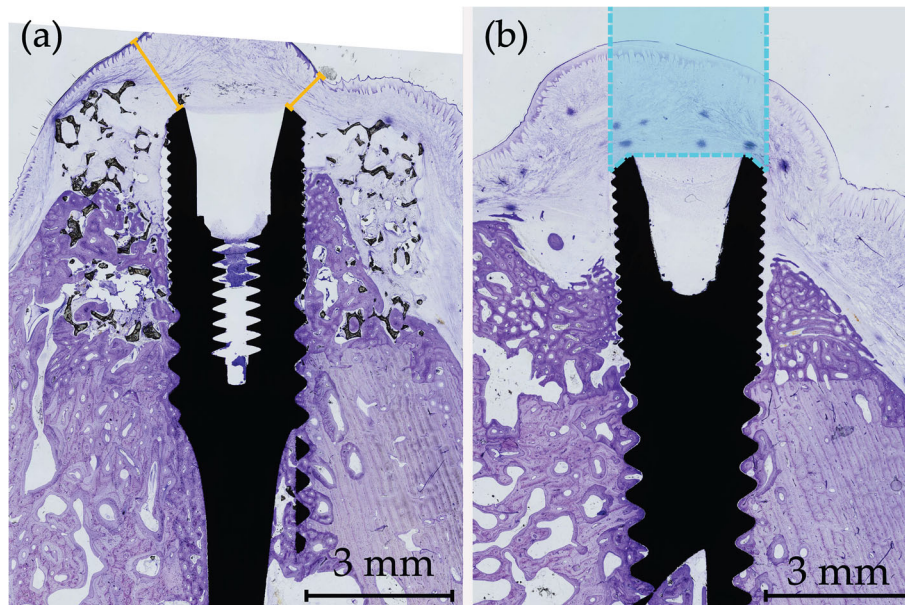


**Fig. 4** Soft tissue measurements in histological samples. Lingual side left and buccal side right for both figures. **a** Shortest distance from implant shoulder to oral cavity marked in yellow. **b** Area of soft tissue above the implant measured within the dotted blue lines

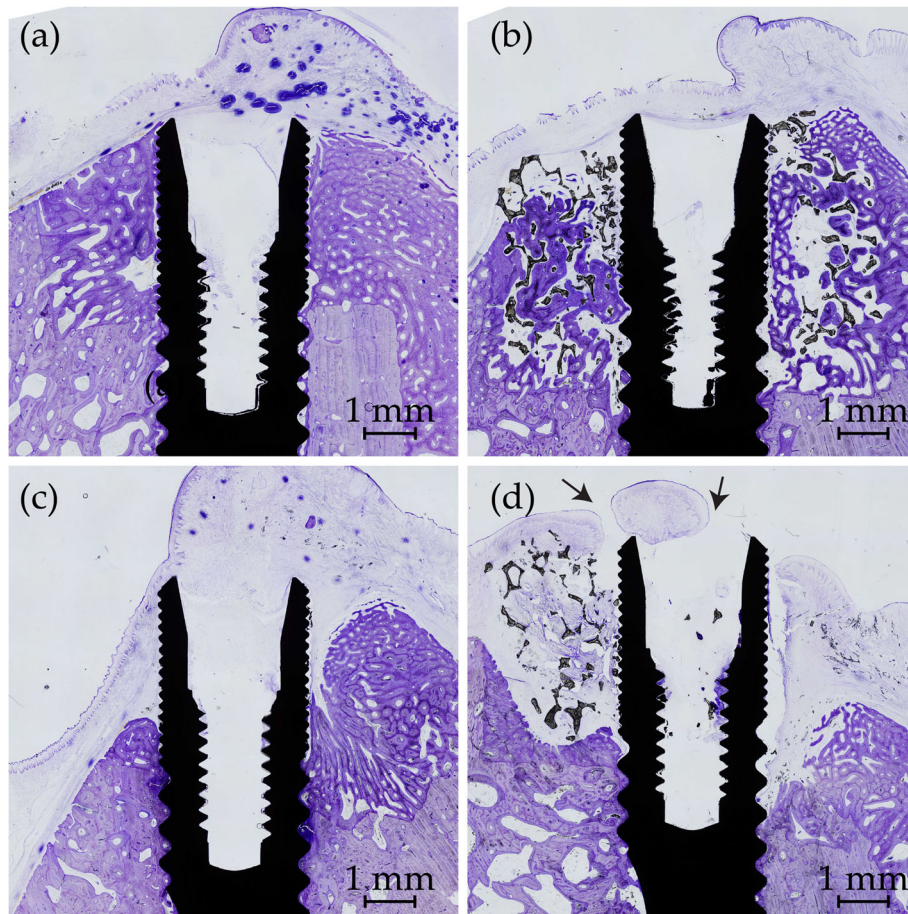


**Fig. 5** Histological samples of best (a-b) and worst (c-d) samples from sham (a) and (c) and TiO<sub>2</sub> (b) and (d). New bone stained deep purple and irregular in shape. Lingual side left and buccal side right for all figures. **a** Complete healing of the defect. **b** Extensive bone growth within the porous scaffold. **c** Resorption of the lingual bone wall and epithelium in contact with the implant. **d** Missing scaffold at the buccal side and no bone contact between bone and scaffold lingually. Arrows: mucosal perforations also visible on both sides

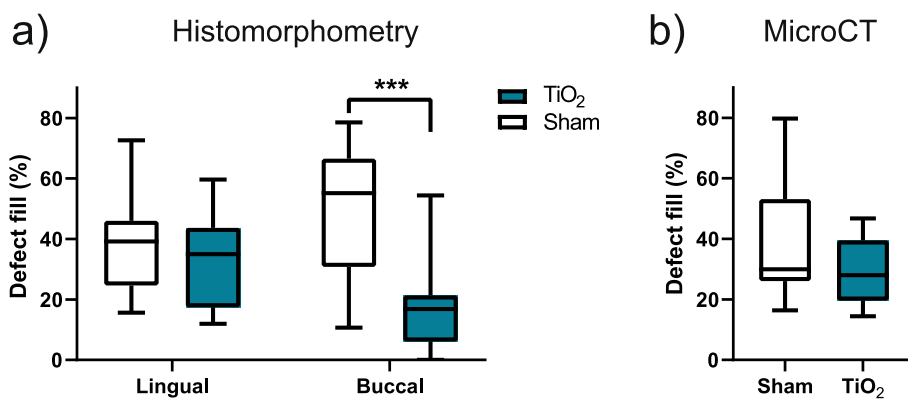


**Fig. 6** Defect fill measured by (a) histomorphometry and (b) microCT. \*\*\*  $p < 0.001$

three sites demonstrated almost complete bone coverage of the implants.

**Histology**

All implants were osseointegrated. New bone formation was clearly distinguishable from the original bone and the defects were readily identified. Except for one sham site (Fig. 5a), no buccal bone wall was completely re-established to the level of the implant shoulder in the defects. The TiO<sub>2</sub> scaffold which was in part missing on MicroCT showed no contact between the TiO<sub>2</sub> scaffold and the bone in histology (Fig. 5d). The remaining 11 scaffolds were in intimate contact with the bone and demonstrated new bone formation in various degrees within the porous scaffold structures.

**Defect fill**

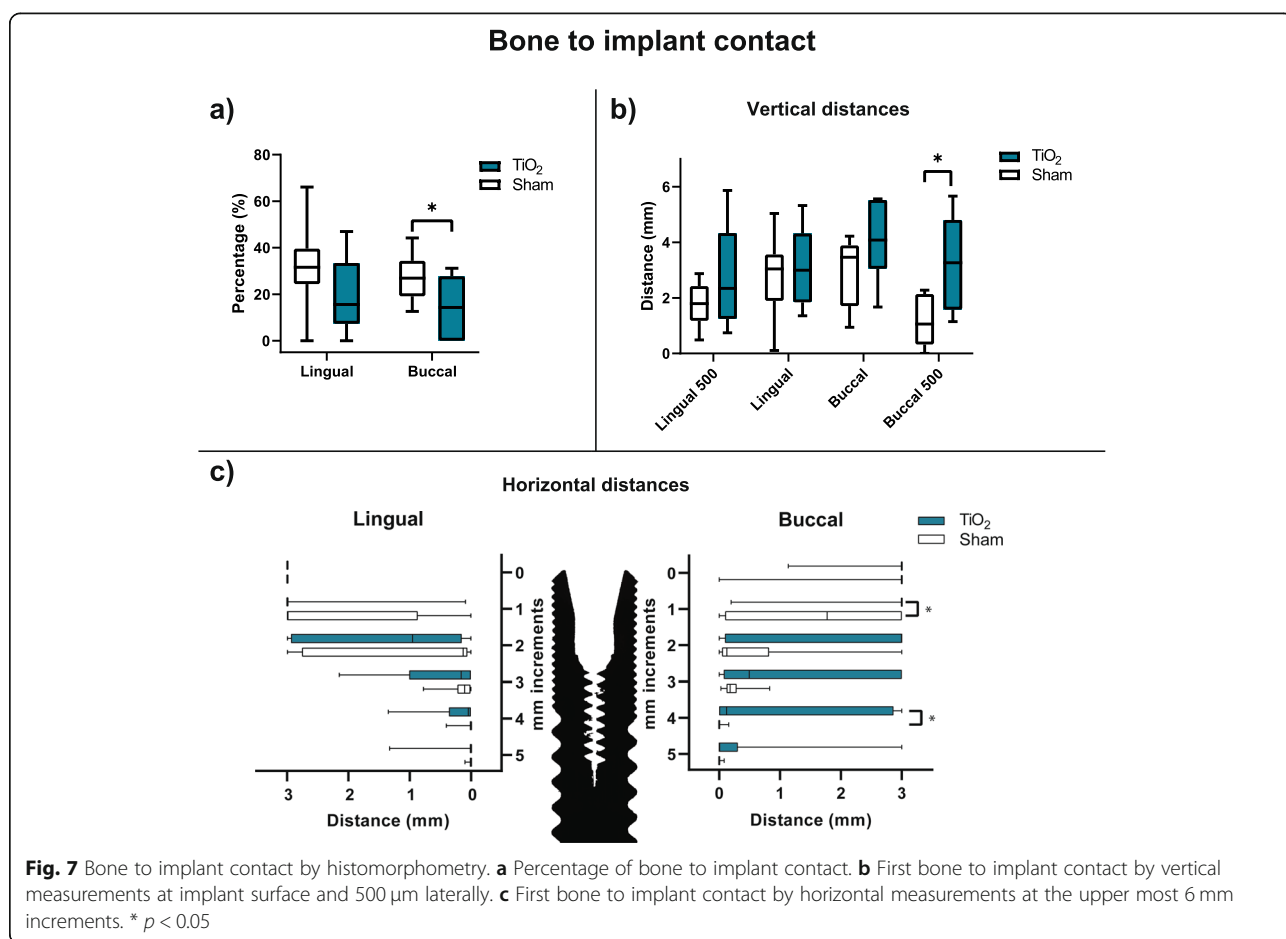
Results are presented in Fig. 6. Histomorphometric results at the buccal sites demonstrated a statistically significant higher fraction of bone fill between the sham group (median: 55.1%, IQR: 30.8-66.6) compared to the TiO<sub>2</sub> scaffolds (median: 16.9%, IQR: 6.1-21.3).

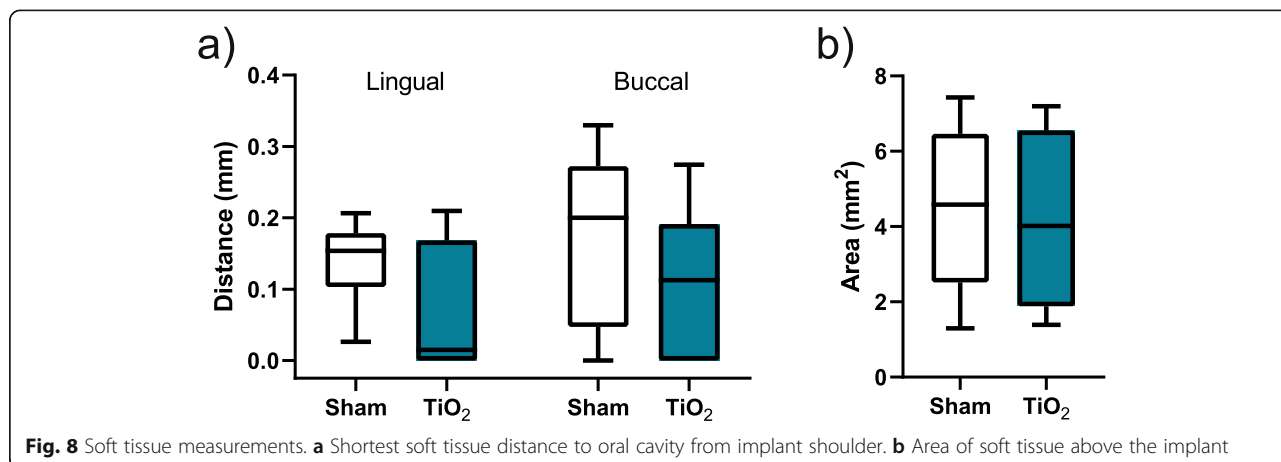
**Bone to implant contact**

The results for %BIC at the uppermost 5 mm of the implants are shown in Fig. 7a. Statistically significant difference was found in the buccal sites between shams (median: 26.9%, IQR: 19.1-34.4) and TiO<sub>2</sub> blocks (median: 14.3%, IQR: 0.0-27.7). No significant difference was found at the lingual sites.

The results for vertical FBIC and FBIC500 are shown in Fig. 7b. No significant difference in FBIC between TiO<sub>2</sub> blocks and sham were found in buccal or lingual sites. For FBIC500, the shams (median: 1.1 mm, IQR: 0.3-2.1) demonstrated a significantly lower value on the buccal side than the TiO<sub>2</sub> blocks (median: 3.3 mm, IQR: 1.6-4.8). No significant difference was found for FBIC500 in lingual sites.

Horizontal width measurements are presented in Fig. 7c. Statistically significant difference was found in buccal sites between sham and TiO<sub>2</sub> scaffold at millimetre 1 (median: 1.8 mm, IQR: 0.9-3.0 and median: 3.0 mm, IQR: 3.0-3.0, respectively) and millimetre 4 (median: 0 mm, IQR: 0.0-0.0 and median: 1.2 mm, IQR: 0.0-2.9, respectively).





### Soft tissue measurements

Results are presented in Fig. 8. No statistically significant differences were found between sham and TiO<sub>2</sub> for either shortest soft tissue distance to oral cavity from implant shoulder or area of soft tissue above the implant.

### Discussion

This study demonstrated less bone formation on the buccal side with the use of TiO<sub>2</sub> scaffold block along with simultaneous implant placement in circumferential defects with buccal bone fenestrations, as compared to sham sites.

In microCT, no significant difference was seen in comparing %DF. However, the region of interest analysed for %DF was different in histomorphometry and microCT. The microCT analysis set out to evaluate a 3D volume within the scaffolds at the upper part of the implants, excluding the interface between the scaffold and adjacent structures. This volume of interest was chosen to evaluate the space within the porous scaffold structures at the upper part of the implant. As previously demonstrated, bone growth occurs from the defect borders [21]. The 3D microCT analysis did not differentiate between buccal and lingual sites.

The fact that differences in defect fill, bone to implant contact and vertical FBIC500 were observed in the buccal but not lingual sites points to the impact of the lack of a buccal bone wall in this model. The TiO<sub>2</sub> scaffold did not improve bone healing at this aspect. A similar defect model in dogs by Botticelli et al. demonstrated an incomplete healing when the buccal bone wall was removed [2]. In comparison, they found a defect resolution in four wall defects for both gap distances evaluated (1 and 2.25 mm). This demonstrated buccal bone fenestrations as a challenging model. In contrast to the aforementioned study by Botticelli et al., no collagen membrane was used to cover the defects in the present study. Guided bone regeneration (GBR) is defined as the

use of a barrier membrane to direct the growth of new bone and has become a predictable therapeutic method used routinely [22, 23]. Barrier membranes should maintain the space for bone formation and exclude soft tissue invasion of the defect and are commonly used in augmentation procedures. In parallel with its barrier function, the membrane plays an active role in hosting and modulating the molecular activities during GBR [24]. However, their clinical efficacy is debated [25]. Several studies have shown defects healed both with and without membrane for immediate implant placement in four wall defects [26–28]. When used in the bone ring technique, studies have reported no benefits of a membrane [29, 30]. As such, it was opted not to use a membrane in the present study to avoid confounding factors and to assess the bone regeneration capacity of the TiO<sub>2</sub> scaffolds.

Barrier membranes are also used to ensure the stability of bone graft materials and it can be argued that this aspect is not necessary in a block graft, which furthermore is non-resorbable. Additionally, comparison with the use of empty defects would be cumbersome with the use of membranes as the inadequate mechanical properties of a collagen membrane would likely render insufficient space maintenance in the relatively large defects, compared to the TiO<sub>2</sub> scaffolds. Closing the site without the use of a membrane covering the scaffold material resulted consequently in a direct contact between the gingival flap and the TiO<sub>2</sub> scaffold. Soft tissue measurements were performed on histological samples to evaluate any effect of the TiO<sub>2</sub> scaffold on soft tissue and no differences were found in neither buccal nor lingual sites. The results may indicate that the scaffolds were well tolerated by the soft tissue, even when suspended over the scaffold ridge in the buccal sites. A non-resorbable membrane with enhanced mechanical strength could have been considered and may have had a positive influence on the bone reconstruction and soft tissue dimensions.

In the present study, nine out of twelve TiO<sub>2</sub> scaffolds were intact at the end of the study. The new bone formation within the porous structures in eleven out of twelve scaffolds may indicate sufficient mechanical stability of the scaffolds for bone healing. Fractured scaffold edges were not found as previously reported [31]. This can be explained by three-wall defects in the present study, which provide stability and shelters the scaffold from external forces in contrast to its use in lateral bone augmentation models. The aforementioned study also used a fixation screw to secure the block, which resulted in partial scaffold fracture around the screw due to stress concentration. The press-fit installation of the scaffold may have provided more even stress distribution for the brittle TiO<sub>2</sub> scaffolds, thereby maintained the augmented volume throughout the evaluated period. In both studies, the scaffold allowed easy chairside adaptation with dental burs or scissors. This enabled efficient shaping of the scaffold to fill the augmented space, which is advantageous for bone graft substitute materials [10]. In comparison, particulate graft materials often require a flexible membrane for mechanical stabilisation, which also limits the expandable space. Alternatively, a stiff barrier like titanium meshes needs to be manually bent and shaped in a time consuming process and ill adapted meshes increase the risk of mucosal rupture and exposure of the mesh [32].

Mucosal perforations to the oral cavity were found clinically at five sites, four of which in the TiO<sub>2</sub> scaffold group. An implant cover screw, which is temporarily used to close the implant lumen during osseointegration, could have potentially resulted in less mucosal perforations. However, bone growth was confirmed within the porous scaffold structures at all but one of the TiO<sub>2</sub> scaffold sites. As it was a challenging defect model, a longer healing time might show continued bone growth, and the single time point evaluated is a limiting factor of this study. In comparison, when GBR is performed in a two staged approach, implant placement is carried out from 6 to 12 months after GBR surgery [33].

The results suggest that the TiO<sub>2</sub> scaffolds hold the basic requirements for a bone substitute; osteoconductive, biocompatible, space-making capability and volume maintenance [34], also confirmed in previous *in vivo* studies [18, 19, 31]. However, the TiO<sub>2</sub> scaffolds are lacking osteoinductive properties as bone formation is seen only from the lateral borders of the grafts, originating from the parent bone. Different strategies have been proposed to improve new bone formation and *in vitro* studies applying various coatings to the scaffold have shown possibilities for increased osteogenic potential [35–37]. More recently, cationic doping of TiO<sub>2</sub> scaffolds with Ca, Sr or Mg have shown ion release in addition to the benefit of increased mechanical strength

[38]. The released Mg resulted in significantly increased osteogenic differentiation. As the ions Ca, Sr and Mg influence bone biology [39–41], doping could be a prospect for further investigation.

## Conclusions

Less bone formation was observed on the buccal side with the use of TiO<sub>2</sub> scaffold block in combination with simultaneous implant placement in circumferential defects with buccal bone dehiscences, as compared to sham sites.

## Abbreviations

%BIC: Percentage of bone-to-implant contact; FBIC: First bone-to-implant contact; FBIC500: First bone-to-implant contact 500 μm lateral to the implant; GBR: Guided bone regeneration; MicroCT: Microcomputed tomography; TiO<sub>2</sub>: Titanium dioxide; VOI: Volume of interest

## Acknowledgements

Not applicable.

## Authors' contributions

Conceptualization, JEE, SPL and HJH; methodology, MKLT, MPM, HT, AV; surgery, JEE, SPL, HJR, JCW, AGC, FMG, MPM; formal analysis, MKLT, AH, LRH, HT; writing—original draft preparation, MKLT; writing—review and editing, AV and HJH; supervision, HT, AV and HJH; funding acquisition, JEE, HJH. All authors have read and agreed to the published version of the manuscript.

## Funding

Research was funded by the Norwegian Research Council grant no. 228415. Implants was provided by Dentsply Sirona through the grant I-AS-14-009 "Immediate placement of dental implants and titanium dioxide scaffolds".

## Availability of data and materials

All data is available upon request to the corresponding author.

## Declarations

### Ethics approval and consent to participate

The Regional Ethics Committee for Animal Research of the University of Santiago de Compostela approved the protocol (Ref. AE-LU-001/002/14).

### Consent for publication

Not applicable.

### Competing interests

Haugen, Ellingsen, Tiainen and Lyngstadaas are inventors of the technology behind the production of TiO<sub>2</sub> scaffold (WO2014044672, WO2008078164). The commercial rights for the TiO<sub>2</sub> scaffold belongs to Corticalis AS. Haugen, Ellingsen, Lyngstadaas, Rønold and Wohlfahrt are shareholder of Corticalis AS.

### Author details

<sup>1</sup>Department of Biomaterials, Institute of Clinical Dentistry, University of Oslo, 0317 Oslo, Norway. <sup>2</sup>Department of Periodontology, Institute of Clinical Dentistry, Faculty of Dentistry, University of Oslo, Oslo, Norway. <sup>3</sup>Department of Prosthetic Dentistry and Oral Function, Institute of Clinical Dentistry, Faculty of Dentistry, University of Oslo, Oslo, Norway. <sup>4</sup>Universidad de Santiago de Compostela, Facultad de Veterinaria, Campus Universitario, s/n, 27002 Lugo, Spain. <sup>5</sup>Ibonelab S.L., Laboratory of Biomaterials, Avda. da Coruña, 500 (CEI-NODUS), 27003 Lugo, Spain.

Received: 29 June 2021 Accepted: 15 November 2021

Published online: 25 November 2021

## References

- Schropp L, Wenzel A, Kostopoulos L, Karring T. Bone healing and soft tissue contour changes following single-tooth extraction: a clinical and

- radiographic 12-month prospective study. *Int J Periodontics Restorative Dentistry*. 2003;23(4):313–23.
2. Botticelli D, Berglundh T, Lindhe J. Resolution of bone defects of varying dimension and configuration in the marginal portion of the peri-implant bone. *J Clin Periodontol*. 2004;31(4):309–17.
  3. Paolantonio M, Dolci M, Scarano A, D'Archivio D, Di Placido G, Tumini V, et al. Immediate implantation in fresh extraction sockets. A controlled clinical and histological study in Man. *J Periodontol*. 2001;72(11):1560–71.
  4. Ortega-Martínez J, Pérez-Pascual T, Mareque-Bueno S, Hernández-Alfaro F, Ferrés-Padró E. Immediate implants following tooth extraction. A systematic review. *Med Oral Patol Oral Cir Bucal*. 2012;17(2):e251–e61.
  5. Nkenke E, Schultze-Mosgau S, Kloss F, Neukam FW, Radespiel-Tröger M. Morbidity of harvesting of chin grafts: a prospective study. *Clin Oral Implants Res*. 2001;12(5):495–502.
  6. Nkenke E, Neukam FW. Autogenous bone harvesting and grafting in advanced jaw resorption: morbidity, resorption and implant survival. *Eur J Oral Implantol*. 2014;7(Suppl 2):S203–17.
  7. Araujo MG, Lindhe J. Socket grafting with the use of autologous bone: an experimental study in the dog. *Clin Oral Implants Res*. 2011;22(1):9–13.
  8. Sanz-Sánchez I, Ortiz-Vigón A, Sanz-Martín I, Figuero E, Sanz M. Effectiveness of lateral bone augmentation on the alveolar crest dimension: a systematic review and Meta-analysis. *J Dent Res*. 2015;94(9 Suppl):1285–42s.
  9. Sogal A, Tofe AJ. Risk assessment of bovine spongiform encephalopathy transmission through bone graft material derived from bovine bone used for dental applications. *J Periodontol*. 1999;70(9):1053–63.
  10. Haugen HJ, Lyngstadaas SP, Rossi F, Perale G. Bone grafts: which is the ideal biomaterial? *J Clin Periodontol*. 2019;46(S21):92–102.
  11. Giesenhagen B, Martin N, Donkiewicz P, Perić Kačarević Ž, Smeets R, Jung O, et al. Vertical bone augmentation in a single-tooth gap with an allogenic bone ring: clinical considerations. *J Esthet Restor Dent*. 2018;30(6):480–3.
  12. Miller RJ, Korn RJ, Miller RJ. Indications for simultaneous implantation and bone augmentation using the allograft bone ring technique. *Int J Perio Res Dent*. 2020;40:345–52.
  13. Sáez-Alcaide LM, Brinkmann JC-B, Sánchez-Labrador L, Pérez-González F, Molinero-Mourelle P, López-Quiles J. Effectiveness of the bone ring technique and simultaneous implant placement for vertical ridge augmentation: a systematic review. *Int J Implant Dent*. 2020;6(1):82.
  14. Gaikwad AM, Joshi AA, Padhye AM, Nadgere JB. Autogenous bone ring for vertical bone augmentation procedure with simultaneous implant placement: a systematic review of histologic and histomorphometric outcomes in animal studies. *J Prosthet Dent*. 2021;126(5):626–35. <https://doi.org/10.1016/j.prosdent.2020.09.001>.
  15. Sabetrasekh R, Tiainen H, Lyngstadaas SP, Reseland J, Haugen H. A novel ultra-porous titanium dioxide ceramic with excellent biocompatibility. *J Biomater Appl*. 2010;25(6):559–80.
  16. Tiainen H, Wiedmer D, Haugen HJ. Processing of highly porous TiO<sub>2</sub> bone scaffolds with improved compressive strength. *J Eur Ceram Soc*. 2013;33(1):15–24.
  17. Tiainen H, Lyngstadaas SP, Ellingsen JE, Haugen HJ. Ultra-porous titanium oxide scaffold with high compressive strength. *J Mater Sci Mater Med*. 2010; 21(10):2783–92.
  18. Tiainen H, Wohlfahrt JC, Verket A, Lyngstadaas SP, Haugen HJ. Bone formation in TiO<sub>2</sub> bone scaffolds in extraction sockets of minipigs. *Acta Biomater*. 2012;8(6):2384–91.
  19. Verket A, Müller B, Wohlfahrt JC, Lyngstadaas SP, Ellingsen JE, Jostein Haugen H, et al. TiO<sub>2</sub> scaffolds in peri-implant dehiscence defects: an experimental pilot study. *Clin Oral Implants Res*. 2016;27(10):1200–6.
  20. Botticelli D, Berglundh T, Lindhe J. The influence of a biomaterial on the closure of a marginal hard tissue defect adjacent to implants. *Clin Oral Implants Res*. 2004;15(3):285–92.
  21. Botticelli D, Berglundh T, Buser D, Lindhe J. Appositional bone formation in marginal defects at implants. *Clin Oral Implants Res*. 2003;14(1):1–9.
  22. Hämmerle CH, Karring T. Guided bone regeneration at oral implant sites. *Periodontology 2000*. 1998;17(1):151–75.
  23. Buser D, Dula K, Belsler UC, Hirt H-P, Berthold H. Localized ridge augmentation using guided bone regeneration. II. Surgical procedure in the mandible. *Int J Periodontics Restorative Dentistry*. 1995;15(1):10–29.
  24. Omar O, Elgali I, Dahlin C, Thomsen P. Barrier membranes: more than the barrier effect? *J Clin Periodontol*. 2019;46(S21):103–23.
  25. Hu C, Gong T, Lin W, Yuan Q, Man Y. Immediate implant placement into posterior sockets with or without buccal bone dehiscence defects: a retrospective cohort study. *J Dent*. 2017;65:95–100.
  26. Chen ST, Darby IB, Reynolds EC. A prospective clinical study of non-submerged immediate implants: clinical outcomes and esthetic results. *Clin Oral Implants Res*. 2007;18(5):552–62.
  27. Covani U, Cornelini R, Barone A. Bucco-lingual bone remodeling around implants placed into immediate extraction sockets: a case series. *J Periodontol*. 2003;74(2):268–73.
  28. Botticelli D, Berglundh T, Buser D, Lindhe J. The jumping distance revisited. *Clin Oral Implants Res*. 2003;14(1):35–42.
  29. Haga-Tsujimura M, Nakahara K, Kobayashi E, Igarashi K, Schaller B, Saulacic N. Single-staged implant placement using bone ring technique with and without membrane placement: an experimental study in the beagle dog. *Clin Oral Implants Res*. 2018;29(3):263–76.
  30. Nakahara K, Haga-Tsujimura M, Igarashi K, Kobayashi E, Schaller B, Lang NP, et al. Single-staged implant placement using the bone ring technique with and without membrane placement: Micro-CT analysis in a preclinical in vivo study. *Clin Oral Implants Res*. 2020;31(1):29–36.
  31. Thieu MKL, Haugen HJ, Sanz-Esporrin J, Sanz M, Lyngstadaas SP, Verket A. Guided bone regeneration of chronic non-contained bone defects using a volume stable porous block TiO<sub>2</sub> scaffold: an experimental in vivo study. *Clin Oral Implants Res*. 2021;32(3):369–81.
  32. Xie Y, Li S, Zhang T, Wang C, Cai X. Titanium mesh for bone augmentation in oral implantology: current application and progress. *Int J Oral Sci*. 2020; 12(1):37.
  33. Buser D, Chappuis V, Belsler UC, Chen S. Implant placement post extraction in esthetic single tooth sites: when immediate, when early, when late? *Periodontology 2000*. 2017;73(1):84–102.
  34. Yamada M, Egusa H. Current bone substitutes for implant dentistry. *J Prosthodont Res*. 2018;62(2):152–61.
  35. Verket A, Tiainen H, Haugen HJ, Lyngstadaas SP, Nilsen O, Reseland JE. Enhanced osteoblast differentiation on scaffolds coated with TiO<sub>2</sub> compared to SiO<sub>2</sub> and CaP coatings. *Biointerphases*. 2012;7(1-4):36.
  36. Pullisaar H, Reseland JE, Haugen HJ, Brinckmann JE, Ostrup E. Simvastatin coating of TiO<sub>2</sub> scaffold induces osteogenic differentiation of human adipose tissue-derived mesenchymal stem cells. *Biochem Biophys Res Commun*. 2014;447(1):139–44.
  37. Rubert M, Pullisaar H, Gómez-Florit M, Ramis JM, Tiainen H, Haugen HJ, et al. Effect of TiO<sub>2</sub> scaffolds coated with alginate hydrogel containing a proline-rich peptide on osteoblast growth and differentiation in vitro. *J Biomed Mater Res A*. 2013;101A(6):1768–77.
  38. Klemm A, Gomez-Florit M, Carvalho PA, Wachendörfer M, Gomes ME, Haugen HJ, et al. Grain boundary corrosion in TiO<sub>2</sub> bone scaffolds doped with group II cations. *J Eur Ceram Soc*. 2019;39(4):1577–85.
  39. Yoshizawa S, Brown A, Barchowsky A, Sfeir C. Magnesium ion stimulation of bone marrow stromal cells enhances osteogenic activity, simulating the effect of magnesium alloy degradation. *Acta Biomater*. 2014;10(6):2834–42.
  40. Pors NS. The biological role of strontium. *Bone*. 2004;35(3):583–8.
  41. Blair HC, Robinson LJ, Huang CL-H, Sun L, Friedman PA, Schlesinger PH, et al. Calcium and bone disease. *BioFactors*. 2011;37(3):159–67.

## Publisher's Note

Springer Nature remains neutral with regard to jurisdictional claims in published maps and institutional affiliations.

### Ready to submit your research? Choose BMC and benefit from:

- fast, convenient online submission
- thorough peer review by experienced researchers in your field
- rapid publication on acceptance
- support for research data, including large and complex data types
- gold Open Access which fosters wider collaboration and increased citations
- maximum visibility for your research: over 100M website views per year

At BMC, research is always in progress.

Learn more [biomedcentral.com/submissions](https://www.biomedcentral.com/submissions)











# Guided bone regeneration of chronic non-contained bone defects using a volume stable porous block TiO<sub>2</sub> scaffold: An experimental in vivo study

Minh Khai Le Thieu<sup>1,2</sup>  | Håvard Jostein Haugen<sup>2</sup>  | Javier Sanz-Esporrin<sup>3</sup>  |  
Mariano Sanz<sup>3</sup>  | Ståle Petter Lyngstadaas<sup>2</sup> | Anders Verket<sup>1</sup> 

<sup>1</sup>Department of Periodontology, Institute of Clinical Dentistry, Faculty of Dentistry, University of Oslo, Oslo, Norway

<sup>2</sup>Department of Biomaterials, Institute of Clinical Dentistry, Faculty of Dentistry, University of Oslo, Oslo, Norway

<sup>3</sup>ETEP Research Group, Faculty of Odontology, University Complutense of Madrid, Madrid, Spain

## Correspondence

Anders Verket, Department of Periodontology, Institute of Clinical Dentistry, Faculty of Dentistry, University of Oslo, Box 1109 Blindern, 0317 Oslo, Norway.  
Email: anderver@odont.uio.no

## Funding information

Norges Forskningsråd, Grant/Award Number: FRINATEK grant number 231530

## Abstract

**Objectives:** To evaluate new lateral bone formation and lateral volume augmentation by guided bone regeneration (GBR) in chronic non-contained bone defects with the use of a non-resorbable TiO<sub>2</sub>-block.

**Materials and methods:** Three buccal bone defects were created in each hemimandible of eight beagle dogs and allowed to heal for 8 weeks before treatment by GBR. Each hemimandible was randomly allocated to 4- or 12-week healing time after GBR, and three intervention groups were assigned by block randomization: TiO<sub>2</sub> block: TiO<sub>2</sub>-scaffold and a collagen membrane, DBBM particles: Deproteinized bovine bone mineral (DBBM) and a collagen membrane, Empty control: Collagen membrane only. Microcomputed tomography (microCT) was used to measure the lateral bone formation and width augmentation. Histological outcomes included descriptive analysis and histomorphometric measurements.

**Results:** MicroCT analysis demonstrated increasing new bone formation from 4 to 12 weeks of healing. The greatest width of mineralized bone was seen in the empty controls, and the largest lateral volume augmentation was observed in the TiO<sub>2</sub> block sites. The DBBM particles demonstrated more mineralized bone in the grafted area than the TiO<sub>2</sub> blocks, but small amounts and less than the empty control sites.

**Conclusion:** The TiO<sub>2</sub> blocks rendered the largest lateral volume augmentation but also less new bone formation compared with the DBBM particles. The most new lateral bone formation outward from the bone defect margins was observed in the empty controls, indicating that the presence of either graft material leads to slow appositional bone growth.

## KEYWORDS

animal experimentation, bone regeneration, bone substitutes, guided tissue regeneration, xenografts

This is an open access article under the terms of the Creative Commons Attribution-NonCommercial-NoDerivs License, which permits use and distribution in any medium, provided the original work is properly cited, the use is non-commercial and no modifications or adaptations are made.

© 2021 The Authors. Clinical Oral Implants Research published by John Wiley & Sons Ltd.

## 1 | INTRODUCTION

Missing teeth are commonly replaced with dental implants. However, patients often present insufficient bone volume, which may jeopardize predictable stability and aesthetic outcomes of the implant-supported restorative treatment (Tonetti et al., 2008). Following tooth loss, bone resorption occurs in both vertical and horizontal dimensions (Schropp et al., 2003). Other causes of bone loss include infections as in periodontitis and periapical pathology, trauma, benign and malignant tumours and congenital conditions. Different bone regenerative interventions have demonstrated efficacy for augmenting the alveolar ridge bone and providing enough volume available for successful implant placement (Sanz & Vignoletti, 2015; Sanz-Sanchez et al., 2015).

Among these interventions, guided bone regeneration (GBR) has been the most frequently used. Its principle is based on the exclusion of non-osteogenic cells by a cell occlusive membrane, which allows growth of bone-forming cells, ultimately leading to new bone tissue (Nyman et al., 1982; Retzepi & Donos, 2010). The predominant type of membranes used in GBR today is resorbable collagen membranes, although these have limited mechanical strength (Sanz et al., 2019). Therefore, the use of bone graft materials as scaffolds to maintain space for new bone formation is often required (Elgali et al., 2017; McAllister & Haghghat, 2007). Autologous bone grafts are considered the gold standard due to their osteogenic, osteoconductive and osteoinductive properties (Moy & Aghaloo, 2019), however, their often limited availability, and the requirement of more invasive surgeries when harvested extra-orally may limit its use. Drawbacks associated with autografts include donor site morbidity and post-operative pain (Clavero & Lundgren, 2003; Nkenke et al., 2001; Raghoobar et al., 2001; Schaaf et al., 2010) and their unpredictable rate of resorption, which could hamper their space-maintaining function in a GBR procedure (Chiapasco et al., 2006; Nkenke & Neukam, 2014). Alternative bone replacement grafts are allografts or xenografts, which need to be processed and sterilized prior to their use, what greatly reduces or eradicates their osteoinductive and osteogenic potential. One major concern with allografts and xenografts is the risk of disease transmission from graft to host (Sogal & Tofe, 1999). In spite of these limitations, bovine-derived bone replacement grafts have been extensively documented for bone augmentation, mainly with GBR procedures (Benic & Hämmerle, 2014; Ortiz-Vigón et al., 2018; Sanz & Vignoletti, 2015; Sanz-Sanchez et al., 2015). In Europe, current changes in regulations of medical devices by the European Union may increase the use of synthetic materials (Haugen et al., 2019).

The use of synthetic bone replacement grafts may overcome the aforementioned challenges due to their controlled production environments and biocompatible properties. Synthetic materials can also be tailored for appropriate macro- and microstructures, interconnectivity and mechanical properties. Commercial synthetic bone graft substitutes are widely available and several studies have

shown osteoconductive properties suitable for bone augmentation (Carson & Bostrom, 2007; Hürzeler et al., 1996), but long-term clinical efficacy is lacking (Sanz-Sanchez et al., 2015).

The TiO<sub>2</sub> block used in this study is a ceramic bone graft substitute with porous architecture which allows formation of bone and vascularization, compressive strength similar to trabecular bone and biocompatible properties (Tiainen et al., 2013; Tiainen et al., 2012; Verket et al., 2012). Previous preclinical studies have demonstrated bone ingrowth and angiogenesis within the structures of the TiO<sub>2</sub> block in extraction sockets and in peri-implant dehiscence defects (Haugen et al., 2013; Tiainen et al., 2012). In these studies, acute healing models were used. The use of acute defects to assess healing for osseous regenerative therapy is useful from a materials perspective, but has its limits in terms of clinical relevance, since it is well-known that such defects possess great potential for spontaneous healing (Hanisch et al., 2003). It was, therefore, the aim of this *in vivo* experimental investigation to evaluate the potential of the TiO<sub>2</sub> block for use in lateral augmentation using a validated chronic bone defect model. The objectives of this experimental study were to evaluate lateral bone formation and lateral volume augmentation in a chronic non-contained bone defect when using a non-resorbable synthetic block made of titanium dioxide in a guided bone regeneration (GBR) procedure.

## 2 | MATERIALS AND METHODS

### 2.1 | Scaffold preparation

Ceramic TiO<sub>2</sub> scaffolds were produced as described by Tiainen et al. (Tiainen et al., 2013). In short, polymer sponges were coated and sintered three times. The slurries were prepared from TiO<sub>2</sub> powder (Kronos 1171, Kronos Titan GmbH, Leverkusen, Germany) and sterilized water in following proportions: 65 g powder in 25 ml water, 40 g powder in 25 ml water and 20 g powder in 25 ml water. The third coating was done under vacuum infiltration. After the final sintering, the dimensions of the rectangular scaffold blocks were approximately 11 mm × 11 mm × 8 mm. Prior to use, the scaffolds were steam sterilized at 121°C for 15 min.

### 2.2 | Study design

For each animal, the hemimandibles were randomly allocated for either 4 or 12 weeks healing time. Three defect sites; anterior, middle and posterior, were created in each hemimandible and allowed to heal for 8 weeks prior to GBR procedures (Figure 1). The three defect sites were randomly allocated to the following treatment group:

1. TiO<sub>2</sub> block: TiO<sub>2</sub> scaffold (Corticalis AS, Oslo, Norway) covered by a collagen membrane (Bio-Gide®; Geistlich Pharma AG, 6110 Wolhusen, Switzerland)

2. DBBM particles: A xenograft of deproteinized bovine bone mineral (DBBM) (Bio-Oss® Granules 0.25-1mm, Geistlich Pharma AG, 6110 Wolhusen, Switzerland) covered by a collagen membrane (Bio-Gide®; Geistlich Pharma AG, 6110 Wolhusen, Switzerland)
3. Empty control: A collagen membrane covered the defect (Bio-Gide®; Geistlich Pharma AG, 6110 Wolhusen, Switzerland)

Randomization of the interventions was performed using a random block computer-generated list (IBM SPSS Statistics® V20. Macro !RNDSEQ V2011.09.09 (c) JM.Domenech). Randomization sequence was generated using a blocking, balanced restricted randomization (block size: 3), stratified by side (healing time) and position in the jaw (anterior, middle and posterior). Randomization was performed to distribute equally all treatment groups within each healing group. So in each hemimandible (healing time), all treatment groups should be present, randomized for position (anterior, middle and posterior) and considering hemimandible side as a factor as well. All groups were randomized for the defect position and the side (right or left), resulting in presence of all groups in all hemimandibles equally distributed by position and healing on both sides (right and left).

### 2.3 | Animals and surgical procedures

The study was designed in accordance with the ARRIVE (Animal Research: Reporting of In Vivo Experiments) guidelines for preclinical research (Kilkenny et al., 2010). The protocol was approved by the Ethical committee at the Jesús Usón Minimally Invasive Surgery Centre (Caceres, Spain) and by the Director General of Agriculture and Livestock (approval code: 2018209020003431).

Eight female beagle dogs (weight, 11–14 kg) were used. The animals were fed on soft pellet diet and maintained in individual kennels. They were kept in a 12:12 light/dark cycle at 21–22°C and daily monitored by a veterinarian. All animals were inspected to ensure absence of oral disease or dental conditions that would preclude the placement of the graft materials. The animals were monitored for any signs or symptoms of illness 2 weeks prior to the start of the study.

The animals were sedated with propofol (2 mg/kg/i.v., Propovet, Abbott Laboratories, Kent, UK), general anaesthesia was maintained under mechanically induced respiration of 2.5%–4% of isoflurane (Isoba-vet, Schering-Plough, Madrid, Spain). The animals

were pre-medicated with acepromazine (0.05 mg/kg/i.m., Calmo Meosan, Pfizer, Madrid, Spain). As analgesics, morphine (0.3 mg/kg/i.m., Morfina Braun 2%, B. Braun Medical, Barcelona, Spain) was administered in addition to infiltration with Lidocaine 2% with epinephrine 1:100,000 (2% Xylocaine Dental, Dentsply, York, PA, USA). After surgeries, the animals were administered Morphine (0.3 mg/kg/i.m.) for the first 24 hr and meloxicam (0.1 mg kg<sup>-1</sup> s<sup>-1</sup>.i.d./p.o., Metacam, Boehringer Ingelheim España, Barcelona, Spain) for 3 days after surgeries to control pain. Antibiotic therapy was set with amoxicillin (22 mg kg<sup>-1</sup> s<sup>-1</sup>.i.d./s.c., Amoxoil retard, Syva, León, Spain) for seven days after the surgeries.

**Surgery 1 (week 0):** Defect creation for 12-weeks healing time (Figure 2a). Extraction and defect creation were performed according to the protocol of Sanz et al. (2017).

**Surgery 2 (week 8):** Regeneration of 12 weeks healing sites and defect creation for 4 weeks healing sites. Bone augmentation was performed on the defects made in surgery 1. Full-thickness flaps were raised on the buccal and lingual side. The cortical bone plate was perforated using a small, round bur. The three groups (TiO<sub>2</sub> blocks, DBBM particles and empty controls) were allocated by block randomization to the edentulous areas. The distribution between groups and sites is shown in Table 1. Allocation to the treatment was concealed by means of sealed envelopes until the moment of the surgical grafting procedure. The regenerative therapy could not be blinded as treatment groups differed in shape and form of fixation. The rectangular TiO<sub>2</sub> blocks were shaped with a diamond bur to fit the alveolar ridge, and sharp edges were smoothed before fixation by a bone block fixation screw 1.5 mm diameter and 10.0 mm length (Straumann AG, CH-4002 Basel, Switzerland) (Figure 2b). The fixation screw length was always adapted to the width of the alveolar bone. For the DBBM particles, between 0.1 g and 0.2 g of Bio-Oss® was used for each defect depending on the size. All three sites were then covered with a Bio-Gide® membrane, secured by two titanium pins (Botiss titan pins 3 mm, Straumann AG, CH-4002 Basel, Switzerland) at the apical corners on the buccal side of the alveolar bone (Figure 2c). The flap was passively adapted and primary wound closure was obtained. In the contralateral hemimandible, defect creation was done as described for surgery 1.

**Surgery 3 (week 16):** Regeneration of 4 weeks group, performing the same GBR procedure as in surgery 2.

At week 20, the animals were euthanized with a lethal dose of sodium pentobarbital (40–60 mg/kg/i.v., Dolethal, Vetoquinol, France). The mandibles were dissected and fixed in formalin.

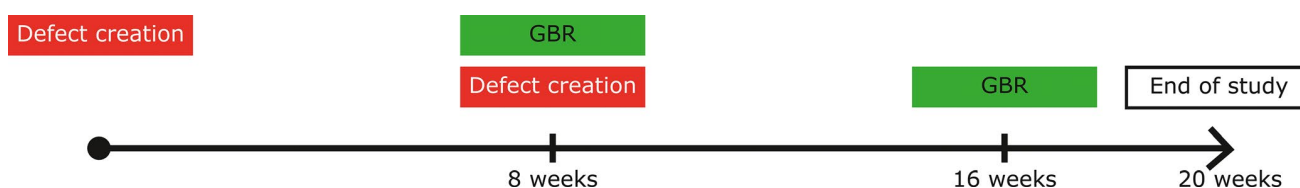
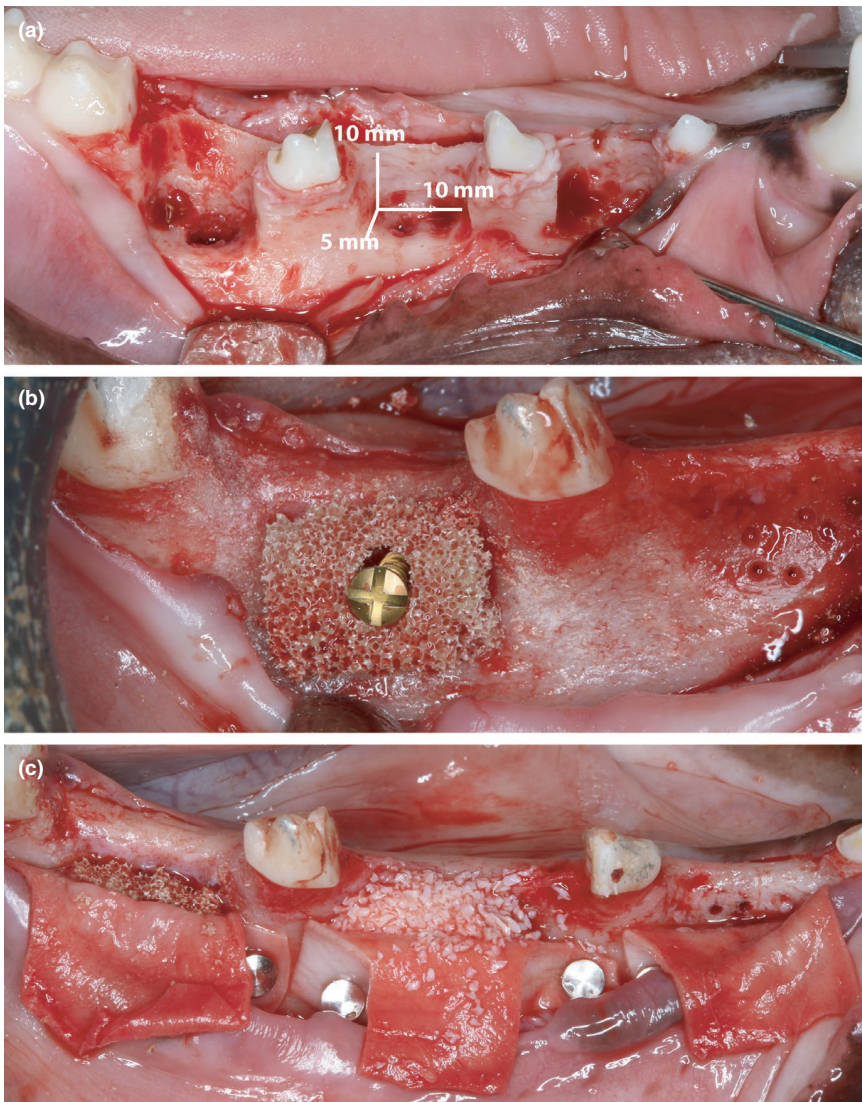


FIGURE 1 Timeline of the study design



**FIGURE 2** Clinical photographs depicting the experimental model. (a) After hemisections and extractions the defects were made, measuring approximately  $5 \times 10 \times 10$  mm each. The defects were labelled anterior, middle and posterior site, according to the location on the hemimandible (b) Fixation of the  $\text{TiO}_2$  scaffold with a screw in the posterior site. Cortical perforations made in the middle site. (c) After placement of graft materials, membranes and pins to secure the membrane prior to flap adaptation and suturing

	4 Week			12 Week		
	Anterior	Middle	Posterior	Anterior	Middle	Posterior
Empty control	2	2	4	3	2	3
DBBM particles	3	2	3	3	4	1
$\text{TiO}_2$ block	3	4	1	2	2	4

**TABLE 1** Allocation of materials to sites by block randomization

#### 2.4 | Microcomputed tomography scanning

Microcomputed tomographic imaging (microCT) of the samples was performed (SkyScan 2211, Bruker microCT, Kontich, Belgium) with a resolution of  $10 \mu\text{m}$ , using 70 kV and  $65 \mu\text{A}$ , with 3 average images every  $0.67$  degrees for a 360-degree rotation with  $0.5$  mm aluminium filter. The data were reconstructed using NRecon software (Bruker microCT, Kontich, Belgium) with ring artefact correction and beam hardening correction of 40%. The reconstructed images were analysed in CTan (Bruker microCT, Kontich, Belgium). The alveolar ridge was measured in

bucco-lingual direction for bone width and overall width included graft materials, as well as the distance of bone ingrowth within the grafted area for the  $\text{TiO}_2$  blocks and DBBM particles, defined from the borders of the graft materials. The average of five measurements was included for each site. For the DBBM particles and empty control; one at the mesio-distal centre of the defect and one and two millimetre to each side of the centre. In the measurements of the  $\text{TiO}_2$  blocks, 1 mm from each side of fixation screw was excluded, to avoid the scattering from the fixation screw. The measurements were done in millimetre increments from the tip of the alveolar crest and 6 mm in apical direction (Figure 3a).

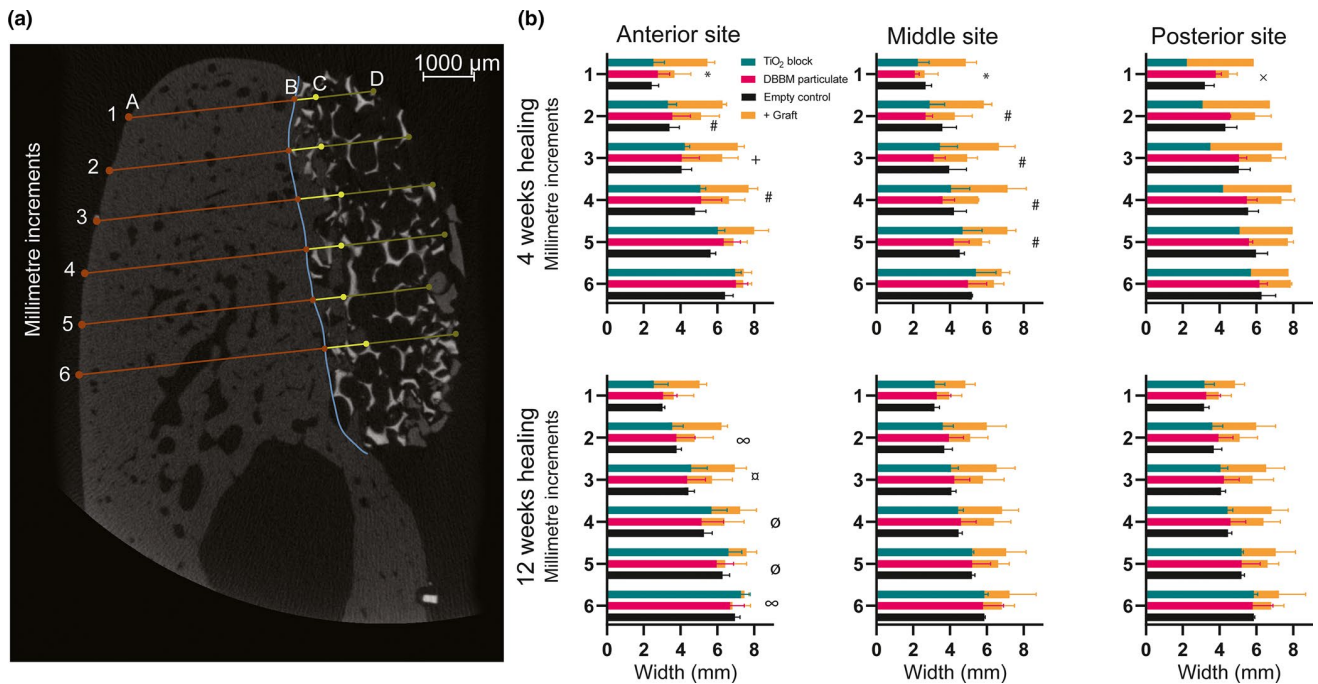


**FIGURE 3** (a) Illustration of the measurements performed on microCT scans at the six increments. (A) marking the lingual bone border, (B) marking the assumed border of the parent bone, (C) marking the regenerated buccal bone border, (D) marking the external border of the augmented area. Bone width = Distance AC. Bone width included graft = Distance AD. New bone = Distance BC. (b) Bar charts showing alveolar bone width and total width included graft material from microCT measurements at the six millimetre increments. Statistically significant difference between groups ( $p < .05$ ) denoted by: # TiO<sub>2</sub> + graft versus TiO<sub>2</sub>, TiO<sub>2</sub> + graft versus DBBM and TiO<sub>2</sub> + graft versus empty, \* TiO<sub>2</sub> + graft versus empty, TiO<sub>2</sub> + graft versus DBBM, TiO<sub>2</sub> + graft versus DBBM + graft and TiO<sub>2</sub> + graft versus TiO<sub>2</sub>, ∞ TiO<sub>2</sub> + graft versus TiO<sub>2</sub>, × TiO<sub>2</sub> + graft versus TiO<sub>2</sub> and TiO<sub>2</sub> + graft versus empty, ∩, TiO<sub>2</sub> + graft versus TiO<sub>2</sub> and TiO<sub>2</sub> + graft versus DBBM, ∅ TiO<sub>2</sub> + graft versus TiO<sub>2</sub>, TiO<sub>2</sub> + graft versus DBBM, TiO<sub>2</sub> + graft versus empty and TiO<sub>2</sub> versus empty

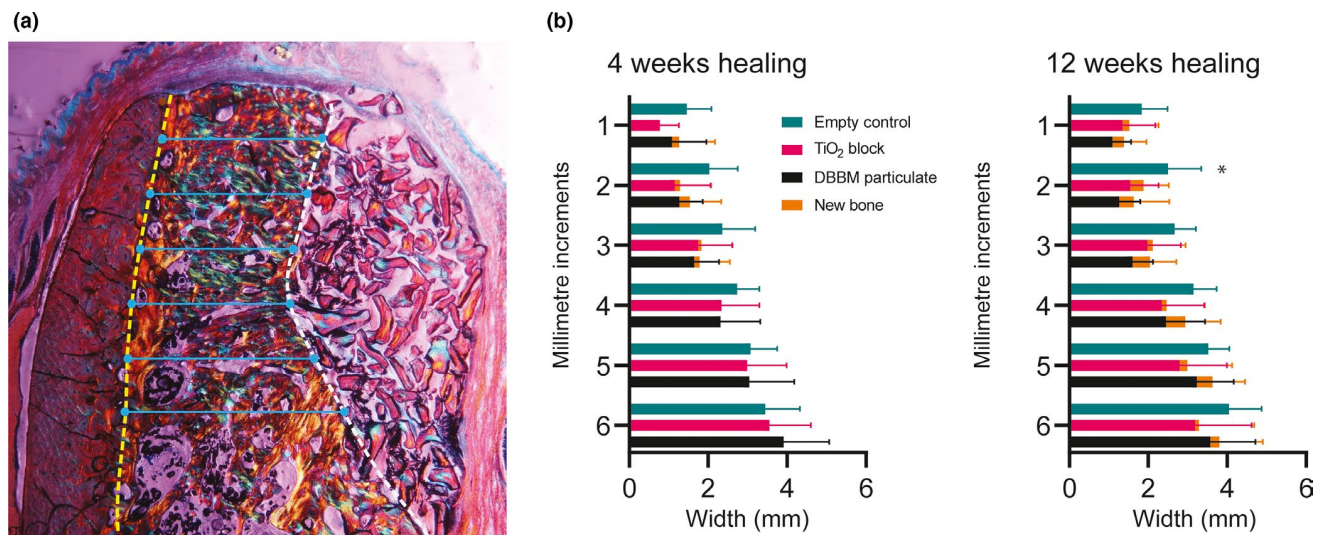


**FIGURE 4** (a) Illustration of the histomorphometric width measurements. Yellow dotted line denotes polarized line from defect creation. White dotted line denotes graft start. Blue lines denote the six increments measured. (b) Bar charts showing width from polarized line to graft start and polarized line to lateral bone border at the six millimetre increments. Denoted by asterisk (\*): Statistically significant difference ( $p < .05$ ) between empty control and DBBM particle group

Intra-examiner reliability was validated by repeated measurements of ten sites with a 1-week interval. Volumetric measurements of the grafts were also done for DBBM particles and TiO<sub>2</sub>

blocks. The outline of the graft was manually traced throughout the defect sites, and the volume constituted by graft materials was calculated.

## 2.5 | Histological preparation

The samples were dehydrated in an ascending series of alcohol and xylene baths prior to embedding in methyl methacrylate and polymerized at  $-20^{\circ}\text{C}$ . The most central section of the defect site was chosen for analysis. The sections were obtained by cutting the embedded blocks with an Exakt 300 diamond band saw (Exakt, Norderstedt, Germany) followed by grinding and polishing to a thickness of approximately  $80\ \mu\text{m}$  with an Exakt 400CS. The sections were stained with Levai-Laczko staining and scanned using an AxioScan Z1 (Carl Zeiss, Germany). Histological analysis was performed using Photoshop CS6 (Adobe Systems, USA) and ImageJ (ImageJ 1.52a, National Institutes of Health, USA).

## 2.6 | Histological analyses

For histomorphometric bone width measurements, polarized light was used to demarcate a vertical line from which new bone was formed after defect creation. The distance from the defects created to the DBBM particles or  $\text{TiO}_2$  blocks were measured and assumed as a constant distance of spontaneous healing (Figure 4a). This was used to assess the width of new bone formation in the empty controls. The use of polarized light did not allow for discrimination between bone formation by spontaneous healing and bone formation following augmentation. Intra-examiner reliability was validated by repeated measurements of ten random sites with a 1-week interval.

For area measurements, the region of interest (ROI) was defined from the borders of the scaffold materials in bucco-lingual direction. The fixation screw was excluded from the analysis. The percentage of new bone and graft material within the ROI was measured (Figure 5). For the empty control sites, area measurements were not applicable as the defect shape varied at the regeneration time point and no graft material could be used as a reference point to define the ROI.

## 2.7 | Statistics

Comparison across groups were performed using parametric one-way analysis of variance (ANOVA) for normalized datasets. Pairwise multiple comparison procedures were done by Holm-Sidak method. When normality test or equal variance test failed, Kruskal-Wallis one-way ANOVA on ranks was performed and pairwise multiple comparison procedures were done by Dunn's method. All statistical analyses were performed using SigmaPlot 14 (Systat Software, San Jose, CA, USA). Statistical significance was set at the 0.05 level. Intra-correlation reliability for repeated measures of alveolar width in microCT and histology were calculated using intraclass correlation coefficient (ICC) two-way mixed effect model, absolute agreement. ICC (95% CI) for the repeated measurements were as follows: 0.985 for the measurements on microCT and 0.930 on histology.

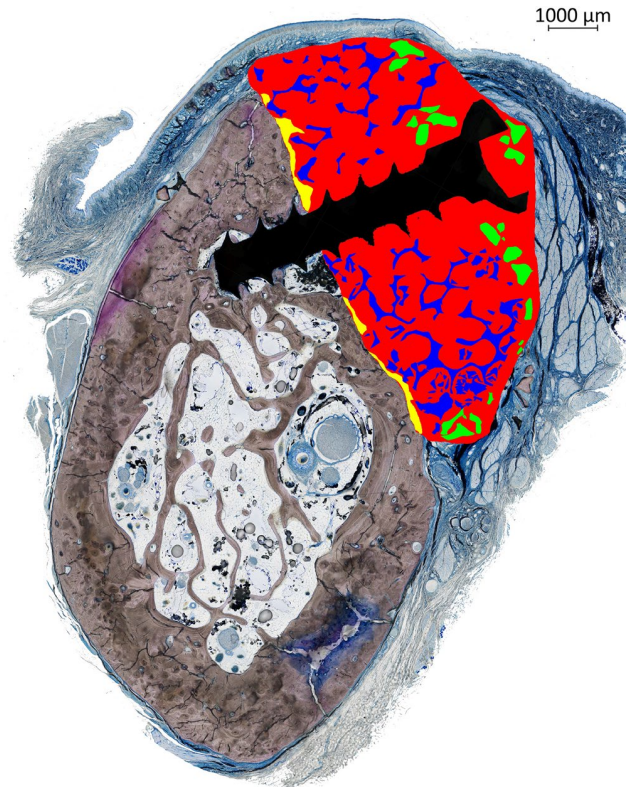


**FIGURE 5** Illustration of the histomorphometric measurements. The coloured area defined as the region of interest, fixation screw excluded in black. Green = DBBM, blue =  $\text{TiO}_2$  scaffold, yellow = new bone within graft material, red = non-mineralized connective tissue

## 3 | RESULTS

Post-operative healing following surgery was uneventful. At the time of euthanasia, the top lateral part of three  $\text{TiO}_2$  blocks in the 4-week healing sites was partially exposed, but was included in subsequent analyses. MicroCT analysis showed one posterior site in the 4-week DBBM particles group without DBBM materials, which was excluded from following analysis. Accordingly, the number of units analysed in this group was one less than presented in Table 1.

### 3.1 | MicroCT

The microCT analysis demonstrated similar total alveolar bone width for all groups. The overall width including lateral volume augmentation by the graft materials was larger for the  $\text{TiO}_2$  block group compared with the DBBM particulate and empty control groups (Figure 3b, Table S1). At the 4-week healing time, only minute quantities of lateral bone formation were observed within grafted sites. At 12 weeks, the DBBM particulate group demonstrated no statistically significant differences in lateral bone formation versus the  $\text{TiO}_2$  block group (Table 2). The  $\text{TiO}_2$  blocks constituted a significantly

**TABLE 2** Results of linear measurements on microCT reconstructions for width of new bone formation (mm), measured at the six millimetre increments

Mm Increments	4 W DBBM group mm (SD)	4 W TiO <sub>2</sub> group mm (SD)	12 W DBBM group mm (SD)	12 W TiO <sub>2</sub> group mm (SD)
1	0.06 (0.15)	0.02 (0.06)	0.37 (0.44)	0.19 (0.19)
2	0.06 (0.13)	0.02 (0.05)	0.56 (0.61)	0.17 (0.15)
3	0.02 (0.04)	0.03 (0.07)	0.41 (0.64)	0.08 (0.09)
4	0 (0)	0.02 (0.06)	0.30 (0.28)	0.08 (0.13)
5	0.02 (0.06)	0 (0)	0.25 (0.33)	0.07 (0.07)
6	0 (0)	0 (0)	0.16 (0.27)	0.10 (0.23)

Note: Presented as mean values with standard deviation. No statistically significant difference was found between positive control and test group at 4 and 12 weeks healing time.

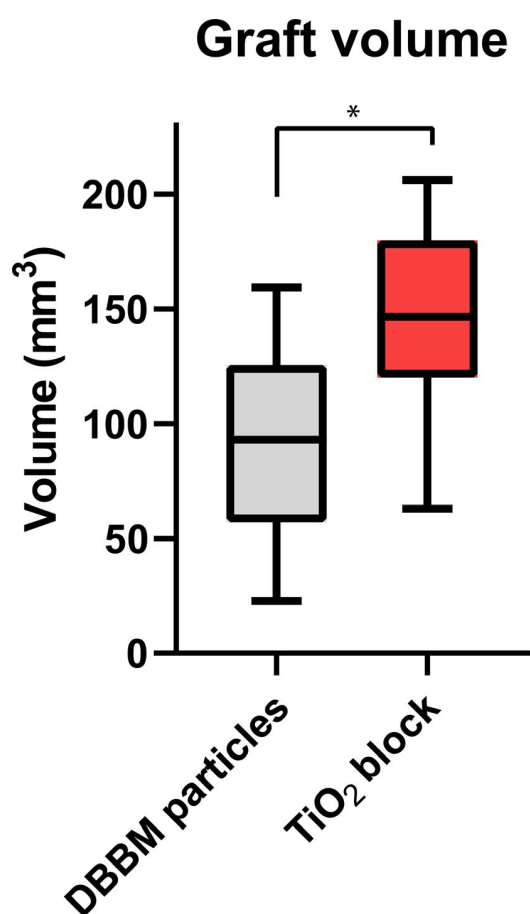


**FIGURE 6** Bar chart of graft volumes. Statistically significant difference ( $p < .001$ ) denoted by asterisk (\*)

larger volume (mean:  $145.8 \text{ mm}^3 \pm 39.2 \text{ mm}^3$ ) compared with the DBBM particles (mean:  $92.9 \text{ mm}^3 \pm 42.3 \text{ mm}^3$ ,  $p < .001$ ) (Figure 6).

The TiO<sub>2</sub> block sites maintained a convex profile, but eight seemed over-contoured to varying degrees compared with a normal ridge. Twelve out of sixteen scaffolds had either bone ingrowth within the porous structures or were in intimate contact with the bone. One scaffold was only partly in contact and three were not in contact with bone. Three out of these four scaffolds were those

exposed clinically. In large, the scaffolds maintained their shape, but fractures were observed, usually at the edges and around the fixation screw. Scaffold segments accumulated at the bottom of the defect in sites of fracture (Figure 3a). In the DBBM particulate group, the arrangement of granules varied from natural ridge shapes, to a more scattered distribution. Eleven sites in this group demonstrated migration of DBBM particles towards the lingual side or apically below the defect base. Clusters of granules were in all but one site in close contact with bone. Stray granules were frequently observed in the sites of TiO<sub>2</sub> blocks and empty controls. This was also found for fractured TiO<sub>2</sub> scaffold pieces, but to a less extent. In the empty controls, five sites contained both DBBM granules and pieces of scaffold, and six sites contained DBBM granules. Thus, only five empty control sites were exempt of graft material migration from the adjacent sites of TiO<sub>2</sub> blocks and DBBM particles. These migrated particles were in general not confined or in contact with bone and appeared free-floating on the microCT scans. The ridge profile was in these sites concave. Ridge profiles were well-contoured when graft materials were not observed.

### 3.2 | Histology

In general, there was more new bone formation after 12 than 4 weeks healing in all groups. The contour of the alveolar bone in the empty controls after 12 weeks appeared to follow the natural contour of the alveolar bone in contrast to the DBBM particles and TiO<sub>2</sub> blocks (Figure 7). In the TiO<sub>2</sub> block group, 12 of the scaffolds were clearly integrated or in close contact with the bone (Figure 8), whereas four presented visible space between the scaffold and bone confirming the microCT results. The scaffolds were for the most part intact, although sections close to the fixation screw demonstrated broken struts in the central part, as described for microCT analysis. These TiO<sub>2</sub> particles could be found at the apical portion of the defect but did not seem to affect the healing process (Figure 7c).

Within the TiO<sub>2</sub> blocks and DBBM granules in close contact with bone organized dense laminar features could be observed, which may be compatible with early mineralization. This was more pronounced in

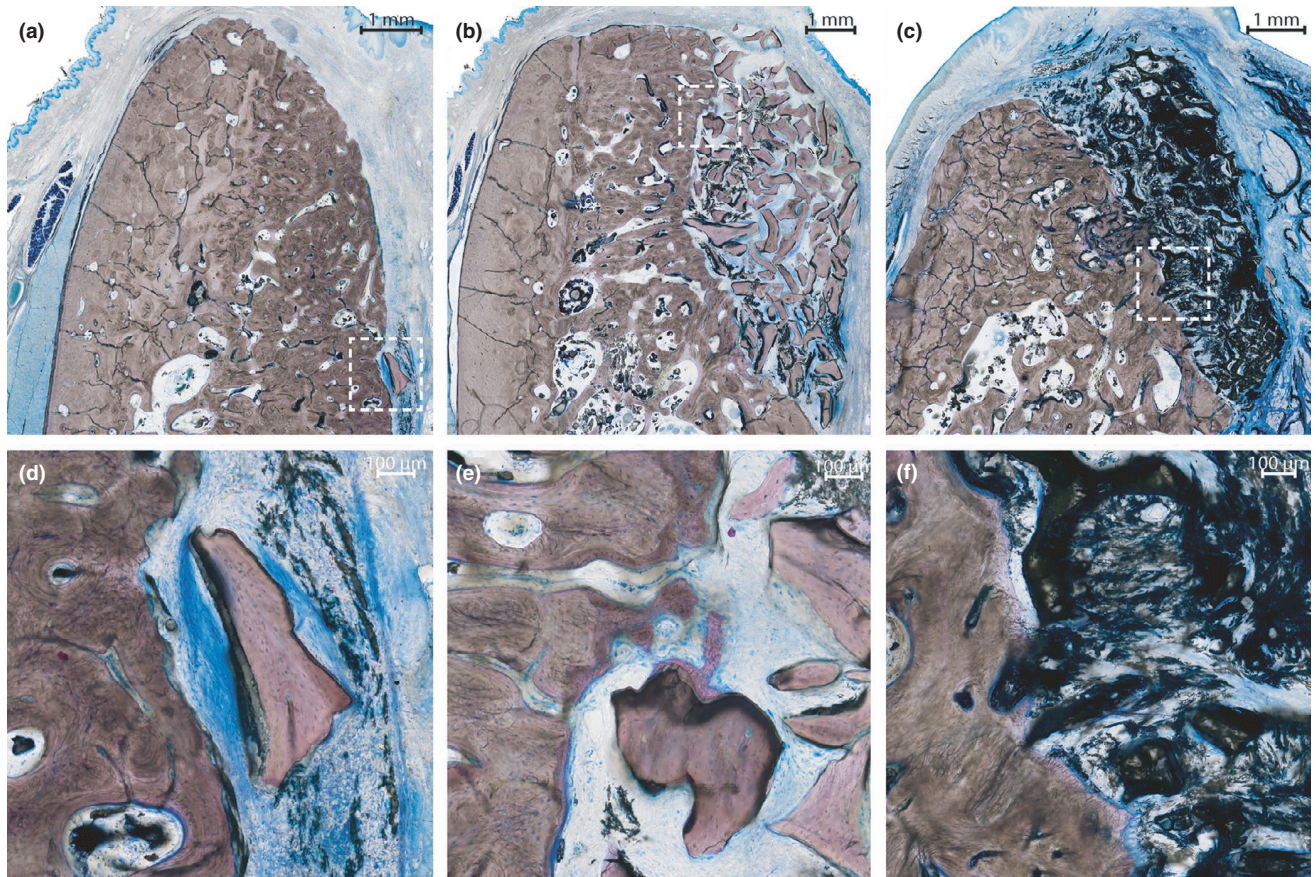


**FIGURE 7** Histological samples of 4-week healing time. (a) Negative control, (b) positive control and (c) test group. All sites demonstrated well-contoured profiles of bone and grafted area. (d - e) Higher magnification images of the highlighted areas above. (d) DBBM granule migrated from adjacent site. Note that the particle is not in contact with bone. (e - f) Grafted material in close contact with parent bone. Note the dense, unidentified lamina structures between the graft materials, particularly pronounced in the test group (f)

the TiO<sub>2</sub> blocks than in the DBBM particles (Figure 7e,f) and could also be seen in close contact with new bone (Figure 8d). These structures were also observed in the empty controls, but to a much less extent and only if graft particles had migrated from adjacent sites (Figure 7d). In DBBM particulate and TiO<sub>2</sub> block sites where new bone was seen, this was confined to the regions of the graft in contact with parent bone. No new bone formation was found at the lateral regions of the grafts.

The shape of the grafted area varied greatly for the DBBM particles, some of which formed a natural shape of the alveolar ridge, while other sites contained only scarce amounts of graft particles. Both DBBM particles and broken scaffold struts were often found outside of their confined sites, not in contact with bone. This was more pronounced for the DBBM particles as DBBM particles could be found in most of the adjacent sites.

### 3.3 | Histomorphometry

The bone width measurements are presented in Figure 4b. For the coronal four millimetres, the empty control sites demonstrated more lateral new bone formation than the sites with graft materials. A

statistically significant difference was observed at 12-week healing, millimetre increment 2, between DBBM particulate group and empty control group.

The area analyses are presented in Table 3. At 4 weeks healing time, the DBBM particulate sites demonstrated a statistically significant higher fraction of new bone of  $1.87\% \pm 2.55\%$  compared with  $0.17\% \pm 0.33\%$  in the TiO<sub>2</sub> blocks ( $p = .021$ ). The TiO<sub>2</sub> blocks had a higher porosity and thus constituted a significantly smaller fraction of the ROI than the DBBM particles,  $12.06\% \pm 4.38\%$  compared with  $22.63\% \pm 10.12\%$  ( $p = .037$ ). At 12 weeks healing time, no statistically significant difference was found between DBBM particulate and TiO<sub>2</sub> block sites for new bone formation. Both groups demonstrated an increase in the fraction of new bone from 4 to 12 weeks healing time. The DBBM particles increased to  $9.69\% \pm 11.27\%$  while the TiO<sub>2</sub> blocks increased to  $5.48\% \pm 5.29\%$ , which was a statistically significant difference compared with the new bone fraction at 4 weeks healing time ( $p = .003$ ).

In the TiO<sub>2</sub> blocks, migrated DBBM granules constituted  $2.2\% \pm 2.1\%$  and  $3.4\% \pm 2.5\%$  of the ROI at 4 weeks and 12 weeks healing time, respectively. For the DBBM particles, the fraction of migrated TiO<sub>2</sub> scaffold pieces was  $0.1\% \pm 0.3\%$  and  $0.4\% \pm 0.7\%$ .



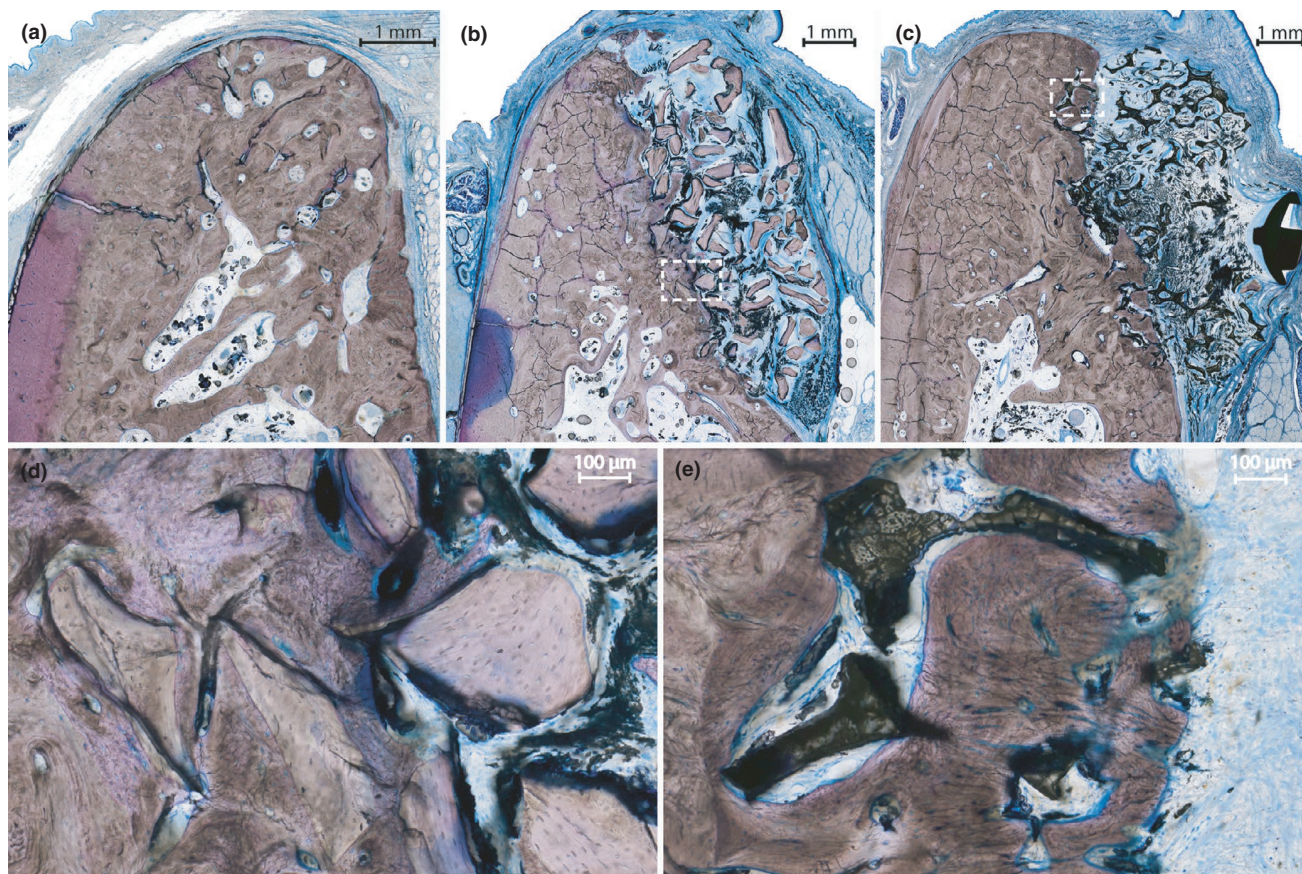


**FIGURE 8** Histological samples of 12-week healing time. (a) Negative control, (b) positive control and (c) test group. (d) Higher magnification images of the highlighted area in (b). DBBM granules clearly integrated in bone and novel bone formation at the interface. Note the dense, unidentified laminar structures in contact with novel bone (e) Higher magnification images of the highlighted area in (c) demonstrated bone growth within the porous structures of the scaffold

**TABLE 3** Results of histomorphometric measurements for the constituents within the region of interest (ROI)

	4 Week		12 Week	
	Mean %	SD	Mean %	SD
<b>DBBM particles group</b>				
DBBM particles	22.6	10.1	19.5	6.6
TiO <sub>2</sub>	0.1	0.3	0.4	0.7
New bone	1.9	2.6	9.7	11.3
<b>TiO<sub>2</sub> block group</b>				
DBBM particles	2.2	2.1	3.4	2.5
TiO <sub>2</sub>	12.1	4.4	14.0	3.7
New bone	0.2	0.3	5.5	5.3

## 4 | DISCUSSION

This study demonstrated that lateral augmentation by GBR in chronic bone defects with the use of a synthetic bone TiO<sub>2</sub> block and a collagen membrane withheld a greater width and volume augmentation, but presented less new bone formation at 4 and 12 weeks, as compared to DBBM particles or empty controls.

The TiO<sub>2</sub> blocks have in previous studies demonstrated potential for angiogenesis and bone ingrowth in acute defect models (H. J. Haugen et al., 2013; Tiainen et al., 2012; Verket et al., 2016). In the present study, new bone formation within the grafted region was also observed in a chronic bone defect model. The extent of new bone formation is in part similar to other studies in chronic bone defects. Sanz et al. utilized the same surgical protocol in the beagle dog, but different healing times and a DBBM in a collagen matrix (Sanz et al., 2017). The reported amount of graft material within the region of interest when using DBBM in collagen and a collagen membrane was 17%, 22% and 16% after 2 weeks, 6 weeks and 3 months, respectively. These findings are comparable with the present study, but the authors reported a considerably higher amount of new mineralized tissue formation: 7%, 26% and 36% after the three healing times, respectively. However, the horizontal linear measurements of new mineralized tissue after 3 months were  $0.79 \pm 0.39$  mm,  $0.35 \pm 0.24$  mm and  $0.46 \pm 0.6$  mm, which coincided more with the results of the present study. The differences may partly be due to different histological processing and thresholding, or differences in the defined total grafted area. Even though the DBBM material was embedded in collagen blocks in the study by Sanz and co-workers, particles were still found to

migrate to adjacent membrane-covered sites and constituted 6%–7% of the ROI at all three-time points. Lee et al. employed a similar defect model, also in the beagle dog, to evaluate two different biphasic calcium phosphate (BCP) block bone grafts and two different collagen membranes (Lee et al., 2020). Their horizontal linear histomorphometric analysis showed increased bone width at four weeks, ranging from 0.05 mm to 1.01 mm for the different materials tested. However, the measurements after 8 weeks healing were comparable with the results found in the present study after 12 weeks, with a range from 0.00 mm to 1.13 mm. After 16 weeks, one of the BCP materials rendered increased bone width varying from 0.29 mm to 3.24 mm at the five incremental measuring points, while the other material ranged from 0.08 mm to 0.37 mm. The authors hypothesized a slow bone formation process in this defect model. Slow bone formation was also found by Araújo et al. when autologous bone and DBBM blocks were compared in a chronic bone healing defect model in dogs (Araújo et al., 2002). They reported an amount of new mineralized bone of  $23\% \pm 3\%$  for DBBM and  $47\% \pm 5\%$  for autologous bone after 6 months. The authors found that DBBM blocks maintained its volume and resorbed slowly. They reported that the new bone within the graft extended from the parent bone. Only limited bone formation was observed in peripheral areas.

The present study found a similar osteoconductive growth pattern for both graft materials. For all groups, the average total width of the alveolar bone increased from the 4-week healing time to 12-week healing time. The gain was largest for the empty controls, followed by the DBBM particles and TiO<sub>2</sub> blocks. This suggests slow bone regeneration in this model and particularly for the grafted sites. These findings coincide with a network meta-analysis by Al-Moraissi et al. suggesting that materials with a slow resorption rate results in slower bone formation compared to autogenous grafts (Al-Moraissi et al., 2020). However, studies have also reported higher regeneration of bone at the early stages of healing in chronic bone defects (Schmid et al., 1997; Stavropoulos et al., 2001). A longer observation period in the present study would provide further information about the scaffold's osteoconductive potential.

The TiO<sub>2</sub> blocks' ability to withhold the augmented volume over the observed healing times in the present study was confirmed both by two-dimensional width measurements and volumetric measurements of the grafts. This suggests a potential for this material to be combined with growth factors or osteoinductive factors to enhance new bone formation. Bone morphogenetic proteins (BMP) and fibroblast growth factor (FGF) are potent osteoinductive factors which may be used for bone regeneration (Dimitriou et al., 2011; Hallman & Thor, 2008). The porous structure of the TiO<sub>2</sub> block may provide a suitable carrier system for such factors (McKay et al., 2007), which may yield an osteoinductive biomaterial with sufficient mechanical strength.

The histomorphometric analysis showed a higher density of the TiO<sub>2</sub> scaffold in this study compared with a study by Verket et al. in the minipig (Anders Verket et al., 2016). The difference could be due to the different animal and study designs, evaluating an acute

dehiscence defect versus a lateral augmentation in a chronic bone defect model. As the defects in the present study were non-contained, the loading exerted on the scaffold was probably higher. Dogs may grind their cheeks against the cage upon surgery assorting additional mechanical stresses to the bone graft, which differs from a clinical situation.

Three TiO<sub>2</sub> blocks were partly exposed at the final healing time, whereas no exposure of the DBBM particulate graft was observed. A recent systematic review on allogeneic and autogenous block grafts reported considerable graft exposure incidences with the use of block grafts for horizontal ridge augmentation (Starch-Jensen et al., 2020). It is not unreasonable that a rigid block graft is more prone to exposure as compared to the more adaptable nature of particulate grafts. Hence, a limitation of the study is the comparison not only of two materials with different surface topography and chemical composition but also with widely different architectural design. A previous *in vitro* study demonstrated a higher porosity for TiO<sub>2</sub> particles as compared to DBBM particles and a higher interconnectivity at pore sizes required for vascular growth (Sabetrasekh et al., 2010). This corroborates the histomorphometric findings from the present study. Despite this difference, the more bone ingrowth in DBBM particle sites could be due to the particulate nature of this material as compared a rigid block. A previous clinical study compared corticocancellous allograft blocks to a particulate graft mix of DBBM and autogenous bone for mandibular augmentation (Amorfini et al., 2014). The authors reported similar volumes of regenerated bone as assessed by CBCT after 1 year.

Even though fractures of the TiO<sub>2</sub> blocks were observed, the architecture was maintained suggesting adequate mechanical strength in this model. Combined with its non-resorbable property, this may be considered an advantage in cases where the space-maintaining function is needed for a longer time period. The differences between acute and chronic models may explain the noticeably lower amount of new bone formation within the TiO<sub>2</sub> blocks in the present study. Verket et al. reported a mean new bone fraction of  $37\% \pm 14.6\%$  by histomorphometric measurements, while Haugen et al. reported a median fraction of 31.7% (26.5%–38.3%) by volumetric microCT measurements (H. J. Haugen et al., 2013; Anders Verket et al., 2016). GBR in chronic defects is clinically more relevant and challenging, as freshly created and contained defects do not represent a clinical situation.

Complications with exposure of fixation screws or grafts, biofilm formation and inflammation are frequently reported in GBR (Olsen et al., 2004; Schwarz et al., 2010; Simion et al., 2006; Yeo et al., 2012). Four of the scaffolds were not in intimate contact with bone, despite the use of both fixation screw, membrane and pins (Mir-Mari et al., 2016). Three of these were found clinically exposed at the end of the study. One may speculate whether the scaffolds were erroneously fixated or disengaged during healing. The fixation screw had a relatively small head, which concentrated the tightening forces on a small area of the brittle scaffolds. A better force distribution could potentially improve stability for this particular material. In

the present study, DBBM granules and broken TiO<sub>2</sub> block particles were found to migrate to adjacent defect sites. This may have affected the results for the empty control sites, as only five were truly empty at the time of harvest.

The analysis of chronic bone defects is challenging since each defect heals uniquely. Borders and baselines are difficult to define and subjective thresholds reduce the validity of the analysis. This complicates comparison of different sites and materials. In the present study, the contour of the graft materials was assumed the baseline border for GBR. The TiO<sub>2</sub> blocks were fixed and thus defining the baseline border for GBR by the contour of the graft materials seems rational. Some dislocation of the DBBM particles cannot be ruled out, which may have led to discrepancies of the defined baseline border for this group. In the study by Sanz et al., polarized light was used to distinguish the line of demarcation between parent bone and newly formed bone (Sanz et al., 2017). Attempts to replicate this method failed to discriminate between bone formed after defect creation and following augmentation. A longer healing time of 3 months prior to GBR compared with 2 months in the present study could explain why this was not achievable. More samples and control groups may provide further and more precise comparisons between the groups. The histological analysis in this study could not precisely identify all structures within the grafted materials and further studies, histological and immunohistochemical analyses are warranted.

## 5 | CONCLUSION

In conclusion, within the limitations of the study, the largest lateral volume augmentation was obtained with the non-resorbable TiO<sub>2</sub> blocks. The TiO<sub>2</sub> blocks demonstrated less new bone formation than the DBBM particles. However, the largest width of mineralized bone was observed with the use of a collagen membrane only.

### ACKNOWLEDGEMENTS

The authors would like to express their gratitude to Hanna Tiainen at the Department of Biomaterials, Faculty of Dentistry, University of Oslo, Catherine Anne Hayward and Liebert Parreiras Nogueira at the Clinical Oral Research Laboratory, Faculty of Dentistry, University of Oslo for their help preparing and analysing the materials. Special thanks to the investigators Javier Núñez, Rafael Pla, Fernando Luengo, Riccardo Di Raimondo and Georgios Antonoglou from the Complutense University, Madrid, Spain. This work was supported by the Research Council of Norway (FRINATEK grant number 231530).

### CONFLICT OF INTEREST

Lyngstadaas and Haugen hold patents for the technology for the TiO<sub>2</sub> bone graft substitute (EP Patent 2,121,053, US Patent 9,629,941). The rights for these patents are shared between the University of Oslo and Corticalis AS. Haugen and Lyngstadaas are shareholders and board members of Corticalis AS. The other authors report no conflicts of interest related to this study.

### AUTHOR CONTRIBUTION

**Minh Khai Le Thieu:** Formal analysis (equal); Investigation (equal); Visualization (equal); Writing-original draft (lead); Writing-review & editing (equal). **Håvard Jostein Jostein Haugen:** Conceptualization (equal); Funding acquisition (equal); Investigation (equal); Methodology (equal); Project administration (equal); Resources (equal); Writing-original draft (equal); Writing-review & editing (equal). **Javier Sanz-Esporrin:** Conceptualization (equal); Investigation (equal); Writing-original draft (equal); Writing-review & editing (equal). **Mariano Sanz:** Conceptualization (equal); Funding acquisition (equal); Methodology (equal); Writing-original draft (equal); Writing-review & editing (equal). **Staalet Petter Lyngstadaas:** Investigation (equal); Writing-original draft (equal); Writing-review & editing (equal). **Anders Verket:** Investigation (equal); Supervision (equal); Writing-original draft (equal); Writing-review & editing (equal).

### DATA AVAILABILITY STATEMENT

The data that support the findings of this study are available from the corresponding author upon reasonable request.

### ORCID

Minh Khai Le Thieu  <https://orcid.org/0000-0003-1712-9276>

Håvard Jostein Haugen  <https://orcid.org/0000-0002-6690-7233>

Javier Sanz-Esporrin  <https://orcid.org/0000-0003-0859-3149>

Mariano Sanz  <https://orcid.org/0000-0002-6293-5755>

Anders Verket  <https://orcid.org/0000-0002-4862-9030>

### REFERENCES

- Al-Moraissi, E. A., Alkhatari, A. S., Abotaleb, B., Altairi, N. H., & Del Fabbro, M. (2020). Do osteoconductive bone substitutes result in similar bone regeneration for maxillary sinus augmentation when compared to osteogenic and osteoinductive bone grafts? A systematic review and frequentist network meta-analysis. *International Journal of Oral and Maxillofacial Surgery*, 49(1), 107–120. <https://doi.org/10.1016/j.ijom.2019.05.004>
- Amorfini, L., Migliorati, M., Signori, A., Silvestrini-Biavati, A., & Benedicenti, S. (2014). Block allograft technique versus standard guided bone regeneration: A randomized clinical trial. *Clinical Implant Dentistry and Related Research*, 16(5), 655–667. <https://doi.org/10.1111/cid.12040>
- Araújo, M. G., Sonohara, M., Hayacibara, R., Cardaropoli, G., & Lindhe, J. (2002). Lateral ridge augmentation by the use of grafts comprised of autologous bone or a biomaterial. An experiment in the dog. *Journal of Clinical Periodontology*, 29(12), 1122–1131. <https://doi.org/10.1034/j.1600-051X.2002.291213.x>
- Benic, G. I., & Hämmerle, C. H. F. (2014). Horizontal bone augmentation by means of guided bone regeneration. *Periodontology 2000*, 66(1), 13–40. <https://doi.org/10.1111/prd.12039>
- Carson, J. S., & Bostrom, M. P. G. (2007). Synthetic bone scaffolds and fracture repair. *Injury*, 38(1), S33–S37. <https://doi.org/10.1016/j.injury.2007.02.008>
- Chiapasco, M., Zaniboni, M., & Boisco, M. (2006). Augmentation procedures for the rehabilitation of deficient edentulous ridges with oral implants. *Clin Oral Implants Res*, 17(S2), 136–159. <https://doi.org/10.1111/j.1600-0501.2006.01357.x>
- Clavero, J., & Lundgren, S. (2003). Ramus or chin grafts for maxillary sinus inlay and local onlay augmentation: Comparison of donor site

- morbidity and complications. *Clinical Implant Dentistry and Related Research*, 5(3), 154–160. <https://doi.org/10.1111/j.1708-8208.2003.tb00197.x>
- Dimitriou, R., Jones, E., McGonagle, D., & Giannoudis, P. V. (2011). Bone regeneration: Current concepts and future directions. *BMC Medicine*, 9, 66. <https://doi.org/10.1186/1741-7015-9-66>
- Elgali, I., Omar, O., Dahlin, C., & Thomsen, P. (2017). Guided bone regeneration: Materials and biological mechanisms revisited. *European Journal of Oral Sciences*, 125(5), 315–337. <https://doi.org/10.1111/eos.12364>
- Hallman, M., & Thor, A. (2008). Bone substitutes and growth factors as an alternative/complement to autogenous bone for grafting in implant dentistry. *Periodontology 2000*, 47(1), 172–192. <https://doi.org/10.1111/j.1600-0757.2008.00251.x>
- Hanisch, O., Sorensen, R. G., Kinoshita, A., Spiekermann, H., Wozney, J. M., & Wikesjö, U. M. E. (2003). Effect of recombinant human bone morphogenetic protein-2 in dehiscence defects with non-submerged immediate implants: An experimental study in cynomolgus monkeys. *Journal of Periodontology*, 74(5), 648–657. <https://doi.org/10.1902/jop.2003.74.5.648>
- Haugen, H. J., Lyngstadaas, S. P., Rossi, F., & Perale, G. (2019). Bone grafts: Which is the ideal biomaterial? *Journal of Clinical Periodontology*, 46(S21), 92–102. <https://doi.org/10.1111/jcpe.13058>
- Haugen, H. J., Monjo, M., Rubert, M., Verket, A., Lyngstadaas, S. P., Ellingsen, J. E., Rønold, H. J., & Wohlfahrt, J. C. (2013). Porous ceramic titanium dioxide scaffolds promote bone formation in rabbit peri-implant cortical defect model. *Acta Biomaterialia*, 9(2), 5390–5399. <https://doi.org/10.1016/j.actbio.2012.09.009>
- Hürzeler, M. B., Kirsch, A., Ackermann, K. L., & Quiñones, C. R. (1996). Reconstruction of the severely resorbed maxilla with dental implants in the augmented maxillary sinus: A 5-year clinical investigation. *International Journal of Oral and Maxillofacial Implants*, 11(4), 466–475.
- Kilkenny, C., Browne, W. J., Cuthill, I. C., Emerson, M., & Altman, D. G. (2010). Improving bioscience research reporting: The ARRIVE guidelines for reporting animal research. *PLOS Biology*, 8(6), e1000412. <https://doi.org/10.1371/journal.pbio.1000412>
- Lee, J.-T., Cha, J.-K., Kim, S., Jung, U.-W., Thoma, D. S., & Jung, R. E. (2020). Lateral onlay grafting using different combinations of soft-type synthetic block grafts and resorbable collagen membranes: An experimental in vivo study. *Clinical Oral Implants Research*, 31(4), 303–314. <https://doi.org/10.1111/clr.13566>
- McAllister, B. S., & Haghghat, K. (2007). Bone augmentation techniques. *Journal of Periodontology*, 78(3), 377–396. <https://doi.org/10.1902/jop.2007.060048>
- McKay, W. F., Peckham, S. M., & Badura, J. M. (2007). A comprehensive clinical review of recombinant human bone morphogenetic protein-2 (INFUSE Bone Graft). *International Orthopaedics*, 31(6), 729–734. <https://doi.org/10.1007/s00264-007-0418-6>
- Mir-Mari, J., Wui, H., Jung, R. E., Hämmerle, C. H. F., & Benic, G. I. (2016). Influence of blinded wound closure on the volume stability of different GBR materials: An in vitro cone-beam computed tomographic examination. *Clinical Oral Implants Research*, 27(2), 258–265. <https://doi.org/10.1111/clr.12590>
- Moy, P. K., & Aghaloo, T. (2019). Risk factors in bone augmentation procedures. *Periodontology 2000*, 81(1), 76–90. <https://doi.org/10.1111/prd.12285>
- Nkenke, E., & Neukam, F. W. (2014). Autogenous bone harvesting and grafting in advanced jaw resorption: Morbidity, resorption and implant survival. *European Journal of Oral Implantology*, 7(Suppl 2), S203–217.
- Nkenke, E., Schultze-Mosgau, S., Kloss, F., Neukam, F. W., & Radespiel-Tröger, M. (2001). Morbidity of harvesting of chin grafts: A prospective study. *Clinical Oral Implants Research*, 12(5), 495–502. <https://doi.org/10.1034/j.1600-0501.2001.120510.x>
- Nyman, S., Gottlow, J., Karring, T., & Lindhe, J. (1982). The regenerative potential of the periodontal ligament. An experimental study in the monkey. *Journal of Clinical Periodontology*, 9(3), 257–265. <https://doi.org/10.1111/j.1600-051x.1982.tb02065.x>
- Olsen, M. L., Aaboe, M., Hjørting-Hansen, E., & Hansen, A. K. (2004). Problems related to an intraoral approach for experimental surgery on minipigs. *Clinical Oral Implants Research*, 15(3), 333–338. <https://doi.org/10.1111/j.1600-0501.2004.01016.x>
- Ortiz-Vigón, A., Suarez, I., Martínez-Villa, S., Sanz-Martín, I., Bollain, J., & Sanz, M. (2018). Safety and performance of a novel collagenated xenogeneic bone block for lateral alveolar crest augmentation for staged implant placement. *Clinical Oral Implants Research*, 29(1), 36–45. <https://doi.org/10.1111/clr.13036>
- Raghoobar, G. M., Louwse, C., Kalk, W. W. I., & Vissink, A. (2001). Morbidity of chin bone harvesting. *Clinical Oral Implants Research*, 12(5), 503–507. <https://doi.org/10.1034/j.1600-0501.2001.120511.x>
- Retzepi, M., & Donos, N. (2010). Guided Bone Regeneration: Biological principle and therapeutic applications. *Clinical Oral Implants Research*, 21(6), 567–576. <https://doi.org/10.1111/j.1600-0501.2010.01922.x>
- Sabetrasekh, R., Tiainen, H., Lyngstadaas, S. P., Reseland, J., & Haugen, H. (2010). A novel ultra-porous titanium dioxide ceramic with excellent biocompatibility. *Journal of Biomaterials Applications*, 25(6), 559–580. <https://doi.org/10.1177/0885328209354925>
- Sanz, M., Dahlin, C., Apatzidou, D., Artzi, Z., Bozic, D., Calciolari, E., & Schliephake, H. (2019). Biomaterials and regenerative technologies used in bone regeneration in the craniomaxillofacial region: Consensus report of group 2 of the 15th European Workshop on Periodontology on Bone Regeneration. *Journal of Clinical Periodontology*, 46(Suppl 21), 82–91. <https://doi.org/10.1111/jcpe.13123>
- Sanz, M., Ferrantino, L., Vignoletti, F., de Sanctis, M., & Berglundh, T. (2017). Guided bone regeneration of non-contained mandibular buccal bone defects using deproteinized bovine bone mineral and a collagen membrane: An experimental in vivo investigation. *Clinical Oral Implants Research*, 28(11), 1466–1476. <https://doi.org/10.1111/clr.13014>
- Sanz, M., & Vignoletti, F. (2015). Key aspects on the use of bone substitutes for bone regeneration of edentulous ridges. *Dental Materials*, 31(6), 640–647. <https://doi.org/10.1016/j.dental.2015.03.005>
- Sanz-Sanchez, I., Ortiz-Vigón, A., Sanz-Martín, I., Figuero, E., & Sanz, M. (2015). Effectiveness of lateral bone augmentation on the alveolar crest dimension: A systematic review and meta-analysis. *Journal of Dental Research*, 94(9 Suppl), 128s–142s. <https://doi.org/10.1177/0022034515594780>
- Schaaf, H., Lendeckel, S., Howaldt, H.-P., & Streckbein, P. (2010). Donor site morbidity after bone harvesting from the anterior iliac crest. *Oral Surgery, Oral Medicine, Oral Pathology, Oral Radiology, and Endodontology*, 109(1), 52–58. <https://doi.org/10.1016/j.tripl.2009.08.023>
- Schmid, J., Hämmerle, C. H. F., Flickiger, L., Winkler, J. R., Olah, A. J., Gogolewskiz, S., & Lang, N. P. (1997). Blood-filled spaces with and without filler materials in guided bone regeneration. A comparative experimental study in the rabbit using bioresorbable membranes. *Clinical Oral Implants Research*, 8(2), 75–81. <https://doi.org/10.1034/j.1600-0501.1997.080201.x>
- Schropp, L., Wenzel, A., Kostopoulos, L., & Karring, T. (2003). Bone healing and soft tissue contour changes following single-tooth extraction: A clinical and radiographic 12-month prospective study. *International Journal of Periodontics and Restorative Dentistry*, 23(4), 313–323.
- Schwarz, F., Ferrari, D., Podolsky, L., Mihatovic, I., & Becker, J. (2010). Initial pattern of angiogenesis and bone formation following lateral ridge augmentation using rhPDGF and guided bone regeneration: An immunohistochemical study in dogs. *Clinical Oral Implants Research*, 21(1), 90–99. <https://doi.org/10.1111/j.1600-0501.2009.01845.x>
- Simion, M., Rocchietta, I., Kim, D., Nevins, M., & Fiorellini, J. (2006). Vertical ridge augmentation by means of deproteinized bovine bone

- block and recombinant human platelet-derived growth factor-BB: A histologic study in a dog model. *International Journal of Periodontics and Restorative Dentistry*, 26(5), 415–423.
- Sogal, A., & Tofe, A. J. (1999). Risk assessment of bovine spongiform encephalopathy transmission through bone graft material derived from bovine bone used for dental applications. *Journal of Periodontology*, 70(9), 1053–1063. <https://doi.org/10.1902/jop.1999.70.9.1053>
- Starch-Jensen, T., Deluiz, D., & Tinoco, E. M. B. (2020). Horizontal alveolar ridge augmentation with allogeneic bone block graft compared with autogenous bone block graft: A systematic review. *Journal of Oral & Maxillofacial Research*, 11(1), e1. <https://doi.org/10.5037/jomr.2020.11101>
- Stavropoulos, A., Kostopoulos, L., Mardas, N., Randel Nyengaard, J., & Karring, T. (2001). Deproteinized bovine bone used as an adjunct to guided bone augmentation: An experimental study in the rat. *Clinical Implant Dentistry and Related Research*, 3(3), 156–165. <https://doi.org/10.1111/j.1708-8208.2001.tb00136.x>
- Tiainen, H., Wiedmer, D., & Haugen, H. J. (2013). Processing of highly porous TiO<sub>2</sub> bone scaffolds with improved compressive strength. *Journal of the European Ceramic Society*, 33(1), 15–24. <https://doi.org/10.1016/j.jeurceramsoc.2012.08.016>
- Tiainen, H., Wohlfahrt, J. C., Verket, A., Lyngstadaas, S. P., & Haugen, H. J. (2012). Bone formation in TiO<sub>2</sub> bone scaffolds in extraction sockets of minipigs. *Acta Biomaterialia*, 8(6), 2384–2391. <https://doi.org/10.1016/j.actbio.2012.02.020>
- Tonetti, M. S., Hämmerle, C. H. F., & European Workshop on Periodontology Group C (2008). Advances in bone augmentation to enable dental implant placement: Consensus Report of the Sixth European Workshop on Periodontology. *Journal of Clinical Periodontology*, 35(s8), 168–172. <https://doi.org/10.1111/j.1600-051X.2008.01268.x>
- Verket, A., Müller, B., Wohlfahrt, J. C., Lyngstadaas, S. P., Ellingsen, J. E., Jostein Haugen, H., & Tiainen, H. (2016). TiO<sub>2</sub> scaffolds in peri-implant dehiscence defects: An experimental pilot study. *Clinical Oral Implants Research*, 27(10), 1200–1206. <https://doi.org/10.1111/clr.12725>
- Verket, A., Tiainen, H., Haugen, H. J., Lyngstadaas, S. P., Nilsen, O., & Reseland, J. E. (2012). Enhanced osteoblast differentiation on scaffolds coated with TiO<sub>2</sub> compared to SiO<sub>2</sub> and CaP coatings. *Biointerphases*, 7(1–4), 36. <https://doi.org/10.1007/s13758-012-0036-8>
- Yeo, A., Cheok, C., Teoh, S. H., Zhang, Z. Y., Buser, D., & Bosshardt, D. D. (2012). Lateral ridge augmentation using a PCL-TCP scaffold in a clinically relevant but challenging micropig model. *Clinical Oral Implants Research*, 23(12), 1322–1332. <https://doi.org/10.1111/j.1600-0501.2011.02366.x>

## SUPPORTING INFORMATION

Additional supporting information may be found online in the Supporting Information section.

**How to cite this article:** Thieu MKL, Haugen HJ, Sanz-Esporrin J, Sanz M, Lyngstadaas SP, Verket A. Guided bone regeneration of chronic non-contained bone defects using a volume stable porous block TiO<sub>2</sub> scaffold: An experimental in vivo study. *Clin Oral Impl Res*. 2021;00:1–13. <https://doi.org/10.1111/clr.13708>
















# Immunohistochemical comparison of lateral bone augmentation using a synthetic TiO<sub>2</sub> block or a xenogeneic graft in chronic alveolar defects

Minh Khai Le Thieu DDS, MSc<sup>1,2</sup>  | Sabine Stoetzel PhD<sup>2</sup> | Maryam Rahmati PhD<sup>1</sup> |  
 Thaqif El Khassawna PhD<sup>2</sup>  | Anders Verket DDS, PhD<sup>3</sup>  |  
 Javier Sanz-Esporrin DDS, PhD<sup>4</sup>  | Mariano Sanz MD, DDS, PhD<sup>4</sup>  |  
 Jan Eirik Ellingsen DDS, PhD<sup>5</sup>  | Håvard Jostein Haugen PhD<sup>1</sup> 

<sup>1</sup>Department of Periodontology, Institute of Clinical Dentistry, Faculty of Dentistry, University of Oslo, Oslo, Norway

<sup>2</sup>Department of Biomaterials, Institute of Clinical Dentistry, Faculty of Dentistry, University of Oslo, Oslo, Norway

<sup>3</sup>Department of Experimental Trauma Surgery, Faculty of Medicine, Justus-Liebig University Giessen, Giessen, Germany

<sup>4</sup>Periodontology, University Complutense of Madrid, Madrid, Spain

<sup>5</sup>Department of Prosthetics and Oral Function, University of Oslo, Oslo, Norway

## Correspondence

Håvard Jostein Haugen, Department of Biomaterials, Faculty of Dentistry, Institute of Clinical Dentistry, University of Oslo, Box 1109 Blindern, 0317 Oslo, Norway.  
 Email: [h.j.haugen@odont.uio.no](mailto:h.j.haugen@odont.uio.no)

## Funding information

Marie Skłodowska-Curie Actions (MSCA), Grant/Award Number: 811226; Norges Forskningsråd, Grant/Award Number: 231530; European Training Network; the Research Council; Research Council of Norway (FRINATEK)

## Abstract

**Objectives:** To evaluate osteogenic markers and alveolar ridge profile changes in guided bone regeneration (GBR) of chronic noncontained bone defects using a non-resorbable TiO<sub>2</sub> block.

**Materials and Methods:** Three buccal bone defects were created in each hemimandible of eight beagle dogs and allowed to heal for 8 weeks before GBR. Treatment was assigned by block randomization: TiO<sub>2</sub> block: TiO<sub>2</sub>-scaffold and a collagen membrane, DBBM particulates: Deproteinized bovine bone mineral (DBBM) and a collagen membrane, Empty control: Only collagen membrane. Bone regeneration was assessed on two different healing timepoints: early (4 weeks) and late healing (12 weeks) using several immunohistochemistry markers including alpha-smooth muscle actin ( $\alpha$ -SMA), osteopontin, osteocalcin, tartrate-resistant acid phosphatase, and collagen type I. Histomorphometry was performed on Movat Pentachrome-stained and Von Kossa/Van Gieson-stained sections. Stereolithographic (STL) models were used to compare alveolar profile changes.

**Results:** The percentage of  $\alpha$ -SMA and osteopontin increased in TiO<sub>2</sub> group after 12 weeks of healing at the bone-scaffold interface, while collagen type I increased in the empty control group. In the defect area,  $\alpha$ -SMA decreased in the empty control group, while collagen type I increased in the DBBM group. All groups maintained alveolar profile from 4 to 12 weeks, but TiO<sub>2</sub> group demonstrated the widest soft tissue contour profile.

**Conclusions:** The present findings suggested contact osteogenesis when GBR is performed with a TiO<sub>2</sub> block or DBBM particulates. The increase in osteopontin indicated a potential for bone formation beyond 12 weeks. The alveolar profile data indicated a sustained lateral increase in lateral bone augmentation using a TiO<sub>2</sub> block and a collagen membrane, as compared with DBBM and a collagen membrane or a collagen membrane alone.

This is an open access article under the terms of the [Creative Commons Attribution](https://creativecommons.org/licenses/by/4.0/) License, which permits use, distribution and reproduction in any medium, provided the original work is properly cited.

© 2022 The Authors. *Clinical Implant Dentistry and Related Research* published by Wiley Periodicals LLC.

**KEYWORDS**

animal experimentation, bone regeneration, bone substitutes, guided tissue regeneration, immunohistochemistry, xenografts

**What is known**

Lateral bone augmentation in chronic alveolar defects using a bone graft material usually leads to contact osteogenesis. Histological analysis may be used to describe the morphological situation, but gives limited information of the potential for bone formation.

**What this study adds**

Immunohistological data obtained by microtome sectioning MMA embedded samples indicates potential for further bone formation beyond 12 weeks healing.

## 1 | INTRODUCTION

Guided bone regeneration (GBR) employs a membrane as a mechanical barrier to avoid soft tissue involvement in the healing process. Thereby, the osteogenic potential that achieves bone augmentation arises from the bony defect's walls. The standard protocol commonly combines graft material with a membrane to create space for new bone formation and avoid soft tissue infiltration. Although some clinical studies have shown predictable bone gain,<sup>1,2</sup> others have reported less bone formation when using a graft material compared with when using the membrane alone.<sup>3–6</sup>

In a previous *in vivo* experimental study,<sup>7</sup> GBR with a collagen membrane alone was compared with deproteinized bovine bone mineral (DBBM) and a ceramic TiO<sub>2</sub> scaffold. Less bone formation was observed in the TiO<sub>2</sub> and DBBM groups when compared with membrane alone group at the final follow-up time point after 12 weeks of healing. However, the groups using bone replacement grafts demonstrated increased volumetric lateral bone augmentation. In this study, however, these findings were assessed by microcomputed tomography and histomorphometry, where information could not be obtained on the osteogenic dynamics during this observation period.

Osteogenesis during GBR undergoes a complex process of fine-tuned coordinated phases. Initially, an inflammatory phase occurs where leukocytes, including macrophages, are recruited. Subsequently, new blood vessels form and osteoblasts deposit an extracellular matrix. A matrix maturation phase then follows before the final mineralization phase, where osteoblasts remodel woven bone into mature lamellar bone.<sup>8,9</sup> The different stages of osteoblast growth and differentiation can be identified either by specific gene expression or by quantifying protein secretion using histochemical methods. In the proliferation phase, there is a characteristic peak in collagen type 1 during the formation of bone extracellular matrix. Subsequently, during the matrix maturation phase, collagen type I decreases and osteopontin and osteocalcin increase, reaching their maximal expression during the mineralization phase.<sup>10</sup> Other histochemical markers like tartrate-resistant acid phosphatase (TRAP) and alpha-smooth muscle actin ( $\alpha$ -SMA) represent biological cues for osteoclast activity and blood vessel formation, respectively. Hence, the quantification of

these markers by histochemical analysis can study the stages of bone development, including the required neoangiogenesis and bone remodeling processes.

Therefore, the primary aim of this study was to assess the osteogenic potential by evaluation and quantification of osteogenic markers by immunohistochemistry (IHC), when using a bioabsorbable membrane alone compared with the use of either an additional TiO<sub>2</sub> block or DBBM particulates as bone replacement grafts. The secondary aim was to assess the changes in the alveolar ridge soft tissue profile from baseline to 4 weeks and 12 weeks by histomorphometry.

## 2 | MATERIALS AND METHODS

### 2.1 | Materials

A timeline of the study design is shown in Figure 1A. Porous ceramic TiO<sub>2</sub> scaffold blocks were produced by foam replication. Teeth extraction and defect creation were performed according to the protocol of Sanz and colleagues<sup>11</sup> Three standardized defects were created in each hemi mandible to a standardized box shape measuring 10 mm mesiodistally, 10 mm apicocoronally, and 5 mm buccolingually using bone burs under copious saline irrigation, and left to heal for 8 weeks prior to GBR procedures. After 8 weeks healing, GBR surgery was performed on the cortical bone of the one-wall defects. All recipient sites were perforated with round burs, treated with GBR materials (Figure 1B) and primary healing was obtained. The hemimandibles were allocated to either 4 or 12 weeks of healing time. The three defect sites were randomly allocated to the following treatment groups:

1. TiO<sub>2</sub> block: TiO<sub>2</sub> scaffold (Corticalis AS, Oslo, Norway) covered by a collagen membrane (BioGide®; Geistlich Pharma AG, 6110 Wolhusen, Switzerland)
2. DBBM particulates: A xenograft of DBBM (Bio-Oss® Granules 0.25–1 mm, Geistlich Pharma AG, 6110 Wolhusen, Switzerland) covered by a collagen membrane (BioGide®; Geistlich Pharma AG, 6110 Wolhusen, Switzerland)

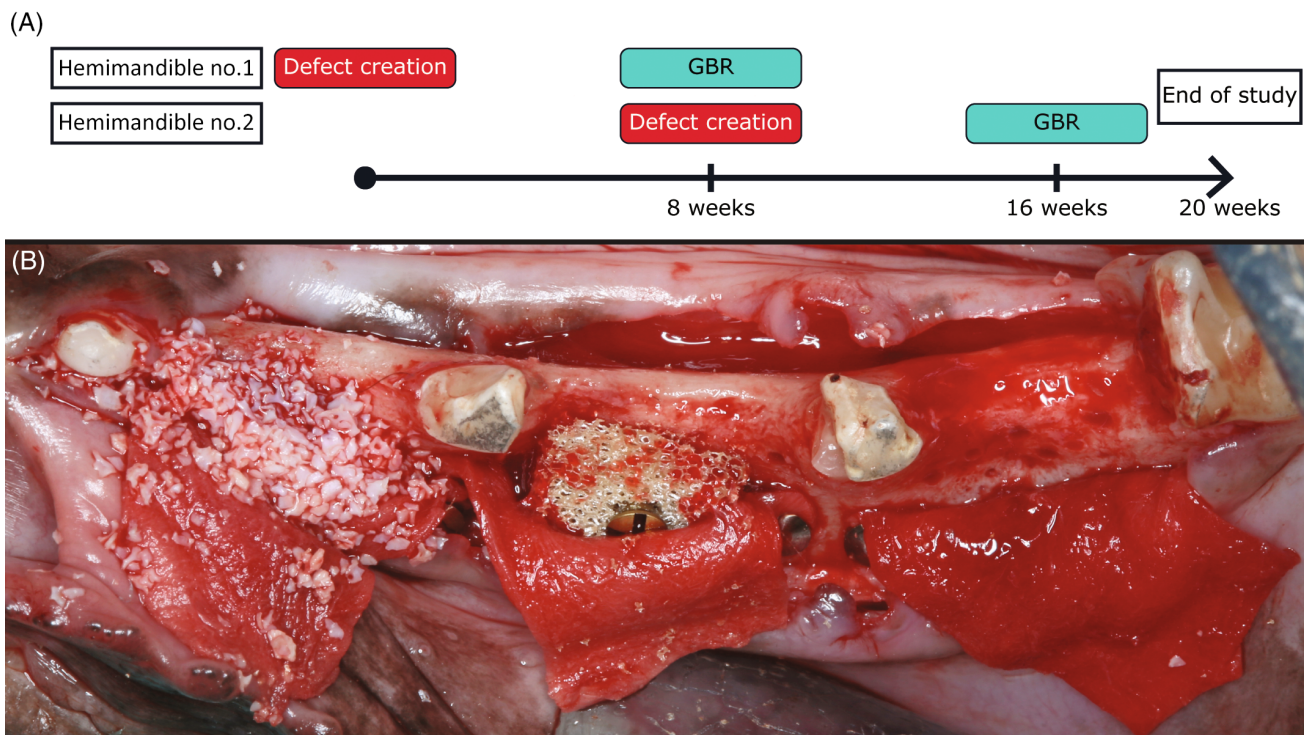


**FIGURE 1** (A) Timeline of the study design. (B) Guided bone regeneration (GBR) procedure on noncontained defects. Showing the anterior defect with deproteinized bovine bone mineral particulates, middle defect with a TiO<sub>2</sub> block secured with a fixation screw and the empty posterior defect. Cortical perforations were performed at all recipient sites. All sites were covered with a collagen membrane stabilized by pin fixation.

3. Empty control: A collagen membrane covered the defect (BioGide<sup>®</sup>; Geistlich Pharma AG, 6110 Wolhusen, Switzerland)

The collagen membranes were fixated at the apical edges by titanium pins (Botiss titan pins 3 mm, Straumann AG, CH-4002 Basel, Switzerland) and the TiO<sub>2</sub> blocks were fixated with a bone block fixation screw 1.5 mm in diameter and 10.0 mm in length (Straumann AG, CH-4002 Basel, Switzerland), adapted to fit the alveolar width. Further details regarding the study design and material preparation have been described previously.<sup>7</sup>

## 2.2 | Animal handling

This experimental *in vivo* investigation was designed in accordance with the ARRIVE (Animal Research: Reporting of *In Vivo* Experiments) guidelines for preclinical research.<sup>12</sup> Its protocol was approved by the Ethical committee at the Jesús Usón Minimally Invasive Surgery Centre (Caceres, Spain) and by the Director General of Agriculture and Livestock (approval code: 2018209020003431).

A total of eight female beagle dogs (weight, 11–14 kg) were used. The animals were kept in a 12:12-light/dark cycle at 21–22°C in individual kennels and fed on soft pellet diet, being daily monitored by a veterinarian. Prior to the study, all animals were inspected to ensure the absence of oral disease or any dental conditions that would preclude bone regenerative intervention. Two weeks prior and throughout

the study, the animals were monitored for any signs or symptoms of systemic disease.

During the surgical interventions, the animals were premedicated with acepromazine (0.05 mg/kg/*i.m.*, Calmo Meosan, Pfizer, Madrid, Spain) and morphine (0.3 mg/kg/*i.m.*, Morfina Braun 2%, B. Braun Medical, Barcelona, Spain). Then they were first sedated with propofol (2 mg/kg/*i.v.*, Propovet, Abbott Laboratories, Kent, UK) and then general anesthesia was applied using 2.5%–4% of isoflurane (Isoba-vet, Schering-Plow, Madrid, Spain) under mechanically induced respiration. The animals were then infiltrated locally with Lidocaine 2% with epinephrine 1:100 000 (2% Xylocaine Dental, Dentsply, York, Pennsylvania) as local anesthetic. After surgeries, the animals were administered Morphine (0.3 mg/kg/*i.m.*) for the first 24 h and meloxicam (0.1 mg/kg/*s.i.d./p.o.*, Metacam, Boehringer Ingelheim España, Barcelona, Spain) for 3 days after surgeries to control pain. Antibiotic therapy with amoxicillin (22 mg/kg/*s.i.d./s.c.*, Amoxoil retard, Syva, León, Spain) was used for 7 days after the surgeries.

At the allocated healing times the animals were euthanized with a lethal dose of sodium pentobarbital (40–60 mg/kg/*i.v.*, Dolethal, Vetoquinol, France) and their mandibles were dissected and fixed in formalin.

## 2.3 | Histological preparation and histomorphometric analysis

Samples were dehydrated in an ascending series of alcohol and xylene baths before embedding in methyl methacrylate and polymerizing at

–20°C. The resulting embedded defect sites were divided into two halves. One was allocated for microcomputed tomography and undecalcified histomorphometry, and was utilized for the recently published results.<sup>7</sup> The other half was allocated to microtome sectioning and staining with Movat Pentachrome and Von Kossa/Van Gieson. At least four representative sites per treatment group per time point were included for IHC staining. These samples were sectioned in the middle of the defect in buccolingual direction in 5- $\mu\text{m}$  thickness onto Kawamoto's film (SECTION-LAB Co. Ltd., Hiroshima, Japan) using a motorized rotary microtome (Thermo/Microm HM 355 S, Thermo Scientific GmbH, Karlsruhe, Germany).

Movat Pentachrome stain was used to quantify collagen.<sup>13</sup> Von Kossa/Van Gieson staining was used to quantify the extracellular matrix mineralization.<sup>14</sup>

Histomorphometry was performed on slides scanned using an AxioScan Z1 (Carl Zeiss, Germany) and analyzed using ImageJ (ImageJ 1.53f51, National Institutes of Health, USA). The Trainable Weka Segmentation plugin for ImageJ was used to quantify the stained areas, as described by Malhan and colleagues<sup>15</sup> In these slides, three regions of interest (ROI) were chosen. (1) The buccal half of the alveolar bone, including the grafted area, measured from the tip of the alveolar crest and extending 10 mm apically (ROI<sub>tot</sub>). (2) An area representing the interface between bone and the graft expanded 200  $\mu\text{m}$  in both buccal and lingual directions (ROI<sub>400</sub>  $\mu\text{m}$ ). In the empty control group, the area between bone and soft tissue was measured, and graft materials were excluded if present. (3) An area was determined from the same interface as for the ROI<sub>400</sub>  $\mu\text{m}$  but only expanded 20  $\mu\text{m}$  in both buccal and lingual directions (ROI<sub>40</sub>  $\mu\text{m}$ ).

## 2.4 | Enzyme histochemical and immunohistochemical preparation and analysis

Sections were deplastified prior to staining. To show TRAP activity, sections were incubated in Sodium Acetate buffer, Naphthol-AS-TR phosphate (N6125-1G, Sigma, Germany) and Sodium Tartrate (Merck, Germany) at 37°C for 60 min.

IHC was done using the following primary antibodies (Abcam Company, Cambridge, UK): rabbit monoclonal (EPR53) to  $\alpha$ -SMA, rabbit polyclonal (OAA100188) to osteopontin, mouse monoclonal (LS-C83497-100) to osteocalcin and rabbit monoclonal (EPR7785) to collagen type I.

To study the blood vessel formation,  $\alpha$ -SMA, osteopontin, osteocalcin, and collagen type-I were diluted in DAKO-Diluent (S 0809), 1:400, 1:400, 1:1200, and 1:1200, respectively. Collagen type-I,  $\alpha$ -SMA, osteocalcin, and osteopontin staining were quantified as described for histomorphometry, using the same ROIs. The number of osteoblasts was counted manually in TRAP-stained sections at the bone interface of ROI<sub>tot</sub>. Blood vessels were classified and quantified as circular, intermediate, or irregular by  $\alpha$ -SMA in ROI<sub>400</sub>  $\mu\text{m}$ .

## 2.5 | Alveolar profile measurements

Individualized impression trays were fabricated for each animal. Silicon impressions of the mandible were taken using a light/heavy putty (Elite HD+, Zhermack spa, RO, Italy) prior to GBR procedure and at the end of study. Cast models were poured with stone (Fujirock type 4, GC, Corp, Tokyo, Japan), then optically scanned using a desktop 3D scanner (Zfx Evolution Scanner, Zimmer Dental, Bolzano, Italy) to obtain STL files. MeshLab 2022.02 was used to align the images.<sup>16</sup> Buccolingual cross-sections were made at the middle of the defect and exported to ImageJ for analysis. ROI was defined as the buccal half of the mandible, from the crest and 6 mm apically or until the mucogingival border. The impression taken prior to GBR procedure was set as a baseline and changes in area were measured in 2 mm increments in a coronal direction.<sup>17</sup>

## 2.6 | Data analysis

Comparisons across groups were performed using parametric one-way analysis of variance (ANOVA) for normalized datasets. Pairwise multiple comparison procedures were done by Holm–Sidak method. When the normality test or equal variance test failed, Kruskal–Wallis one-way ANOVA on ranks was performed, and Dunn's method performed pairwise multiple comparison procedures. All statistical analyses were performed using SigmaPlot 14 (Systat Software, San Jose, California). Statistical significance was set at the 0.05 level.

## 3 | RESULTS

### 3.1 | Histology and histomorphometry

#### 3.1.1 | Movat pentachrome

Mineralized bone was characterized by a dark yellow staining of the collagen. In intimate contact with this mineralized bone was a brighter yellow-stained collagen network between the porous graft materials for both DBBM and TiO<sub>2</sub> groups. This collagen network appeared homogenous but presented fibers in random orientation. Cell nuclei were evenly infiltrated within this collagen network. In addition, a collagen membrane covered the pristine bone in the negative control group and graft materials in DBBM and TiO<sub>2</sub> groups.

The fraction of collagen in the different ROIs is presented in (Figure 2). For ROI<sub>400</sub>  $\mu\text{m}$  at 12 weeks healing time, a significant difference was found between empty control group (median: 87.56%, The interquartile range [IQR]: 81.21–90.46) and DBBM group (median: 68.68%, IQR: 64.72–76.51;  $p < 0.05$ ). The collagen fraction decreased significantly from 4 weeks (median: 83.94%, IQR: 79.14–87.99) to 12 weeks for the DBBM group ( $p < 0.05$ ). The same significant decrease was seen for DBBM group in ROI<sub>40</sub>  $\mu\text{m}$  as well, from 4 weeks (median: 75.48%, IQR: 71.66–76.48) to 12 weeks (median: 67.97%, IQR: 42.34–70.90;  $p < 0.05$ ).

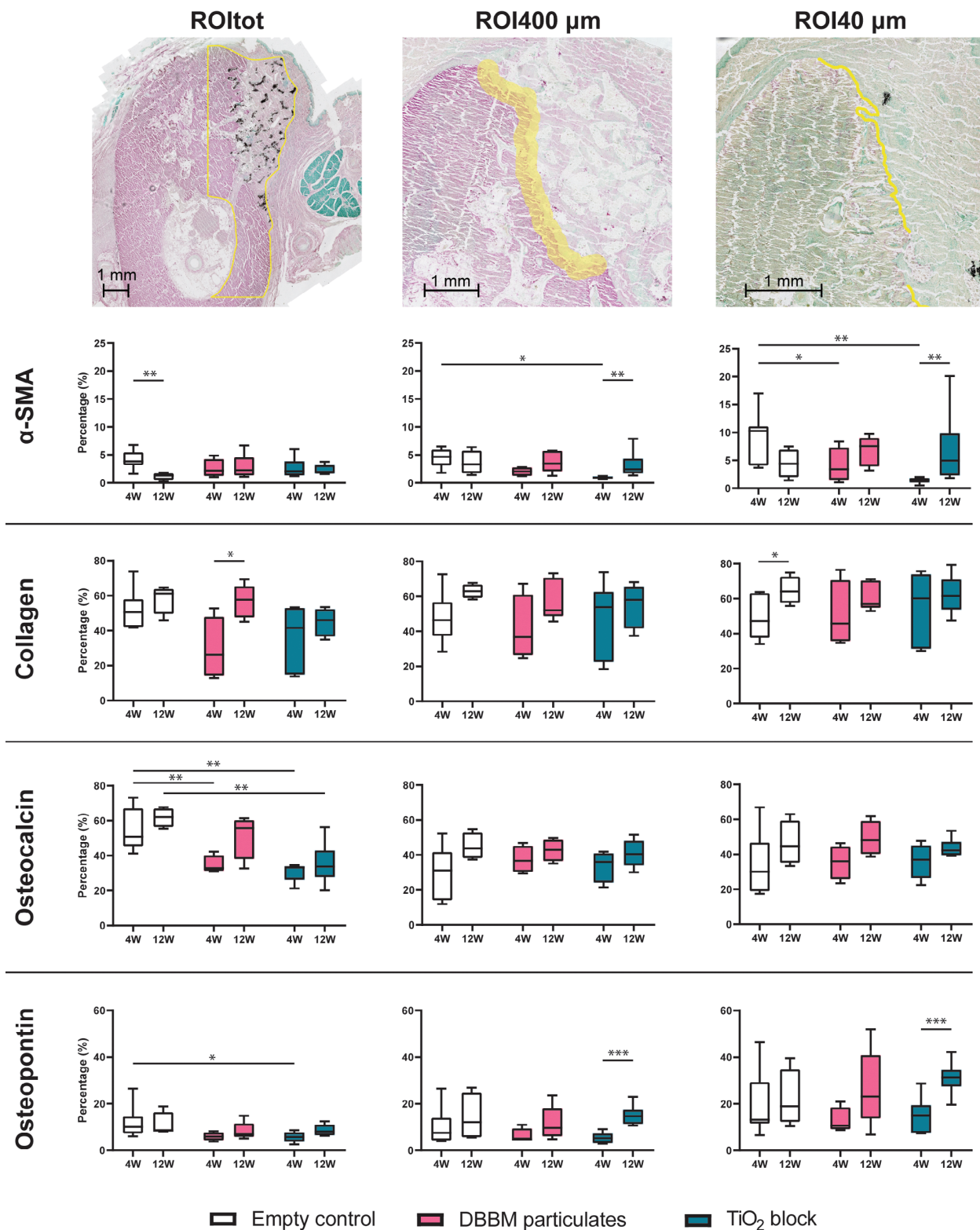


**FIGURE 2** Illustrations of the different regions of interest (ROIs) analyzed. ROI tot showing a TiO<sub>2</sub> sample with osteocalcin stain, ROI 400 μm showing a deproteinized bovine bone mineral (DBBM) sample with collagen stain and ROI 40 μm showing a negative control sample with osteopontin stain. Area with graft material was excluded. Box plots with statistical significance denoted by asterisks: \*p < 0.05, \*\*p < 0.01, \*\*\*p < 0.001. α-SMA, alpha-smooth muscle actin

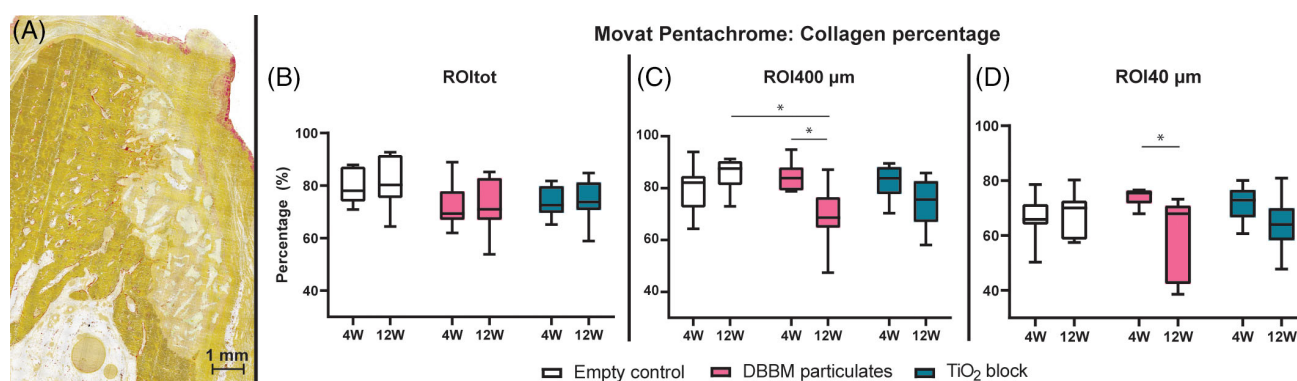


**FIGURE 3** (A) Deproteinized bovine bone mineral (DBBM) particulates seen as light green, mineralized bone in dark yellow, and unmineralized collagen in bright yellow. Percentage of collagen in region of interest (ROI)tot (B), ROI400  $\mu\text{m}$  (C) and ROI40  $\mu\text{m}$  (D). Statistical significance denoted by asterisks: \* $p < 0.05$ . 4 W, 4 weeks; 12 W, 12 weeks

### 3.1.2 | Von Kossa/Van Gieson

A loosely connected extracellular matrix was seen in contact with both DBBM and TiO<sub>2</sub> graft materials and filled the space between the graft materials. The matrix was homogenous and similar for both DBBM and TiO<sub>2</sub> groups.

The fractions of the extra cellular matrix (ECM) are presented in Figure 3B–D. The empty control group exhibited a significantly lower fraction of ECM compared with DBBM group and TiO<sub>2</sub> group at both 4 and 12 weeks. At 4 weeks: DBBM: median: 17.46%, IQR: 14.30–31.12, empty control: median: 6.50%, IQR: 4.03–8.30, TiO<sub>2</sub>: median: 16.97%, IQR: 16.06–25.74. At 12 weeks: DBBM: median: 14.68%, IQR: 9.51–18.44, empty control: median: 4.81%, IQR: 3.65–5.68, TiO<sub>2</sub>: median: 22.00%, IQR: 17.02–27.64.

## 3.2 | Histochemical analyses

### 3.2.1 | Alpha-smooth muscle actin

Blood vessels were evenly distributed in the mineralized bone with no apparent differences between the new and original bone of the alveolar ridge for both 4 and 12 weeks healing time points. The empty defects showed vascularization in the connective tissue buccal to the bone, but only small amounts were observed in the close vicinity of the cortical border (ROI400  $\mu\text{m}$  and ROI40  $\mu\text{m}$ ). Both TiO<sub>2</sub> group and DBBM group had ingrowth of blood vessels from the bone into the grafted area, but primarily at the border. Quantification of blood vessels by type at ROI400  $\mu\text{m}$ ; regular, moderately irregular, and irregular, demonstrated no differences between the group and timepoints (Table S1).

For the ROI tot, the percentage of stained  $\alpha$ -SMA showed a significant decrease from 4 weeks (median: 3.83%, IQR: 3.16–5.47) to 12 weeks (median: 1.29%, IQR: 0.52–1.72) for empty control group ( $p \leq 0.01$ ). For ROI400  $\mu\text{m}$  at 4 weeks, empty control (median: 4.68%, IQR: 3.21–5.95) was significantly higher than TiO<sub>2</sub> group (median:

0.93%, IQR: 0.78–1.15;  $p < 0.05$ ). The TiO<sub>2</sub> group also showed a significant increase from 4 to 12 weeks (median: 2.41%, IQR: 1.70–4.33;  $p < 0.01$ ). For ROI40  $\mu\text{m}$  at 4 weeks, empty control (median: 10.26%, IQR: 4.07–11.10) was significantly higher than both DBBM group (median: 3.43%, IQR: 1.49–7.30) and TiO<sub>2</sub> group (median: 1.03–1.81;  $p < 0.05$ ). TiO<sub>2</sub> group showed a significant increase from 4 to 12 weeks (median: 4.94%, IQR: 2.30–9.84;  $p < 0.01$ ).

### 3.2.2 | Collagen

Collagen type I was detected by IHC in all samples. The mineralized bone was easily distinguishable with increased intensity along the bone border (Figure 4). For TiO<sub>2</sub> and DBBM groups the intensity of collagen staining was weaker between the graft materials compared with mineralized bone, but similar to the surrounding extracellular matrix.

For ROI tot a significant increase was seen for DBBM group from 4 weeks (median: 26.19%, IQR: 14.27–47.94) to 12 weeks (median: 57.76%, IQR: 47.54–65.35;  $p < 0.05$ ). At ROI40  $\mu\text{m}$  a significant increase was seen for empty control group from 4 weeks (median: 47.13%, IQR: 37.54–63.14) to 12 weeks (median: 64.20%, IQR: 57.58–72.60;  $p < 0.05$ ).

### 3.2.3 | Osteocalcin

Osteocalcin intensity was similar across all groups and time points. For example, a homogenous staining of the pristine alveolar bone was observed, and no osteocalcin stain was seen in the grafted area.

For ROI tot, at 4 weeks the negative controls (median: 50.83%, IQR: 45.34–67.03) were significantly higher than both DBBM group (median: 32.86%, IQR: 31.23–40.15) and TiO<sub>2</sub> group (median: 33.17%, IQR: 26.30–33.98;  $p < 0.01$ ). At 12 weeks, a significant difference was found between negative control (median: 62.01%, IQR: 56.35–66.98) and TiO<sub>2</sub> group (median: 33.68%, IQR: 27.76–43.00;  $p < 0.01$ ). No

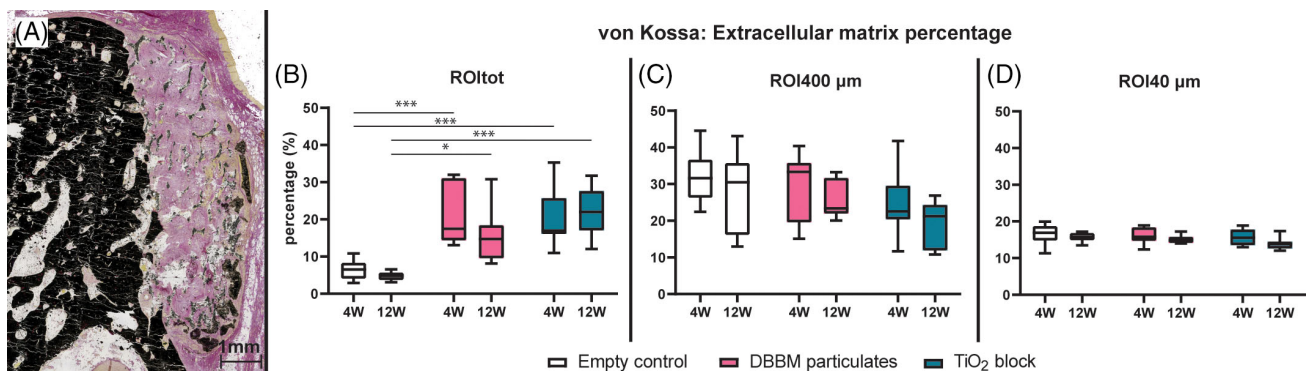


**FIGURE 4** (A) TiO<sub>2</sub> group. Mineralized bone, including deproteinized bovine bone mineral (DBBM) particulates, stained black by Von Kossa/ Van Gieson, while TiO<sub>2</sub> appeared dark gray to black. An extracellular matrix is stained pink within the TiO<sub>2</sub> scaffold and presents less intensity than the surrounding soft tissue and epithelium. Some voids from fracture and tearing of the scaffold are seen. Note migrated DBBM particulates at the bottom of the defect. Percentage of extracellular matrix in region of interest (ROI) tot (B), ROI400 μm (C), and ROI40 μm (D). Statistical significance denoted by asterisks: \* $p < 0.05$ , \*\*\* $p < 0.001$

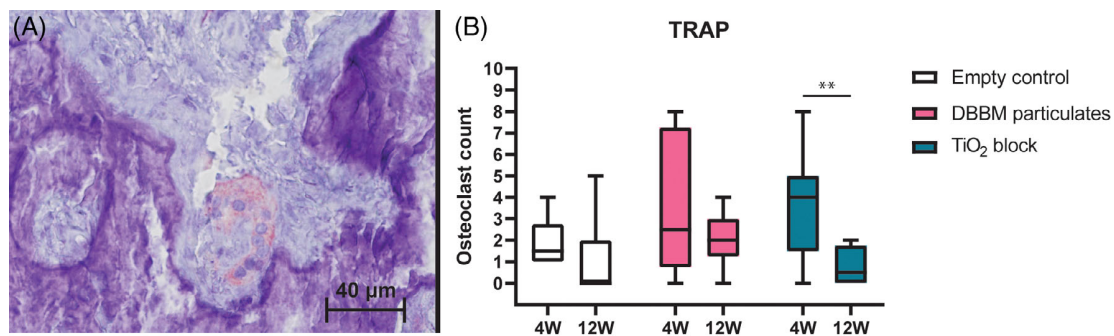


**FIGURE 5** (A) Osteoclast in a Howship lacuna, (B) Double asterisks denote statistical significance ( $p < 0.01$ ). DBBM, deproteinized bovine bone mineral; TRAP, tartrate-resistant acid phosphatase

significant differences were found between the groups or from 4 to 12 weeks for ROI400 or ROI40 μm.

### 3.2.4 | Osteopontin

Osteopontin staining was found along the osteons' borders, resulting in a heterogeneous staining of the mineralized bone. Increased intensity was seen at the cortical borders of the defect site for all groups. Within the grafted areas, the intensity of osteopontin was weaker and observed on the surface of both DBBM and TiO<sub>2</sub>. Osteopontin was not seen in the space between the graft materials. For ROI tot at 4 weeks, empty control (median: 10.09%, IQR: 4.28–7.64) was significantly higher than TiO<sub>2</sub> group (median: 5.77, IQR: 3.71–7.71;  $p < 0.05$ ). For ROI400 μm, TiO<sub>2</sub> group demonstrated a significant increase from 4 weeks (median: 5.22%, IQR: 3.08–7.30) to 12 weeks (median: 14.66%, IQR: 11.31–17.45;  $p < 0.001$ ). This was also seen at ROI40 μm for TiO<sub>2</sub> group from 4 weeks (median: 15.08%, IQR: 7.41–19.49) to 12 weeks (median: 31.24%, IQR: 27.44–34.58;  $p < 0.01$ ).

### 3.2.5 | Tartrate-resistant acid phosphatase

Osteoclasts were identified in 35 out of 46 samples within the ROI. Outside the ROI, osteoclasts were also found on the surface of the DBBM particulates close to the bone (Figure 5A). The TiO<sub>2</sub> group demonstrated a significantly decrease in the number of osteoclasts from 4 weeks (median: 4.0, IQR: 1.5–5) to 12 weeks (median: 0.5, IQR: 0–1.75;  $p < 0.01$ ; Figure 5B).

### 3.3 | Alveolar ridge profile

At 4 weeks of healing, a significant difference was seen between negative control and TiO<sub>2</sub> group at the mid portion, median: 1.38 mm<sup>2</sup>, IQR: –0.30 to 1.88 and median: 3.62 mm<sup>2</sup>, IQR: 2.41–5.22, respectively (Figure 6B;  $p < 0.05$ ). A significant difference between negative control and TiO<sub>2</sub> group were also seen at the low portion, median: 1.24 mm<sup>2</sup>, IQR: 0.89–2.72 and median: 4.65 mm<sup>2</sup>, IQR: 3.38–4.96, respectively ( $p < 0.05$ ). At 12 weeks healing, a significant difference was seen between negative control and TiO<sub>2</sub> group at the mid

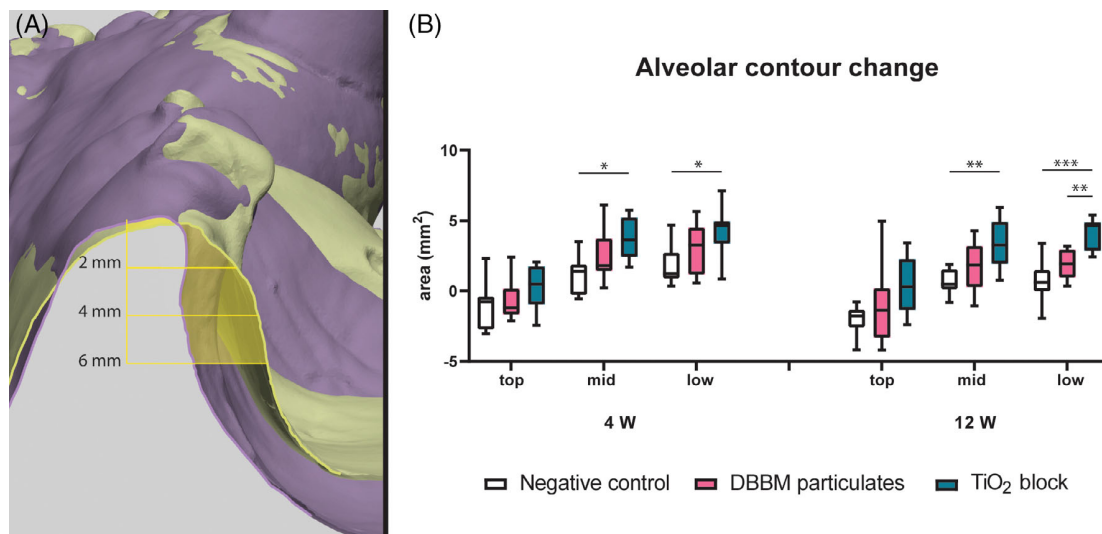


**FIGURE 6** (A) Superimposed stereolithographic images of  $\text{TiO}_2$  sample 4 weeks after guided bone regeneration. The baseline in purple and 4 weeks healing in green. Area difference in ROI is illustrated in yellow. Shown distance from the alveolar crest divides the top, mid, and low segments. (B) Area differences for alveolar contour. Statistical significance denoted by asterisks: \* $p < 0.05$ , \*\* $p < 0.01$ , \*\*\* $p < 0.001$ . DBBM, deproteinized bovine bone mineral

portion, median:  $0.47 \text{ mm}^2$ , IQR:  $0.10\text{--}1.53$  and median:  $3.27 \text{ mm}^2$ , IQR:  $1.92\text{--}4.92$ , respectively ( $p < 0.01$ ). At the low portion, a significant difference between negative control (median:  $0.61 \text{ mm}^2$ , IQR:  $-0.03$  to  $1.48$ ) and  $\text{TiO}_2$  group (median:  $4.66 \text{ mm}^2$ , IQR:  $2.84\text{--}4.90$ ;  $p < 0.001$ ) and DBBM group (median:  $1.93 \text{ mm}^2$ , IQR:  $0.96\text{--}2.95$ ;  $p < 0.01$ ). No significant difference was observed from 4 to 12 weeks of healing in any group.

#### 4 | DISCUSSION

This study demonstrated that GBR in chronic defects using a  $\text{TiO}_2$  block led to an increase of  $\alpha$ -SMA and osteopontin from 4 to 12 weeks at the bone-scaffold interface. In the DBBM group, an increase in collagen type I was observed for ROI<sub>tot</sub>, while the negative control group showed decreased  $\alpha$ -SMA in ROI<sub>tot</sub> and increased collagen type I at ROI<sub>40</sub>  $\mu\text{m}$ . The findings suggest contact osteogenesis when GBR is performed with a  $\text{TiO}_2$  block or DBBM particulates. The increase in osteogenic markers indicates potential for bone formation beyond 12 weeks. In addition, the alveolar profile data showed a sustained lateral increase using a graft material against negative control.

These findings were in accordance with previous studies demonstrating osteoconductivity of  $\text{TiO}_2$  blocks in preclinical models.<sup>7,18</sup> In addition, osteoblasts' enhanced osteopontin and vascular endothelial growth factor secretion by osteoblasts on  $\text{TiO}_2$  have also been demonstrated in cell cultures compared with a  $\text{SiO}_2$  surface.<sup>19</sup> The increased osteopontin at the bone border and around graft materials coincides with previous reports.<sup>20–22</sup> Osteopontin is required for bone formation and facilitates osteoblast and osteoclast adhesion.<sup>23–25</sup> As both osteopontin and blood vessels are essential for osteogenesis, an increase in osteopontin and  $\alpha$ -SMA from 4 to 12 weeks may indicate

a potential for further bone growth. No uniform distribution of osteogenic markers could be found in any site, as can be done by in vitro assessment of osteogenic expression.<sup>10</sup> However, this may be expected as a large site in vivo demonstrates different niches with varying osteogenic development in the augmented compartment. For a more homogeneous comparison, a ROI at the interface between bone and graft was considered to describe the osteogenesis across groups.

For the empty control group,  $\alpha$ -SMA-stained blood vessels significantly decreased from 4 to 12 weeks in ROI<sub>tot</sub>, but not in ROI<sub>40</sub> and ROI<sub>400</sub>  $\mu\text{m}$ . This change was not observed for DBBM or  $\text{TiO}_2$  groups. The different defect areas could explain this result. The regions evaluated for  $\text{TiO}_2$  blocks and DBBM particulates included the area with graft materials and the interface of bone and graft material, whereas empty control sites consisted of bone and adjacent soft tissue. This difference was evident by evaluating the extracellular matrix fraction with Von Kossa/Van Gieson stain, where ROI<sub>tot</sub> constituted primarily mineralized bone in negative controls and no unmineralized grafted area. However, the results could also indicate a lower osteogenic activity at 12 than 4 weeks at negative control sites. Bone graft materials have been shown to delay initial bone regeneration as compared with empty control sites.<sup>6,26</sup> Faster initial healing at empty control sites covered by a collagen membrane was expected compared with DBBM-grafted and  $\text{TiO}_2$ -grafted sites.

One advantage of using graft materials in GBR is space maintenance under the cell occlusive membrane.<sup>27,28</sup> It has been shown by microCT measurements that both DBBM particulates and  $\text{TiO}_2$  blocks preserved the space 12 weeks after GBR procedure. This study corroborated the results in alveolar contour change, which implied the soft tissue profile adapted to the graft materials. The STL images also made it possible to compare baseline alveolar shape prior to surgery



with the shape after 4 and 12 weeks. A minor resorption was found at the top increment in the negative control group, as expected when a flap was raised and the bone crest exposed to perform GBR.<sup>29</sup> A tissue loss at the coronal part was also found for the DBBM group but not for the TiO<sub>2</sub> group. This may be attributed to the different handling and properties of materials used in the chronic, noncontained defects. For example, in the middle and lower part of the ridge, the TiO<sub>2</sub> group was significantly wider than the empty control group. The DBBM group was not statistically significantly wider than the empty control group. This was expected, as a block graft material is more stable than a particulate. Graft dislocation following wound closure may also contribute to the reduced alveolar width at the coronal portion, especially for the particulates. As shown in an *in vitro* study by Mir-Mari and colleagues,<sup>30</sup> compressive forces on the augmented sites could not be totally avoided, even though a clinically tension-free flap closure was achieved. The authors reported enhanced stability of the particulates by application of fixation pins or by the use of a block graft as compared with particulated bone substitutes. The effect of graft dislocation was found to be substantiated in one-wall bone defects as compared with self-contained defects.<sup>31</sup> The authors found GBR with additional membrane fixation resulted in higher volume stability than without fixation and even better stability when a titanium-reinforced membrane or a bone block was used. In this study, the collagen membrane was secured with metal pins. A reinforced membrane may have been beneficial for the particulate group; however, that would add another variable in the healing process. Additionally, DBBM with a resorbable collagen membrane is a commonly used and well-documented procedure for augmentation and therefore chosen as a positive control.<sup>32</sup>

The results from the alveolar ridge profile measurements in this study were partly in agreement with reported findings from Di Raimondo and colleagues,<sup>17</sup> who found a larger increase of the alveolar profile in the apical as compared with the coronal portions and a more significant increase for sites that included graft materials as compared with negative controls. However, the authors also demonstrated that a membrane alone significantly increased the alveolar contour, in contrast to this study. This may be explained by the difference in the defect model, as Di Raimondo and colleagues assessed peri-implant dehiscence defects.

To the best of the authors' knowledge, few studies have reported the IHC characterization of lateral bone augmentation in chronic defects. Schwarz and colleagues<sup>33</sup> reported on GBR with a biphasic hydroxyapatite and beta-tricalcium phosphate compared with a collagen-coated DBBM, whereas Cha and colleagues<sup>34</sup> studied GBR using a biphasic calcium phosphate ceramic compared with DBBM and also empty defects without a membrane. Both authors reported on peri-implant dehiscence defects in dogs, respectively, on acute and chronic defect models.

Cha and colleagues reported a significantly higher osteocalcin intensity at 8 weeks for sites treated with DBBM than sites treated with a biphasic calcium phosphate and empty sites with no membrane. At 16 weeks the osteocalcin intensity was similar across all groups. The authors observed osteocalcin around the mature bone.

Schwarz and colleagues reported osteocalcin antigen reactivity in the connective tissue adjacent to DBBM and beta-tricalcium phosphate granules. This was not seen in this study, where a stable intensity from 4 to 12 weeks was observed in mineralized bone only. The empty control group had the highest intensity in ROI<sub>tot</sub>, but no differences were found otherwise. The lower intensity seen in the DBBM and TiO<sub>2</sub> groups compared with this study's empty control group may indicate early osteogenesis as osteocalcin is a marker of the later stages.<sup>35</sup>

The comparable intensity of osteopontin was found across the groups at 8 and 16 weeks by Cha and colleagues. Osteopontin was situated around bone borders and graft particulates, according to this study. However, in this study, a higher intensity was found in the empty control group than the TiO<sub>2</sub> group at 4 weeks for ROI<sub>tot</sub>, and the TiO<sub>2</sub> group demonstrated increased intensity from 4 to 12 weeks in both ROI<sub>140</sub> and ROI<sub>400</sub> μm.

Cha and colleagues reported no different TRAP counts for the DBBM group as compared with the empty control group, in agreement with this study. The biphasic calcium phosphate bone substitute demonstrated a significant increase in TRAP count from 8 to 16 weeks, which was hypothesized to be due to the resorption and following calcium and phosphate release from the biomaterial. As this study used a nonresorbable scaffold, no change in TRAP count was anticipated for the TiO<sub>2</sub> group. In addition to the different models used by Schwarz and colleagues and Cha and colleagues, these studies also applied different methods for immunohistochemical analysis. Schwarz et al. used the cutting and grinding technique for MMA embedded samples,<sup>36</sup> whereas Cha and colleagues embedded the samples in paraffin. The different techniques may further explain the different results found compared with this study.

When compared with a previous study,<sup>7</sup> where methyl methacrylate sections were prepared by cutting and grinding, the use of microtome sectioned samples in this study presented several benefits. Above all, the 5 μm thin sections could be deplastified and decalcified after microtome sectioning. Decalcifying is usually performed on the bulk sample prior to paraffin embedding and sectioning. However, decalcification would not affect the ceramic TiO<sub>2</sub> scaffold and would be impossible to cut when placed in soft decalcified tissue. The present method described by Malhan and colleagues<sup>15</sup> allowed for histochemical staining of TiO<sub>2</sub> containing samples without the need for specialized equipment like laser microtomes.<sup>37</sup> By decalcifying 5 μm sections, the process was also quicker than bulk decalcifying. In addition, this technique yielded a higher number of sections as no material was lost by cutting and grinding. Ultimately, this may reduce the required number of animals, according to the principles of humane experimental technique.<sup>38</sup> In this study, the thinner sections also resulted in better image quality. As previously reported, a dense structure was observed as a dark substance between the graft materials.<sup>7</sup> With the thinner sections, a collagen network in the extracellular matrix was clearly identified from Movat Pentachrom and Von Kossa/Van Gieson stain. However, there were challenges with the methacrylate infiltration. Some samples were not adequately fixated. As a result, some sections had to be excluded in the analyses.

This study results should be interpreted with care due to the experimental nature of the study as well as the limited number of animals. In addition, the heterogeneity in study designs for GBR makes a comparison between studies challenging. The low number of treatment groups was also a limitation, and a DBBM material in block configuration could have served as a more relevant control in this study design. Further studies should also evaluate if the regenerated tissue obtained with TiO<sub>2</sub> blocks will be stable over time and allow a reliable osseointegration of implants. Finally, despite the indications of osteogenic differentiation, a longer observation time is required to confirm future bone formation.

## 5 | CONCLUSION

In conclusion, within the study's limitations, the findings suggest contact osteogenesis when GBR is performed with a TiO<sub>2</sub> block or DBBM particulates. The increase in osteopontin markers indicates potential for osteogenesis beyond 12 weeks in this model. However, the alveolar profile data indicated a sustained lateral increase in lateral bone augmentation using a TiO<sub>2</sub> block and a collagen membrane, as compared with DBBM and a collagen membrane or a collagen membrane alone.

### AUTHOR CONTRIBUTIONS

Mariano Sanz and Håvard Jostein Haugen prepared the protocol, acquired funding, and critically revised the article. Minh Khai Le Thieu, Sabine Stoetzel, Maryam Rahmati, Thaqif El Khassawna, Anders Verket, Javier Sanz-Esporrin, Jan Eirik Ellingsen, and Håvard Jostein Haugen conducted the study. Minh Khai Le Thieu and Anders Verket interpreted data/analysis. Anders Verket and Javier Sanz-Esporrin led the study. All authors contributed in critical revision of the article. The data that support the findings of this study are available from the corresponding author upon reasonable request.

### ACKNOWLEDGMENTS

Maryam Rahmati was supported by a project "Promoting patient safety by a novel combination of imaging technologies for biodegradable magnesium implants, MgSafe" funded by European Training Network within the framework of Horizon 2020 Marie Skłodowska-Curie Action (MSCA) grant number No 811226 ([www.mgsafe.eu](http://www.mgsafe.eu)). Histological images were acquired at the Norbrain Slide scanning Facility at the Institute of Basic Medical Sciences, University of Oslo, a resource funded by the Research Council of Norway. This work was supported by the Research Council of Norway (FRINATEK) grant number 231530.

### CONFLICT OF INTEREST

Haugen and Ellingsen hold patents for the technology for the TiO<sub>2</sub> bone graft substitute (EP Patent 2121053, US Patent 9629941 US Patent App. 14/427901, US Patent App. 14/427683, and US Patent App. 14/427854). The rights for these patents are shared between the University of Oslo and Corticalis AS. Haugen and Ellingsen are

shareholders and board members of Corticalis AS. The other authors report no conflicts of interest related to this study.

### DATA AVAILABILITY STATEMENT

The data that support the findings of this study are available from the corresponding author upon reasonable request.

### ORCID

Minh Khai Le Thieu  <https://orcid.org/0000-0003-1712-9276>

Thaqif El Khassawna  <https://orcid.org/0000-0002-1187-8578>

Anders Verket  <https://orcid.org/0000-0002-4862-9030>

Javier Sanz-Esporrin  <https://orcid.org/0000-0003-0859-3149>

Mariano Sanz  <https://orcid.org/0000-0002-6293-5755>

Jan Eirik Ellingsen  <https://orcid.org/0000-0001-9182-6251>

Håvard Jostein Haugen  <https://orcid.org/0000-0002-6690-7233>

### REFERENCES

- Elgali I, Omar O, Dahlin C, Thomsen P. Guided bone regeneration: materials and biological mechanisms revisited. *Eur J Oral Sci.* 2017; 125(5):315-337. doi:10.1111/eos.12364
- McAllister BS, Haghghat K. Bone augmentation techniques. *J Periodontol.* 2007;78(3):377-396. doi:10.1902/jop.2007.060048
- Araujo M, Linder E, Wennstrom J, Lindhe J. The influence of Bio-Oss collagen on healing of an extraction socket: an experimental study in the dog. *Int J Periodontics Restorative Dent.* 2008;28(2):123-135.
- Hammerle CH, Olah AJ, Schmid J, et al. The biological effect of natural bone mineral on bone neoformation on the rabbit skull. *Clin Oral Implants Res.* 1997;8(3):198-207. doi:10.1034/j.1600-0501.1997.080306.x
- Schmid J, Hammerle CH, Fluckiger L, et al. Blood-filled spaces with and without filler materials in guided bone regeneration. A comparative experimental study in the rabbit using bioresorbable membranes. *Clin Oral Implants Res.* 1997;8(2):75-81. doi:10.1034/j.1600-0501.1997.080201.x
- Stavropoulos A, Kostopoulos L, Mardas N, Nyengaard JR, Karring T. Deproteinized bovine bone used as an adjunct to guided bone augmentation: an experimental study in the rat. *Clin Implant Dent Relat Res.* 2001;3(3):156-165. doi:10.1111/j.1708-8208.2001.tb00136.x
- Thieu MKL, Haugen HJ, Sanz-Esporrin J, Sanz M, Lyngstadaas SP, Verket A. Guided bone regeneration of chronic non-contained bone defects using a volume stable porous block TiO<sub>2</sub> scaffold: an experimental in vivo study. *Clin Oral Implants Res.* 2021;32(3):369-381. doi:10.1111/clr.13708
- Probst A, Spiegel HU. Cellular mechanisms of bone repair. *J Invest Surg.* 1997;10(3):77-86. doi:10.3109/08941939709032137
- Schindeler A, McDonald MM, Bokko P, Little DG. Bone remodeling during fracture repair: the cellular picture. *Semin Cell Dev Biol.* 2008; 19(5):459-466. doi:10.1016/j.semcdb.2008.07.004
- Stein GS, Lian JB, Stein JL, Van Wijnen AJ, Montecino M. Transcriptional control of osteoblast growth and differentiation. *Physiol Rev.* 1996;76(2):593-629. doi:10.1152/physrev.1996.76.2.593
- Sanz M, Ferrantino L, Vignoletti F, de Sanctis M, Berglundh T. Guided bone regeneration of non-contained mandibular buccal bone defects using deproteinized bovine bone mineral and a collagen membrane: an experimental in vivo investigation. *Clin Oral Implants Res.* 2017; 28(11):1466-1476. doi:10.1111/clr.13014
- Percie du Sert N, Hurst V, Ahluwalia A, et al. The ARRIVE guidelines 2.0: updated guidelines for reporting animal research. *PLoS Biol.* 2020; 18(7):e3000410. doi:10.1371/journal.pbio.3000410

13. Movat HZ. Demonstration of all connective tissue elements in a single section; pentachrome stains. *AMA Arch Pathol.* 1955;60(3): 289-295.
14. Rahmati M, Stotzel S, Khassawna TE, et al. Early osteoimmunomodulatory effects of magnesium-calcium-zinc alloys. *J Tissue Eng.* 2021; 12:204173142111047100. doi:10.1177/204173142111047100
15. Malhan D, Muelke M, Rosch S, et al. An optimized approach to perform bone Histomorphometry. *Front Endocrinol (Lausanne).* 2018; 9(666):666. doi:10.3389/fendo.2018.00666
16. Cignoni, P., Callieri, M., Corsini, M., Dellepiane, M., Ganovelli, F., & Ranzuglia, G. Meshlab: an open-source mesh processing tool. Paper Presented at the Eurographics Italian Chapter Conference; 2008.
17. Di Raimondo R, Sanz-Esporrin J, Sanz-Martin I, et al. Hard and soft tissue changes after guided bone regeneration using two different barrier membranes: an experimental in vivo investigation. *Clin Oral Investig.* 2021;25(4):2213-2227. doi:10.1007/s00784-020-03537-5
18. Verket A, Muller B, Wohlfahrt JC, et al. TiO<sub>2</sub> scaffolds in peri-implant dehiscence defects: an experimental pilot study. *Clin Oral Implants Res.* 2016;27(10):1200-1206. doi:10.1111/clr.12725
19. Verket A, Tainen H, Haugen HJ, Lyngstadaas SP, Nilsen O, Reseland JE. Enhanced osteoblast differentiation on scaffolds coated with TiO<sub>2</sub> compared to SiO<sub>2</sub> and CaP coatings. *Biointerphases.* 2012; 7(1-4):36. doi:10.1007/s13758-012-0036-8
20. Araújo MG, Liljenberg B, Lindhe J. Dynamics of Bio-Oss® Collagen incorporation in fresh extraction wounds: an experimental study in the dog. *Clinical oral implants research.* 2010;21(1):55-64. doi:10.1111/j.1600-0501.2009.01854.x
21. Lindhe J, Araújo MG, Bufler M, Liljenberg B. Biphasic alloplastic graft used to preserve the dimension of the edentulous ridge: an experimental study in the dog. *Clinical oral implants research.* 2013;24(10): 1158-1163. doi:10.1111/j.1600-0501.2012.02527.x
22. Ortiz-Vigón A, Martínez-Villa S, Suarez I, Vignoletti F, Sanz M. Histomorphometric and immunohistochemical evaluation of collagen containing xenogeneic bone blocks used for lateral bone augmentation in staged implant placement. *Int J Implant Dent.* 2017;3(1):24. doi:10.1186/s40729-017-0087-1
23. Mark MP, Butler WT, Prince CW, Finkelman RD, Ruch J-V. Developmental expression of 44-kDa bone phosphoprotein (osteopontin) and bone  $\gamma$ -carboxyglutamic acid (Gla)-containing protein (osteocalcin) in calcifying tissues of rat. *Differentiation.* 1988;37(2):123-136. doi:10.1111/j.1432-0436.1988.tb00804.x
24. Mark MP, Prince CW, Oosawa T, Gay S, Bronckers AL, Butler WT. Immunohistochemical demonstration of a 44-KD phosphoprotein in developing rat bones. *Journal of Histochemistry & Cytochemistry.* 1987;35(7):707-715. doi:10.1177/35.7.3295029
25. Reinholt FP, Hulthén K, Oldberg A, Heinegård D. Osteopontin--a possible anchor of osteoclasts to bone. *Proc Natl Acad Sci U S A.* 1990;87(12):4473-5. doi:10.1073/pnas.87.12.447
26. Trombelli L, Lee MB, Promsudthi A, Guglielmoni PG, Wikesjö UM. Periodontal repair in dogs: histologic observations of guided tissue regeneration with a prostaglandin E1 analog/methacrylate composite. *J Clin Periodontol.* 1999;26(6):381-387. doi:10.1034/j.1600-051x.1999.260608.x
27. Dahlin C, Linde A, Gottlow J, Nyman S. Healing of bone defects by guided tissue regeneration. *Plast Reconstr Surg.* 1988;81(5):672-676. doi:10.1097/00006534-198805000-00004
28. Lundgren D, Lundgren AK, Sennerby L, Nyman S. Augmentation of intramembraneous bone beyond the skeletal envelope using an occlusive titanium barrier. An experimental study in the rabbit. *Clin Oral Implants Res.* 1995;6(2):67-72. doi:10.1034/j.1600-0501.1995.060201.x
29. Bragger U, Pasquali L, Kornman KS. Remodelling of interdental alveolar bone after periodontal flap procedures assessed by means of computer-assisted densitometric image analysis (CADIA). *J Clin Periodontol.* 1988; 15(9):558-564. doi:10.1111/j.1600-051x.1988.tb02129.x
30. Mir-Mari J, Wui H, Jung RE, Hämmerle CH, Benic GI. Influence of blinded wound closure on the volume stability of different GBR materials: an in vitro cone-beam computed tomographic examination. *Clin Oral Implants Res.* 2016;27(2):258-265. doi:10.1111/clr.12590
31. Mertens C, Braun S, Krisam J, Hoffmann J. The influence of wound closure on graft stability: an in vitro comparison of different bone grafting techniques for the treatment of one-wall horizontal bone defects. *Clin Implant Dent Relat Res.* 2019;21(2):284-291. doi:10.1111/cid.12728
32. Sanz-Sanchez I, Ortiz-Vigón A, Sanz-Martin I, Figuero E, Sanz M. Effectiveness of lateral bone augmentation on the alveolar crest dimension: a systematic review and meta-analysis. *J Dent Res.* 2015; 94(9 Suppl):128s-142s. doi:10.1177/0022034515594780
33. Schwarz F, Herten M, Ferrari D, et al. Guided bone regeneration at dehiscence-type defects using biphasic hydroxyapatite + beta tricalcium phosphate (bone ceramic) or a collagen-coated natural bone mineral (Bio-Oss collagen): an immunohistochemical study in dogs. *Int J Oral Maxillofac Surg.* 2007;36(12):1198-1206. doi:10.1016/j.ijom.2007.07.014
34. Cha JK, Pla R, Vignoletti F, Jung UW, Sanz-Esporrin J, Sanz M. Immunohistochemical characteristics of lateral bone augmentation using different biomaterials around chronic peri-implant dehiscence defects: an experimental in vivo study. *Clin Oral Implants Res.* 2021; 32(5):569-580. doi:10.1111/clr.13726
35. Huang W, Yang S, Shao J, Li YP. Signaling and transcriptional regulation in osteoblast commitment and differentiation. *Front Biosci.* 2007; 12(8):3068-3092. doi:10.2741/2296
36. Donath K, Breuner G. A method for the study of undecalcified bones and teeth with attached soft tissues. The sage-Schliff (sawing and grinding) technique. *J Oral Pathol.* 1982;11(4):318-326. doi:10.1111/j.1600-0714.1982.tb00172.x
37. Kunert-Keil C, Richter H, Zeidler-Rentzsch I, Bleeker I, Gredes T. Histological comparison between laser microtome sections and ground specimens of implant-containing tissues. *Ann Anat.* 2019;222: 153-157. doi:10.1016/j.aanat.2018.12.001
38. Russell WMS, Burch RL. *The Principles of Humane Experimental Technique.* Methuen; 1959.

## SUPPORTING INFORMATION

Additional supporting information can be found online in the Supporting Information section at the end of this article.

**How to cite this article:** Thieu MKL, Stoetzel S, Rahmati M, et al. Immunohistochemical comparison of lateral bone augmentation using a synthetic TiO<sub>2</sub> block or a xenogeneic graft in chronic alveolar defects. *Clin Implant Dent Relat Res.* 2022;1-11. doi:10.1111/cid.13143

